CHALMERS
UNIVERSITY OF TECHNOLOGY

Modelling of Fully Electric Vehicle For Driving Simulator

Master's thesis in Mobility Engineering

JINGE GAO
ZIKUN WANG

DEPARTMENT OF MECHANICS AND MARITIME SCIENCES
CHALMERS UNIVERSITY OF TECHNOLOGY
Gothenburg, Sweden 2024
www.chalmers.se

Master's Thesis in Mobility Engineering

Modelling of Fully Electric Vehicle For Driving Simulator

JINGE GAO
ZIKUN WANG

CHALMERS
UNIVERSITY OF TECHNOLOGY

Department of Mechanics and Maritime Sciences
Division of Vehicle Engineering and Autonomous Systems
Chalmers University of Technology
Gothenburg, Sweden 2024

Modelling of Fully Electric Vehicle For Driving Simulator
JINGE GAO
ZIKUN WANG

Supervisor: Smit Saparia, VTI
Sogol Kharrazi, VTI
Fredrik Bruzelius, Mekanik och maritima vetenskaper
Examiner: Fredrik Bruzelius, Mekanik och maritima vetenskaper

Master's Thesis 2024
Department of Mechanics and Maritime Sciences
Chalmers University of Technology
SE-412 96 Gothenburg
Sweden
Telephone +46 31 772 1000

Cover: The SIM IV simulator from VTI.

Typeset in LaTeX
Gothenburg, Sweden 2024

Modeling And Implementation
of a Fully Electric Vehicle Model in Driving Simulator

JINGE GAO
ZIKUN WANG
Department of Mechanics and Maritime Sciences
Division of Vehicle Engineering and Autonomous Systems
Chalmers University of Technology

Abstract

Driving simulators have an important role to play in the automotive industry regarding driver safety and economic benefits, and also carry out some driving behavior studies unsuitable for real roads. Therefore, driving simulators should reflect the real driving experience as much as possible. In order to realize this purpose, it is necessary to develop mathematical car models for driving simulators.

This master's thesis project revises an existing vehicle dynamic model to embody the driving experience of an all-electric vehicle in a driving simulator. The main work of this project is to replace the powertrain system of the original model from an internal combustion engine powertrain to an all-electric vehicle powertrain. This part includes modeling the electric motor, battery, and redistribution of traction force. The features of the all-electric vehicle, such as the one-pedal driving mode, regenerative braking system, and faster response time, are implemented. Also, based on the consideration of regenerative braking, the braking system of the original model was improved in this project so that it can work together with the regenerative braking system. Other parts of the original model were adjusted to fit the relevant parameters of the vehicle used in the experimental tests.

Subsequently, the project conducted real-world driving experiments on a Volvo C40. A series of experiments were carried out on the powertrain system by turning the single pedal mode on and off, as well as hard braking experiments. The experimental data were used to adjust the model's parameters, and the final model was obtained. Through the verification of experimental data, it can be proved that the model carried out in this project can reproduce the real driving experience of an all-electric vehicle in terms of pedal input and speed performance.

In the process of carrying out the above work, a modular structure of the model is realized by revising the original model. The modular design lays the foundation for future work. The process of data collected under the limited experimental environment and the data processing are also made into a guide to assist in future work in the laboratory.

Keywords: Vehicle dynamic model, driving simulator, electric vehicle modeling, powertrain modeling, One Pedal Drive, electric vehicle test, OBD.

Preface

This report presents the outcome of our master's thesis project at the Department of Mechanics and Maritime Sciences at Chalmers University of Technology during the spring of 2024. This thesis was done by a team of two master's students.

With the automotive industry moving towards full electrification, there is a growing demand for dynamic simulation of electric vehicles. Traditional vehicle dynamic models, such as those already available for driving simulators at VTI, are mainly developed based on internal combustion engine vehicles and cannot meet the emerging demand. Therefore, this study aims to create a new dynamic model that specifically addresses the unique characteristics of electric vehicles, such as fast dynamic response, smooth acceleration performance, and driving experience in single-pedal mode.

This thesis details our methodology and steps: First, we used a literature review to learn the basic modeling approach for electric vehicles, and then we simulated a two-motor version of the Volvo C40. By actually operating the model, we collected the necessary data to validate it.

This thesis is structured as follows: the first chapter serves as an introduction and describes the background and objectives of the research. Chapter 2 continues with a detailed literature review showing the structure of the existing model. Chapter 3 discusses the modeling process and ideas for the powertrain and brake models and describes the model's components and operational logic. Chapter 4 explains the experimental equipment and data collection methods. Chapter 5 analyzes the experimental data and adjusts and optimizes the model. The appendix contains the calculation formula of the old model and the complete experimental design.

Acknowledgements

I remember during my interview last December when my future mentors asked if you two had worked together in the past, my answer was "Always." Since enrolling at Chalmers in 2022, Jinge and I have been teaming up on various assignments, projects, and reports. The bond we have developed over the past two years has ultimately manifested itself in our dissertation work. This strong bond has helped us overcome the most difficult moments, and even though we were 8,000 kilometers away from each other, with a six-hour time difference, we did a great job completing our work. I must thank my teammate Jinge for these two years of my master's degree and our lifelong brotherhood.

Many people have been constructive in this journey of writing a dissertation. A big thank you to my supervisor, Smit, who has been a tremendous academic help and has become a valuable friend as time passes. Also, my supervisor, Sogol, has provided us with a lot of academic guidance over the past few months, helping us to stay on the right track and strong in our research. I would also like to express my gratitude to my supervisor, Fredrik, who provided critical corrections to our work and practical solutions when we encountered difficulties during the experiments.

In this thesis project, I would like to give special thanks to Daniel Poveda Pi from Chalmers REVERE Lab for his great support of the experiment. He not only provided invaluable expertise and technical guidance but also gave selfless help and encouragement at all stages of the experiments. Thanks to his support and participation, these ideas could be successfully transformed from conception to practice, and Daniel's contribution not only enhanced the quality of the experiments but also laid a solid foundation for the successful completion of the project. I am deeply fortunate to have had his support and guidance in this project.

Special thanks to Volvo Car for providing the experimental vehicle for this master's thesis project and to Carina Björnsson for her support.

Amicitia enim ex sapientia et amore et moribus bonis et virtute venit.

Zikun Wang, Gothenburg, June 2024

Acknowledgements

It has been a spectacular journey working on this thesis work. The knowledge I have learned, the people I have met, the days of hard work, the nights with rain, and the cozy office have all found their way to the very deep of my memory. There are obstacles on our way, but success finally found its way toward us.

First, I greatly appreciate my teammate Zikun, a cheerful friend who never comes with depression. We worked together throughout our entire master's study, and we are not only a study team but also friends in our spare time. He completed the entire experiment work while I was not able to be here, and beyond doubt, he contributed massively to our project. Even though this thesis work is finished, the bond between us is still unbreakable. Despite the different zones on the planet we are in, the same sun and moon still shine on both of us.

Second, a huge gratitude to our supervisors, Fredrik, Sogol, and Smit. They are the best mentors I have met. They reshaped my academic thoughts and taught me the problem-solving process is more important than the result. Their logical minds and spirit of precision also touched me deeply. I will be glad to work on with them without a second of hesitate.

Finally, a special thanks to REVERE lab and Dianel, thank you for providing real vehicle experiment instruments for this project. The experiment is a memorable experience.

May the force be with you!

Jinge Gao, Gothenburg, June 2024

List of Acronyms

Below is the list of acronyms that have been used throughout this thesis listed in alphabetical order:

ABS	Anti-lock Brake System
AC	Alternating Current
ADAS	Advanced Driver Assistance Systems
BES	Battery Energy Storage
BOS	Break Override System
CAV	Connected and Autonomous Vehicles
CAN	Controller Area Network
COG	Center of Gravity
DER	Distributed Energy Resource
DOF	Degrees of Freedom
EBD	Electric Brake-force Distribution
ECU	Electronic Control Unit
EV	Electric Vehicles
ICE	Internal Combustion Engine
IMU	Inertial measurement unit
OBD	On-Board Diagnostics
OCV	Open Circuit Voltage
OPD	One Pedal Drive
PID	Proportional–Integral–Derivative controller
PMSM	Permanent Magnet Synchronous Motor
RES	Renewable-based Energy Sources
RPM	Revolutions Per Minute
SOC	State of Charge of battery
TCS	Traction Control System
VDM	Vehicle Dynamic Model
VTI	Swedish Road and Transport Research Institute

Nomenclature

Below is the nomenclature of indices, sets, parameters, and variables that have been used throughout this thesis.

Literature Review

v_a	Voltage along the a-axis of the motor.
v_b	Voltage along the b-axis of the motor.
v_c	Voltage along the c-axis of the motor.
ω_e	Electrical angular velocity of the motor.
θ_e	Electrical angular displacement of the motor.
P	Number of mechanical angular displacements of the rotor per one pole of the motor, respectively.
T_m	Electromagnetic torque of the PMSM.
ω_m	Mechanical angular speed of the rotor.
J_m	Moment of inertia of the rotor.
B_m	Viscous friction coefficient of the rotor.
T_L	Load torque applied to the rotor.
i_a, i_b, i_c	Input currents of the PMSM in the abc reference frame.
i_d, i_q, i_0	Transformed currents in the dq0 reference frame.
v_d, v_q	Voltages along the d-axis and q-axis of the motor.
λ_{ds}, λ_{qs}	Flux linkages along the d-axis and q-axis.
L_d, L_q	Inductances along the d-axis and q-axis.
λ_f	Flux linkage due to the rotor magnets.
R_s	Stator winding resistance.
V_{out}	Output voltage of the battery.
V_{OC}	Open-circuit voltage of the battery.
I	Current flowing through the battery.

R_{int}	Internal resistance of the battery.
R_{charge}	Charging resistance of the battery.
$R_{discharge}$	Discharging resistance of the battery.
V_{RC1}, V_{RC2}	Voltage drops across the RC pairs in the battery model.
$\dot{V}_{RC1}$	Rate of change of V_{RC1}.
$\dot{V}_{RC2}$	Rate of change of V_{RC2}.
R_1, C_1, R_2, C_2	Resistances and capacitances in the battery model.
i_d, i_q, i_0	Transformed currents in the dq0 reference frame.
i_a, i_b, i_c	Input currents in the abc reference frame.
θ_e	Electrical angular displacement.
θ_m	Mechanical angular displacement.
T_{max}	Maximum motor output torque.
P	Maximum motor output power.
n	Rotational speed of the motor in RPM.
P_{mec}	Mechanical power output from/applied to the motor.
P_{elec}	Electrical power consumed/generated by the motor.
Pd_{cu}	Upper limit of the pedal range for coasting.
Pd_{cl}	Lower limit of the pedal range for coasting.
τ_r	Regenerative torque .

Electric Vehicle Model

$C_{d,AmpHr}$	Discharged capacity in Ampere-hours.
I	Current flowing through the battery.
N_p	Number of parallel cells in the battery pack.
$C_{AmpHr,0}$	Initial capacity in Ampere-hours.
SOC_0	Initial state of charge.
$C_{AmpHr,Max}$	Maximum capacity in Ampere-hours.
SOC	State of charge.
$w_{motor,ref}$	Reference motor speed.
GR_{tot}	Total gear ratio.
$w_{wheel,left}$ $w_{wheel,right}$	Rotational speeds of the left and right wheels.
w_{motor}	Motor rotational speed.

$V_{nominal}$	Nominal voltage.
V	Actual voltage.
Pd'	A conversion of pedal position to control regenerative brake for OPD mode.
$F_{pedal_{brk}}$	Brake pedal force.
$x_{pedal_{brk}}$	Brake pedal position.
$x_{piston_{brk}}$, $x_{pushrod_{brk}}$	Positions of the brake piston and pushrod.
$l_{gap_{brk}}$	Gap length in the brake system.
F_{out}	Force output from the vacuum booster.
F_d	Force applied by the vacuum booster.
F_{in}	Force input by the brake pushrod.
F_{rs}	Pedal return spring force.
F_{rs_0}	Initial pedal return spring force.
K_{rs}	Elastic coefficient of pedal return spring.
F_{piston}	Force output by the piston.
F_{cs}	Cylinder spring force.
F_{cs_0}	Initial cylinder spring force force.
K_{cs}	Elastic coefficient of cylinder spring.
P_{mc}	Master cylinder pressure.
A_{mc}	Cross-section area of the master cylinder.

Contents

List of Figures

List of Tables

1
Introduction

Globally, there has been a significant shift towards vehicle electrification. This shift has been driven by environmental concerns, technological advances, and government policies to reduce carbon emissions. Countries like Sweden, Norway, China, and the United States have been leaders in adopting electric vehicles (EVs) and have incentivized manufacturers and consumers through various programs[8]. Sweden, as a global pioneer in carbon neutrality, has also made many efforts in this regard. According to the forecast by Mobility Sweden[1], the market share of plug-in passenger cars is expected to reach 35% in 2024, while the market share of electric light trucks will also reach 30%. Governments worldwide are legislating to promote the use of electric vehicles[8], including tax decreases for EV purchasers, greater investment in charging infrastructure, and stricter emission regulations for conventional vehicles. For example, the European Union has set ambitious targets to reduce vehicle emissions, accelerating the transition to electric vehicles.

The road vehicles of the future will not only be electric but also connected and autonomous. CAVs (Connected and Autonomous Vehicles) are expected to enhance road safety, reduce traffic congestion, and improve overall transportation efficiency. Technologies such as 5G connectivity[32], advanced sensors[37], and machine-learning algorithms[25] are efficient for developing these vehicles. Even before fully autonomous vehicles became commonplace, advanced driver assistance systems (ADAS) became standard in many vehicles[28]. These systems, such as automatic emergency braking, lane-keeping assist, and adaptive cruise control, are stepping stones to fully autonomous driving.

The challenge of testing and validating vehicle handling properties has increased with the complexity of their electrification, internet connection, and self-driving level[35]. This challenge will be completed using advanced methods of experiments. A refined vehicle dynamic model will be needed as a basement-level tool for both physical and virtual experiments. Therefore, building a vehicle dynamic model for a driving simulator is a meaningful study.

The thesis project, which will be carried out on the Swedish Road and Transport Research Institute's (VTI) Advanced Driving Simulator software, will provide an existing vehicle dynamics model (VDM) with a powertrain model that can be used to simulate the driving experience of an electric vehicle.

VTI operates as a research institute on several topics in the traffic and transport

fields, including passive safety, road and infrastructure maintenance, tire testing, air quality and noise measurements, and traffic and driving simulation. Of particular note, VTI has over forty years of experience in driving simulation and is an industry leader in conducting simulator experiments and developing simulator technology.

The importance of driving simulators as a tool lies in their ability to help us understand how drivers react under different conditions. Unlike real tests, driving simulator experiments provide better safety and repeatability. For example, some drug[18], alcohol[16], and fatigue tests are dangerous when conducted on real roads[9], whereas driving simulators allow us to test the driver's reactions and the effects of test factors on the driver in a safe environment. To achieve this and to obtain reliable results, driving simulators should provide the driver with as close to a realistic driving experience as possible.

1.1 Driving Simulator

The driving simulator consists of the Dynamic Motion Platform, which simulates the driver's physical sensations of the driving structure.

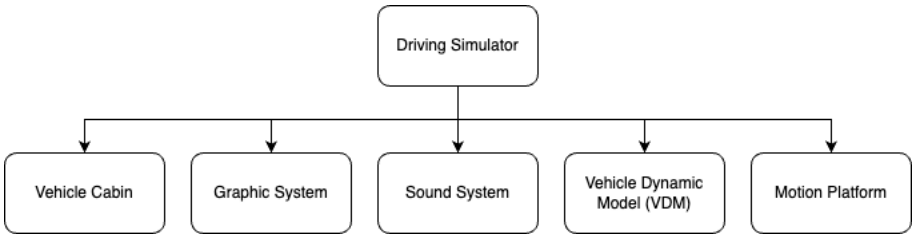

Figure 1.1: Driving Simulator Structure

The car cabin is the primary interface for interaction between the driver and the simulator. VTI SIM IV has a car cabin (from a Volvo XC-60) and a truck cabin (from a Volvo FH 16-700). The cabin provides the driver with an environment close to the real driving experience. This project's model will be used on two motion-based simulators and other mini-simulators.

The graphics system gives the simulator a high-quality driving picture, creating a dynamic visual environment. The sound system comprises several high-quality stereos that reproduce the sound of an actual driving environment. Hearing can have an impact on driver attention and decision-making processes.

The Dynamic Motion Platform hosts the subsystems described above. The Dynamic Motion Platform simulates the driver's physical sensations of driving. The Dynamic Motion Platform provides longitudinal and lateral acceleration for the Sim IV. At the same time, it provides roll, pitch, and yaw angles[15] to provide the driver with a more realistic driving experience.

The VDM developed is an essential component of the simulator system, which this project focuses on. The driver's input signals and road information are fed into the VDM[26], which provides data for the dynamic platform through modeling to reflect the physical sensation of simulated driving in real-time. For electric vehicles, this component should reflect the unique characteristics of electric vehicles, such as instantaneous torque response, battery weight distribution, and regenerative braking systems. Through the development of a unique VDM, the driver can be provided with an exceptional driving experience in EV simulation.

1.2 Goals

How to build accurate vehicle dynamic simulation models of fully electric vehicles?

A vehicle dynamics model that can respond to driver behavior like a real-world vehicle is needed to ensure accuracy. The model should also be able to reflect the unique characteristics of an electric vehicle, such as instantaneous high torque output, regenerative braking, the effect of the weight of the battery on the weight distribution of the entire vehicle, and so on. In addition, the accuracy of the data used in the model is crucial and should have a reliable source.

In this thesis project, the main goal is to modify an existing conventional vehicle dynamics model to a modern pure electric vehicle. The model will be used in all of VTI's driving simulators, which should be able to accurately simulate the vehicle's performance in different environments (e.g., different climates, different road surfaces, different driving styles, etc.) and with varying behaviors of the driver.

This project will get a dynamic model of a car with perfect inputs and outputs. The model is based on a modified VTI model, the simcar14dof model. The modifications to the model are mainly in the replacement of the powertrain module, where the conventional internal combustion engine is replaced by an electric motor. At the same time, the transmission of the electric vehicle is a single transmission, i.e., the clutch and transmission modules of the driveline module will be removed. The new driveline module has a simulation module for the electric motor, which should also be able to give feedback on the dynamic response of the single-pedal mode.

1.3 Clarification of the Issues

Electric Vehicle Handling Characteristics: The handling characteristics of electric vehicles differ from those of conventional vehicles, and these differences stem primarily from the design and powertrain of the electric vehicle. In an electric vehicle, the battery is usually the vehicle's heaviest component, and its location and layout have a decisive impact on the vehicle's center of gravity and weight distribution. Batteries in electric vehicles are usually mounted in the vehicle's chassis[33],

which allows for a lower battery weight distribution and lowers the vehicle's center of gravity.

Instantaneous torque and regenerative braking: The instantaneous torque output and regenerative braking systems of electric vehicles are two key features of their unique driving experience, and they significantly impact the vehicle's acceleration and deceleration behavior. Electric motors can reach maximum torque in a fraction of the time compared to a conventional internal combustion engine. This instantaneous response means an electric vehicle accelerates quickly and smoothly from a standstill. For the driver, this rapid and continuous acceleration is not the same as that of a conventional car[5]. Regenerative braking systems are another unique feature of electric vehicles. When the driver slows down or brakes, the regenerative braking system converts a portion of the kinetic energy into electrical energy fed back into the battery. This not only improves energy efficiency but also changes the deceleration characteristics of the vehicle. This process will differentiate an electric vehicle's dynamic driving experience from a conventional vehicle's[36][22]. The simulation of both can help drivers experience the unique driving experience of electric vehicles in the simulator.

Integration with Existing Models: Since the model for this project was implemented by substituting the power modules of an existing model, there may be some challenges in integrating with the existing model. In addition to replacing the power module, other parameters and designs of the original module that are subject to change should be replaced to ensure the reliability of the new model.

Data Acquisition and Experimental Design: The construction and calibration of this model require the acquisition of data from actual vehicles. This involves experimental design. After acquiring the actual vehicle data, the data should be processed, which puts forward the requirements for data analysis and processing methods.

1.4 Limitations

The tire model is challenging to build, primarily through the magic formula approach. The current magic formula tire model used in the simulator was finished in 2006 due to the EU project VERTEC, and multiple institutions and companies were involved. Most tire companies have produced new generations of tires, especially for electric vehicles[3], and some of the technical specifications of these tires are slightly different from those used in ICE vehicles. It will be hard to modify the tire model, so only the tire size parameters will be updated in this project.
The efficiency of the electric machine and the battery are sensitive to temperature. Considering the effect of temperature on energy consumption is too complex for this project, and the effect will not have a major impact on the simulation results. Therefore, this project chooses to ignore this consideration.

2

Literature Review

Before initiating a modeling and simulation project for all-electric vehicles, a review of previous research not only helps to define the direction of the research but also provides a theoretical basis and technical reference for developing new models. This chapter will first review relevant models, including those presented in previous master's theses and vehicle models developed by VTI.

Subsequently, this chapter will focus on the three core components of this project: the battery, the powertrain, and the braking system. For the battery component, we will review the existing literature on different modeling approaches for batteries, from which we will select a battery modeling scheme that is suitable for the model of this project. Various types of electric motor models will be explored for the powertrain and their application in modeling vehicle dynamics. Finally, a review of the braking system will focus on brake modeling and kinetic energy recovery. This chapter provides the theoretical and practical basis for developing and validating the models for this project in the subsequent chapters.

2.1 Existing Passenger Car Models at VTI

The first vehicle dynamic model is a dynamic model built by Jorge Gómez Fernández for his master's thesis[12], which contains the basic building blocks of the car and was constructed using the Modelica language. Emanuele Obialero then built on that model by refining it and extending it with a vertical dynamic model while improving the performance of the steering system[26]. The second one is a 14DOF model by VTI[17], in Simulink.

2.1.1 Simulink®SimCar 14-DOF model

The Simulink model was built to replace the old FORTRAN-based Vehicle Dynamics Model (VDM)[17], which was challenging to modify. Fig.(2.1) shows the structure of this Simulink model. It comprises seven subsystems: braking, steering, powertrain, wheels, suspension, axles, and chassis.

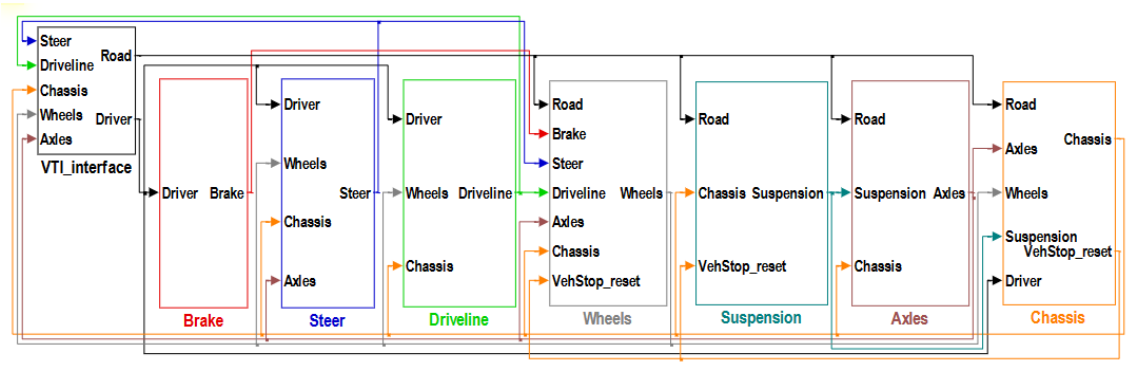

Figure 2.1: Structure of Simulink model Simcar14DOF

The model consists of two parts of inputs. One part of the input is the road information input, which is the road information in the simulated driving space. The other part is the driver's input, which includes the gas pedal signal, clutch signal, steering wheel angle signal, gear signal, brake signal, and whether the ABS function is on or off. The model outputs are the velocity and acceleration of the vehicle in the xy direction and the state of pitch and roll to reflect the vehicle's dynamic response.

2.1.1.1 Powertrain Subsystem

The powertrain model is shown in Fig.(2.2). The inputs to the powertrain model are the gas pedal signal, the gear position signal, the rotational speed of the tires, and the longitudinal speed of the car. This model converts the gear position signal into the total transmission ratio through the gearbox. The clutch signal and the gear position signal are converted into the intermediate parameters of the clutch through the clutch model. Both of these are inputted into the engine model for calculation.

The engine model is shown in Fig.(2.3). In the engine model, the current clutch speed is calculated using the tire speed and total transmission ratio, combined with the speed provided by the engine to get the actual engine speed. This RPM is fed back into the 2D lookup model. In the 2D engine Map diagram model, the torque information is read using the current engine speed and throttle pedal position information to obtain the engine output torque. Integration of this torque divided by the engine's moment of inertia yields the engine's supplied RPM.

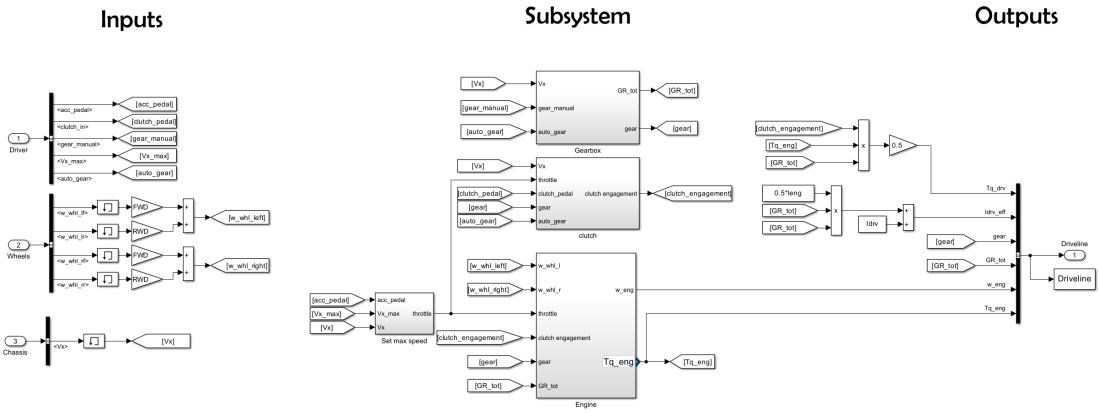

Figure 2.2: Powertrain Subsystem of Simcar14DOF

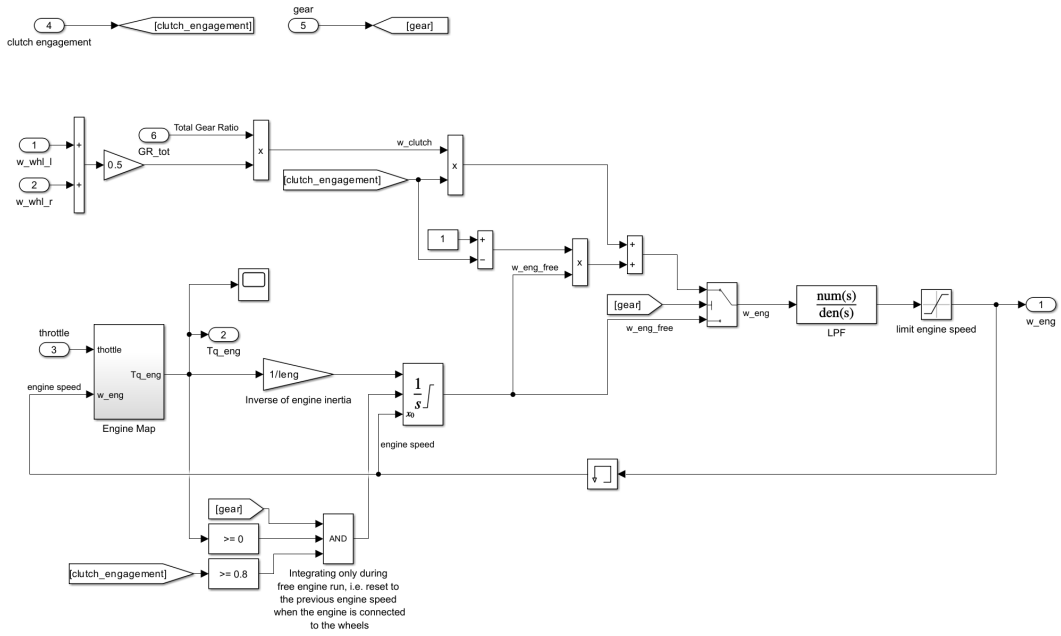

Figure 2.3: ICE Engine Model of Simcar14DOF

2.1.1.2 Brake Subsystem

The brake system is shown in Fig.(2.4). The brake system uses separate hydraulic oil pressures of 4 different brake calipers as inputs and outputs 4 different brake torques on 4 wheel shafts. the brake torques are also controlled by an anti-lock brake system(ABS). ABS detects slip of the different wheels and decides whether to release the brake pressure according to them: if the slip reach certain level, the brake pressure will no longer be transferred to brake torque.

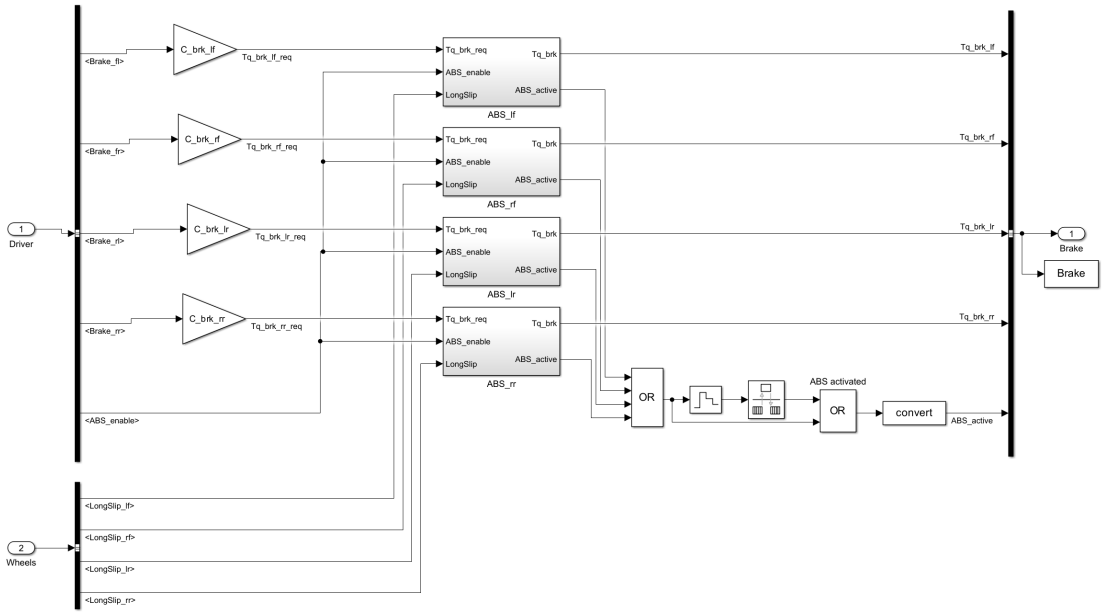

Figure 2.4: Brake Subsystem of Simcar14DOF

2.1.1.3 Wheels Subsystem

This model's tire system consists of four independent wheels, and the dynamics and response of each wheel are calculated separately to ensure the accuracy and practicality of the model. The design of this independent wheel model allows the vehicle to exhibit more realistic behavior under various driving conditions, such as dynamic changes under different road conditions and driving maneuvers.

Each wheel is modeled using a "magic formula" to calculate its longitudinal and lateral forces and rotational speed. This formula describes in detail the complex behavior of tires under various operating conditions. The magic formula can accurately calculate the forces in the longitudinal and transverse directions based on the tire's slips.

The parameters and calculation modules included in the model are derived from the VERTEC project[3], which was dedicated to the study of the dynamic characteristics of tires and provided an exhaustive set of data that includes but is not limited to, longitudinal and transverse slip data of the tires as well as wheel speed. These data are integrated into the model of each wheel and transformed through algorithms into outputs that can be directly applied to the dynamics simulation. The formula for this subsystem can be found in A.1.3.

2.1.1.4 Suspension Subsystem

Inputs to the suspension system include road data from all four tires in the Z-axis direction, reflecting road surface unevenness and other factors affecting vehicle

movement. In addition, the system requires dynamic information from the vehicle chassis. With this combined dynamic information, the suspension system model can accurately calculate the suspension force for each tire in the Z-axis direction. The calculation formulas can be found in A.1.4. These formulas take into account the interaction between the wheels and the road surface, the mass distribution of the vehicle, and the geometric and physical characteristics of the suspension system. By applying these formulas, engineers can simulate the response of the suspension system in real-world driving, resulting in an accurate calculation of the Z-axis direction forces for all four tires. This system only considers one-dimensional force on the suspension system and does not consider impact and movement of contact due to road inclination.

2.1.1.5 Steer Subsystem

The steering system is responsible for converting the steering intention of the driver into the actual movement of the wheels. In this system, the driver's input signals consist mainly of the steering wheel's turning angle. In addition, the system also integrates the lateral and longitudinal forces of the vehicle output from the tire system and the vertical forces of the front wheels provided by the axle system, which are used to simulate the interaction between the tires and the ground during steering.

In the vehicle's steering dynamics model, the front wheels' steering angle is the core parameter, which directly determines the steering radius and path of the vehicle. The steering angle of the front wheels is calculated by the steering wheel angle and the force applied to the tires, and the specific calculation method includes a variety of factors of tire mechanics and steering geometry. the detailed calculation process can be found in the A.1.2. To ensure the accuracy of the results, this calculation is also applied to the rear wheels, but the input steering wheel angle is always 0.0 for the rear wheels.

The steering wheel torque is then calculated by analyzing the torque on each tire. The torque on each tire results from a combination of the friction between the tire and the ground and the torque applied to the wheel as it rotates. After obtaining the torque on each tire, the preliminary steering wheel torque can be calculated by combining the current vehicle speed and the gear ratio of the steering unit. In addition, the steering wheel angle generates an additional torque, and these two parts of the torque need to be added together to obtain the final steering wheel torque. This calculation process is also documented in the A.1.2.

2.1.1.6 Axles Subsystem

The main responsibility of the axle system is to integrate information from multiple systems to simulate forces in the vertical direction of the vehicle. In this system, the axle system first receives the slope information from the road because the slope directly affects the distribution and direction of the forces applied to the vehicle

suspension system. Meanwhile, the force in the Z-axis direction output from the suspension system provides the axle system with information about the vertical forces on the vehicle's four-tire suspension system, while the acceleration of the vehicle in the XY-direction provided by the chassis system reflects the information about the dynamic behavior of the vehicle in the lateral and longitudinal directions. Using these input data, the axle system can calculate the forces on each of the four tires in the vertical direction. The specific calculation method is detailed in A.1.5. In addition, the model precisely models the front and rear axles separately, which is intended to allow for more flexibility in adjusting the parameters of the front and rear axles to suit different driving conditions and vehicle design requirements. By modeling each axle separately, each axle's response characteristics and performance can be adjusted and optimized more accurately.

2.1.1.7 Chassis Subsystem

The input of the chassis subsystem is the tire forces calculated by the wheel subsystem, the z-direction forces calculated by the suspension and axles subsystem, the road data, and the driver's input. The subsystem collects all the longitudinal and lateral forces along with the moments, produces the combined forces and moments on x and y axis. The x and y axis combined forces and moments are then used to calculate linear and angular acceleration in longitudinal and lateral directions, and the accelerations are then integrated into speed, along with the pitch, roll, and yaw behavior. Also, a vehicle stop detection is designed in the subsystem, which detects if the vehicle is stopped or is still on the move. If the vehicle is detected to have stopped, some integrators' outputs in the model will be reset to their initial values. The z-axis forces are also combined, so the vertical movement of the vehicle can be generated.

2.1.2 Modelica Model

Jorge's thesis developed a new vehicle dynamics model[12] from scratch designed for real-time driving simulator applications. His model employs the Modelica® programming language to construct a vehicle dynamics model with ten degrees of freedom, which allows the model to simulate normal driving situations accurately and the vehicle's response under extreme operating conditions, such as emergency crash avoidance. The model validation process included a series of predefined driving maneuvers on a live test track and a series of system tests in a simulator.

Emanuele's paper improves and refines Jorge's vehicle dynamics model for driving simulators[26]. The central goal of the thesis was to make the simulated driving experience more realistic by increasing the model's degrees of freedom and improving the model's vertical dynamics and steering system. This research expanded the model's degrees of freedom from ten to fourteen and specifically added detailed modeling of the vertical dynamics, which includes simulation of the nonlinear properties of the vehicle's suspension system and complex ground interactions. In addition, the thesis

develops a new model of the steering system to provide more accurate and realistic steering feedback. The model was validated by comparing the improved model with dynamic data from actual vehicles and by testing it with multiple drivers in an advanced driving simulator, which showed that the improved model could respond consistently to real-world driving under various driving conditions.

2.1.3 Conclusion

After reviewing the two models, we decided to move on with the simcar14dof model built with Simulink. There are several reasons for choosing it, first, the simcar14dof model is the main passenger car model used in VTI vehicle simulators. Second, comparing to Modelica, we have more experience working with Simulink. Modelica is an equation-based programming language rather than function-based, which is less intuitive for users accustomed to casual modeling approaches. Thus, it is a reasonable approach for this project to modify the current simcar14dof model to a new one and tune it to make it fit a fully electric vehicle.

2.2 Literature Review For New Model

Compared to ICE vehicles, EVs are significantly differentiated by having an electric motor, a battery, and a unique braking system[4] designed to accommodate power recovery. This chapter will conduct a literature review of these three components.

2.2.1 Battery Modeling

The modeling of batteries can take many different forms for different research purposes. For this project, the focus is on the charging and discharging performance of the battery. Therefore, when choosing a modeling approach, the focus should be on how the model is simulated for the charge/discharge performance. For these reasons, the selection of the battery model will not consider the electrochemical model of the battery but will be based on the electrical performance of the battery[30].

2.2.1.1 Ideal Model of Battery

The simplest ideal model of a battery includes only the voltage source itself[13]. The model does not consider the effects of internal resistance, temperature, SoC, etc., on the battery's performance and is used only as a simple voltage source, like Fig.(2.5). The model's parameters include the battery's voltage and capacity. The model will output a constant and stable voltage during operation, and the battery is considered to be empty when the energy consumed reaches its capacity, at which point the output voltage returns to zero. The output voltage is determined by Eq.(2.1).

Figure 2.5: Ideal Model of Battery

$$V_{out} = V_{OC} \tag{2.1}$$

2.2.1.2 Linear Model of Battery

The linear battery model includes a constant voltage source and a constant internal resistance[29]. In this case, the internal resistance reflects the energy loss inside the battery, like Fig. (2.6). The battery's output voltage can be calculated using equation (2.2). The model can reflect the relationship between the energy loss of the battery as the current through the battery varies. However, this model shares a common problem with the ideal battery model discussed in the previous section, i.e., this battery's voltage source is constant. It does not vary with the battery's SoC. This is not consistent with reality. Also, as the operating state of the battery changes, the temperature of the battery changes, and this causes the internal resistance of the battery to change. These factors are not considered in this model.

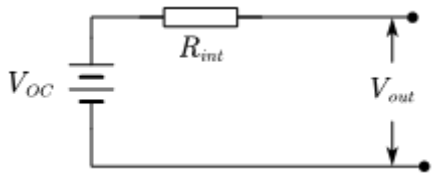

Figure 2.6: Linear Model of Battery

$$V_{out} = V_{OC} - I \cdot R_{int} \tag{2.2}$$

The model applies to scenarios where the SoC of the battery is at an intermediate level and does not change significantly. The SoC and battery temperature will not change significantly shortly for lower charging and discharging rates. It is also essential to consider that the internal resistance of a battery is usually different during the charging and discharging phases. To reflect this difference, the model can be optimized. Fig. (2.7) is the refined battery model. That is, the internal resistance consumption in the charging and discharging phases of the battery is calculated separately using Eq. (2.3) and (2.4).

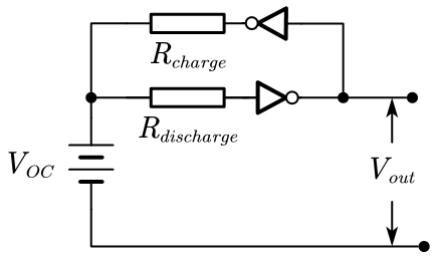

Figure 2.7: Refined Linear Model of Battery

$$\text{Charging: } V_{out} = V_{OC} - I \cdot R_{charge} \tag{2.3}$$

$$\text{Discharging: } V_{out} = V_{OC} - I \cdot R_{discharge} \tag{2.4}$$

2.2.1.3 Thevenin-Based Battery Model

None of the models discussed above simulate the transient response. For this project, the transient response should be modeled to reflect the operating condition of the battery. For this purpose, the Thevenin model is introduced here. The simplest Thevenin model is the first-order Thevenin model[29]. The model contains a voltage source, internal resistance, and a pair of RCs. A pair of RCs is defined as a resistor and a capacitor's parallel circuits (see Fig. (2.8). It can be understood that the model is an addition of a pair of RCs to the model discussed in the previous section to reflect the battery's transient response.

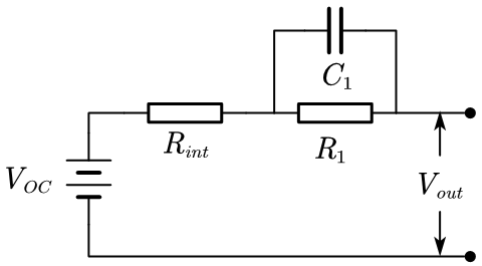

Figure 2.8: 1st Order Thevenin Model

To better reflect the transient response of the battery, a second pair of RCs can be added to this system, i.e., the second-order Thevenin model[29], see Fig. (2.9). The first pair of RCs uses a low time constant to characterize the short-term transient response. The second pair of RCs uses a high time constant to describe the long-term transient response. Meanwhile, this second-order model can correctly reflect the voltage output performance when the current is zero. Eq.(2.5) can describe the output voltage of this model. The first-order derivative of the voltage of the first pair of RCs can be described by Eq.(2.6), and the first-order derivative of the second pair of RCs can be described by Eq.(2.7) To characterize the dynamic response of the

battery better, the effect of the SoC on the voltage source should also be considered.

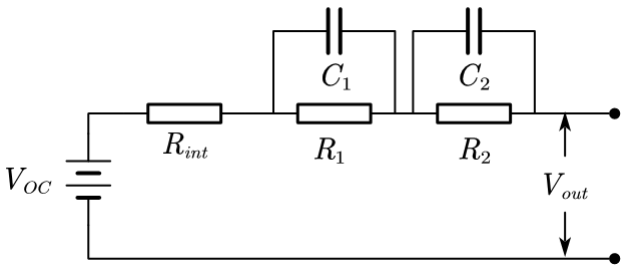

Figure 2.9: 2nd Order Thevenin Model

$$V_{out} = V_{OC} - R_{int} \cdot I - V_{RC1} - V_{RC2} \tag{2.5}$$

$$\dot{V}_{RC1} = -V_{C_1}/R_1 \cdot C_1 + I/C_1 \tag{2.6}$$

$$\dot{V}_{RC2} = -V_{C_2}/R_2 \cdot C_2 + I/C_2 \tag{2.7}$$

2.2.2 Electric Motor Modeling

The most significant difference between conventional and fully electric vehicles is their power source. Electric motors are used in fully electric vehicles, and usually, the motors are 3-phase alternating current (AC) motors because of their fewer mechanical parts, better control ability, and higher efficiency. Significantly, permanent magnet synchronized motors (PMSM) can recover electric energy from kinetic energy. However, the simpler they are mechanically, the more electrically complex they are. Controlling a PMSM to achieve better performance and energy conversion efficiency is always a hot topic.

2.2.2.1 Physical Model of Motors

The usual approach is to model the motor as a whole if its performance is the focus of the study. In this case, the modeling of permanent magnet synchronous motors is more oriented toward detailed analysis. Park et al. discuss integrated modeling and analysis of electric vehicle powertrain dynamics[27], providing insight into the complexities of modeling electrical subsystems alongside conventional vehicle dynamics. Halabi & Tarabsheh, and Zhang et al. focused their research on modeling electric vehicles using Matlab/Simulink to provide a framework for simulating vehicle dynamics[14] and powertrain operation[40] to optimize energy use and system performance.

Meanwhile, for the kinetic energy recovery system unique to electric vehicles, Ji et al. thoroughly investigated the energy recovery mechanism[19], with a particular

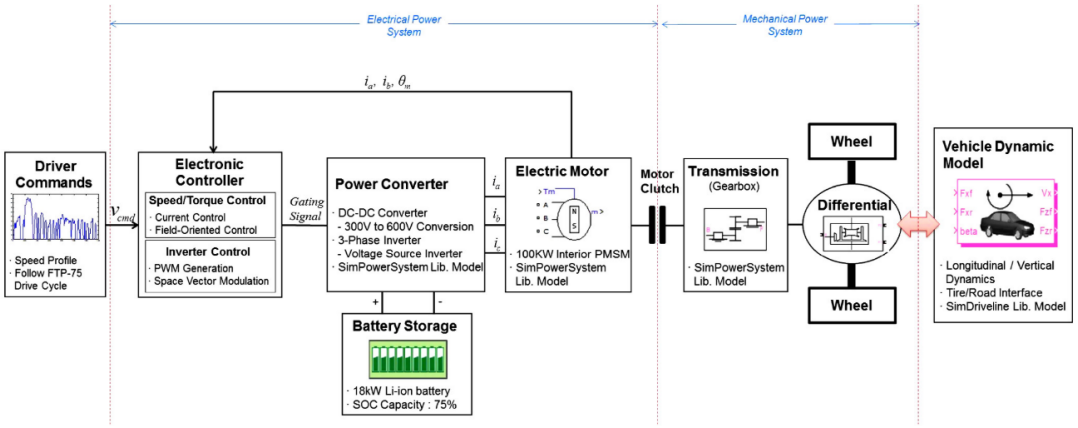

Figure 2.10: Overall Configuration of EV Simulink Model [27]

focus on the regenerative braking system, which improves the energy efficiency of electric vehicles by recovering kinetic energy during the braking phase.

Fig.(2.10) shows the Simulink model[20] developed by Park et al. The model is structured as an all-electric vehicle motor model modeling approach biased toward physical modeling. In this case, the input current of this motor is shown in Eq. (2.8).

$$\begin{bmatrix} i_d \\ i_q \\ i_0 \end{bmatrix} = \frac{2}{3} \begin{bmatrix} \cos\theta_e & \cos\left(\theta_e - \frac{2\pi}{3}\right) & \cos\left(\theta_e + \frac{2\pi}{3}\right) \\ -\sin\theta_e & -\sin\left(\theta_e - \frac{2\pi}{3}\right) & -\sin\left(\theta_e + \frac{2\pi}{3}\right) \\ \frac{1}{\sqrt{2}} & \frac{1}{\sqrt{2}} & \frac{1}{\sqrt{2}} \end{bmatrix} \begin{bmatrix} i_a \\ i_b \\ i_c \end{bmatrix} \tag{2.8}$$

Eq. (2.9) gives the electrical angular displacement of motors.

$$\theta_e = \frac{P}{2}\theta_m = \int \omega_e dt \tag{2.9}$$

The voltage in the direction of Dq can be written as Eq.(2.10), Eq.(2.11) and Eq.(2.12). [24]

$$v_d = R_s i_d + \frac{d\lambda_{ds}}{dt} - \omega_r \lambda_{qs} \tag{2.10}$$

$$v_q = R_s i_q + \frac{d\lambda_{qs}}{dt} + \omega_r \lambda_{ds} \tag{2.11}$$

$$\lambda_{ds} = L_d i_d + \lambda_f, \quad \lambda_{qs} = L_q i_q \tag{2.12}$$

The output torque of PMSM is defined by Eq.(2.13).

$$T_m = \frac{3P}{4}[\lambda_f i_q + (L_d - L_q) i_d i_q] \tag{2.13}$$

The output motor-mechanical dynamics of PMSM is defined by Eq.(2.14).

$$J_m \frac{d\omega_m}{dt} = T_m - T_L - B_m \omega_m \omega_m = \left(\frac{2}{P}\right)\omega_r \tag{2.14}$$

The model simulates the motor control system and the internal structure of a permanent magnet synchronous motor (PMSM) in detail, reproducing the motor's dynamic

performance and response characteristics in real-world operation. This modeling approach, highly dependent on physical properties, poses several challenges. The model's accuracy is highly dependent on the accuracy and completeness of the input parameters. In practice, especially when using prototypes or non-standard equipment, many key motor parameters (e.g., resistance, inductance, flux, etc.) may not be measured in detail or are difficult to obtain. This means that although the model is theoretically accurate, in practice, the simulation results may deviate from the actual motor performance due to inaccurate or missing parameters.

In addition, physical modeling usually requires significant computational resources and complex parameter tuning. In the case of unknown or incomplete parameters, this project needs to estimate these parameters through experiments, reverse engineering, etc. Due to the limitations of the experiments, this project cannot disassemble the motor or analyze it separately. This can lead to inaccurate parameter estimation and affect the final model performance. In this case, the model output may exhibit behavior that does not match the actual operation, thus limiting the model's usefulness. Considering the need to focus on data availability and model adaptability in this project, this modeling approach could not be further explored.

2.2.2.2 Motor Map Approach

The electric motor map is like the external characteristic curve of an internal combustion engine. The motor can carry maximum torque when it works at a certain rotational speed. If the rotational speed is on the x-axis and torque is on the y-axis, this operating condition could be represented by a point in this coordinate. After measuring all the maximum torque at each rotational speed, a curve could be drawn connecting all these operation points, and this curve is called the maximum torque curve. Multiplying this point's horizontal and vertical coordinates gives the power corresponding to that point. Normally, the curve is straight and horizontal as rotational speed increases before the maximum of the maximum output power of this electric motor is reached. Then, the torque drops following the increase of rotational speed, and the curve follows Eq. 2.15. And the curve looks like Fig. 2.11.

$$T_{max} = 9550 \cdot P/n \tag{2.15}$$

For PMSM, the electric motor could also work as a generator, so there will be another curve representing the maximum negative torque when the motor produces the maximum electric power. Furthermore, unlike an ICE, a motor could reverse its rotational direction. So, add all those working conditions together. There are 4 curves in 4 quadrants, like Fig. 2.12.

However, the driving simulator will only be driven forward for our project. Thus, the third and fourth quadrants are not taken into consideration.

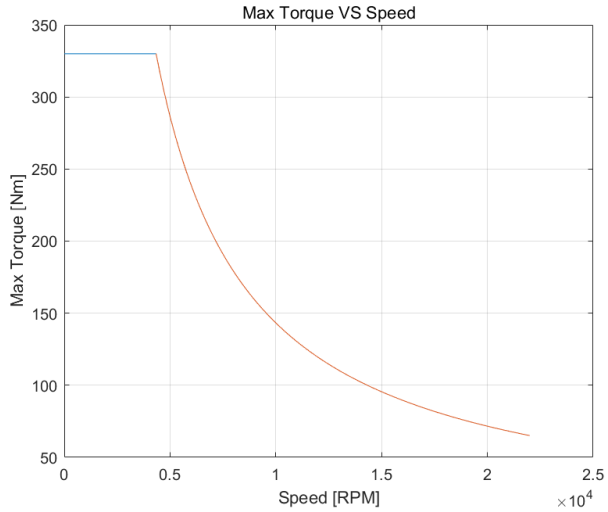

Figure 2.11: Maximum torque curve of an electric motor

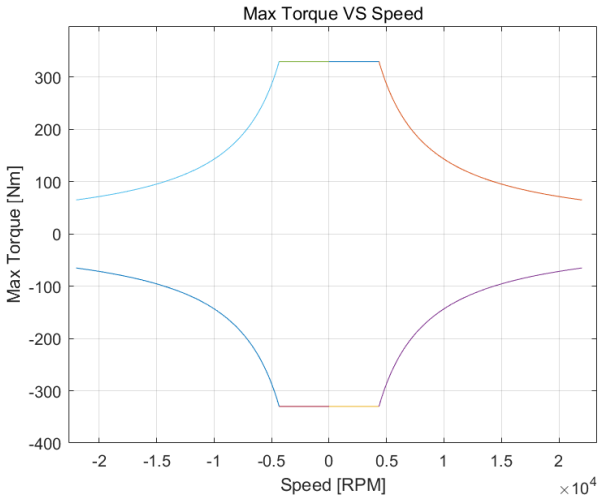

Figure 2.12: Maximum torque curve in 4 quadrants

This coordinate has another dimension if this motor's efficiency is also considered. Each point in the region where the maximum output torque curve and maximum generating torque curve are projected onto the x-axis in this two-dimensional plane corresponds to efficiency. When the PMSM is working as an electric motor, the efficiency corresponds to P_{mec}/P_{elec}; and when it is working as a generator, the efficiency corresponds to P_{elec}/P_{mec}. P_{mec} represents the mechanical power and P_{elec} represents the electrical power. The efficiency of all the points can be connected to form nonintersecting closed curves based on the same values and plotted on a heat map for direct observation. Then, the complete motor map for the first and second quadrants is generated, as shown in Fig. 2.13.

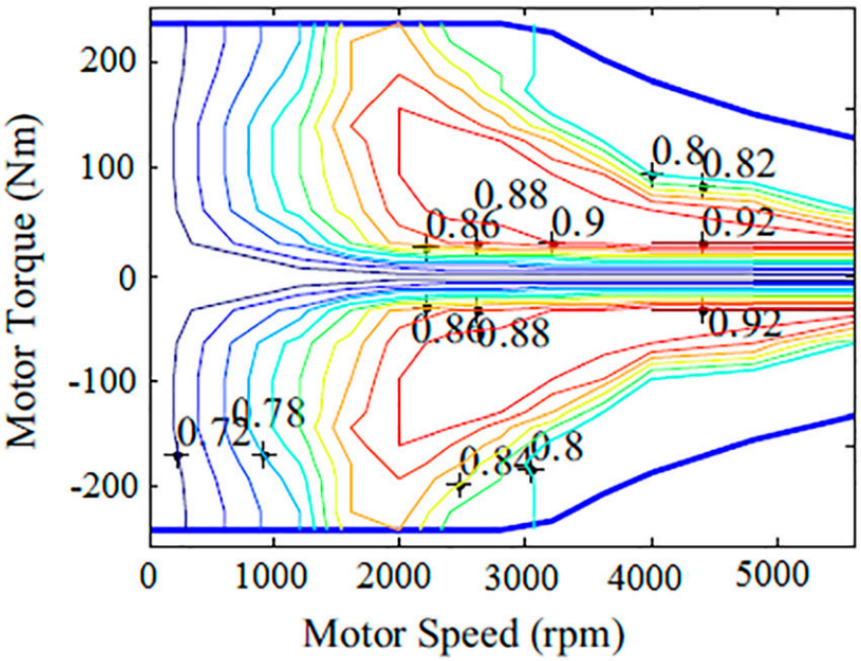

Figure 2.13: A typical motor map with an efficiency of both motor mode and generator mode [19]

2.2.3 OPD Drive Mode Modeling

One pedal drive (OPD) mode is a new feature of fully electric vehicles, where the accelerating pedal can accomplish both accelerating and regenerative braking. It is a feature completely different from the conventional vehicle. Furthermore, this drive mode is equipped within the test vehicle of this project. Thus, the OPD mode is essential for the new vehicle model. Normally, those vehicle companies do not publish the control logic of OPD, so we conducted a literature review on how to design it more academically.

2.2.3.1 Torque Demand Lookup Table Approach

A method to obtain this function is to design a torque demand lookup table(TDLT)[39], also called "fixed pedal map" by us, which is adding another dimension, pedal position, directly to the "motor map," like an internal combustion "engine map" that also includes 3 dimensions representing crankshaft rotational speed, throttle position, and torque output separately. The difference is that the "pedal map" also includes negative torque, which means the vehicle will be driven in regenerative braking mode. When the map is applied, the pedal position and the rotational speed will decide the reference motor torque output together, whereas the rotational speed of the motor is a proportional function of vehicle speed if a fixed gear ratio is applied on the differential or the gearbox. So, the vehicle could define a certain driver's pedal input under a certain speed to accelerate or to brake. An example of the "pedal map" with different drive modes is shown in Fig. 2.14.

The advantages of this modeling approach are obvious. First, this method makes creating several different drive modes easier using the variable "pedal maps"; if the driver wants to switch between drive modes, the simulation model could switch between the maps. Second, the motor map could accurately represent the vehicle's behavior under each certain speed and pedal position if a map is created with rather small spaces of linearly spaced variables. However, the drawbacks still exist, first, the pedal map is bound to only one model of the vehicle, it could not fit if the vehicle parameters are changed, because adjusting the pedal map is creating a new one. Second, creating a pedal map requires tons of tests with different driving speeds and driver's pedal inputs on the test vehicle, through which only the map representing the vehicle's behavior could be accurate. Additionally, this approach could cause endless trouble in tuning the model parameters. Thus, due to the unacceptable drawbacks to us, even if this approach is the most possible one that is used in real-life vehicles as we assumed, we decided to move on to other methods.

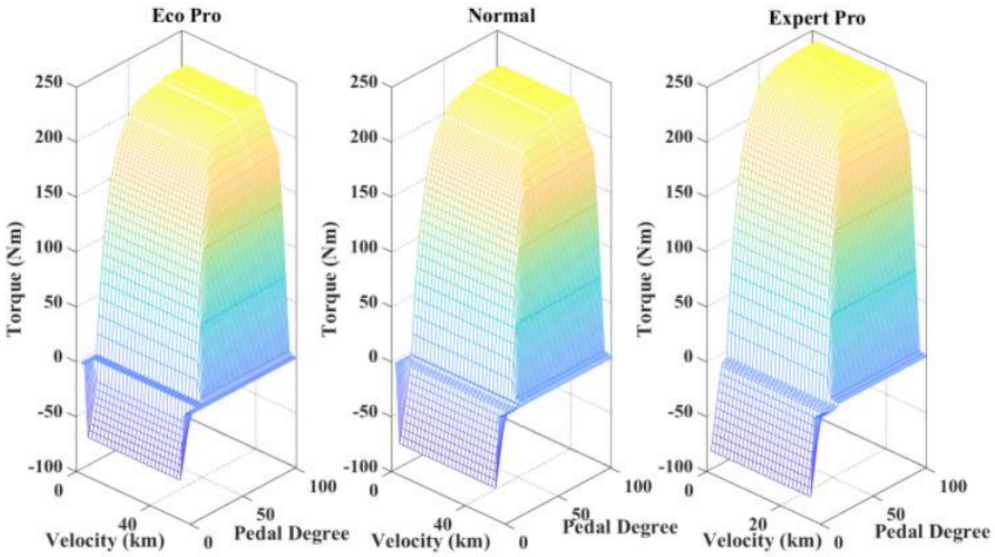

Figure 2.14: An example of a pedal map with different drive modes[39]

2.2.3.2 Sophisticated Pedal Map Approach

From paper[34], we could develop another approach that could also describe variable torque outputs at different velocities and pedal positions. This approach divides the vehicle behavior in OPD mode into three patterns: accelerating, coasting, and regenerating braking. The pedal position is divided into three segments at each longitudinal velocity for a different driving pattern. For example, at 60 km/h, the pedal position segment for coasting is 0.3 to 0.35(for a fully pressed pedal, the position is 1 and 0 for totally released). If the pedal is pressed down to 0.6, the vehicle will accelerate; if the pedal is at 0.32, the vehicle coasts with no mechanic power output from the electric machine; if the pedal is released to 0.05, the vehicle does regenerate brake, and the electric motor gives a negative torque to the axles.

Finding a relationship to divide the pedal position into three segments is essential. If the pedal position is ϕ at the vehicle's maximum speed, the upper limit of the coasting pedal position range could be expressed by Eq. 2.16 & 2.17, where m is a coefficient that could help shape the $Pd_{cu} - V_x$ curve. And to give some headroom for the vehicle to coast within a pedal position range, Pd_{cl} represents the lower limit of the pedal position for coasting, where c_h defines the width of the pedal position range. How the pedal position range for each pattern varies with longitudinal velocity and different coefficient choices could be plotted as Fig. 2.15.

$$Pd_{cu} = \phi\Big(\frac{V_x}{V_{x,max}}\Big)^{\frac{1}{m}} \tag{2.16}$$

$$Pd_{cl} = \phi\Big(\frac{V_x}{V_{x,max}}\Big)^{\frac{1}{m}} - c_h \cdot \Big(\frac{V_x}{V_{x,max}}\Big) \tag{2.17}$$

For the pedal position in regeneration braking, the torque output of the electric motor could be controlled by Eq. 2.18 and 2.19, where a_r, b_r and c_r and ψ are all coefficients to shape the behavior of the regeneration brake response of the pedal. τ_r states the regenerate brake torque given by the electric motor and τ_{rm} is the maximum regenerate brake torque the electric motor could provide. $\frac{d\tau_r}{dPd} = 0$ when $Pd = Pd_{cl}$ is to form a seamless brake response from the pedal. Also, the regenerate torque fraction of the maximum regenerative torque of the motor is controlled by a look-up table, for example, Fig. 2.16.

$$\tau_r = a_r Pd^{\psi} + b_r Pd + c_r \tag{2.18}$$

$$\begin{array}{ll} \tau_r = \tau_{rm} & when Pd = 0 \\ \tau_r = 0 & when Pd = Pd_{cl} \\ \frac{d\tau_r}{dPd} = 0 & when Pd = Pd_{cl} \end{array} \tag{2.19}$$

As for accelerating, the accelerating performance is controlled by the Eq. 2.20, where the Pd_m states a refined pedal range that could "shrink" the full 0-100 pedal-controlled torque output percentage into a shorter pedal movement. It enables the electric motor to output its maximum torque even if the pedal is not pressed fully down, making the vehicle have a fast pedal response at low speeds. τ_a represents the motor torque used to accelerate the vehicle, and τ_{am} is the maximum accelerating torque the motor could provide γ could give the response certain characteristics. The motor's maximum torque is also limited by a look-up table, which is also based on vehicle velocity, preventing the vehicle from losing control at low speed when a large torque is applied to the wheels, which could cause severe tire slip. The examples of look-up tables are shown in Fig. 2.17.

$$\tau_a = \Big(\frac{Pd - Pd_{cu}}{Pd_m - Pd_{cu}}\Big)^{\gamma} \tau_{am} \tag{2.20}$$

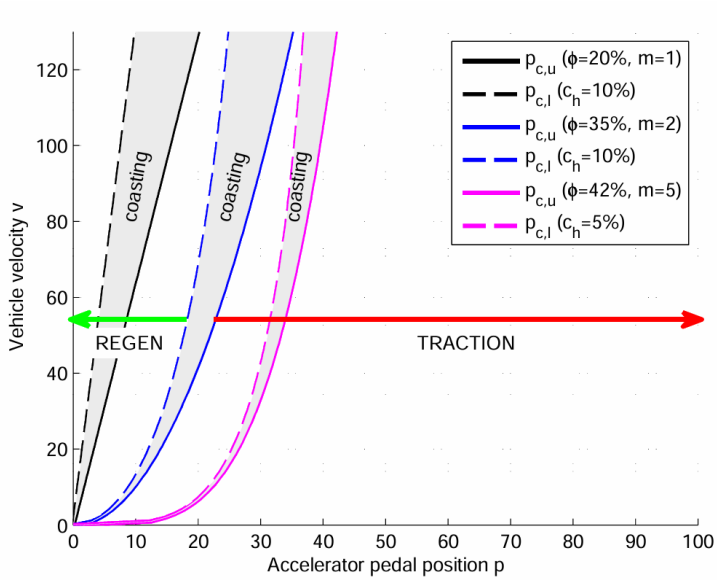

Figure 2.15: Accelerator pedal position divided for each pattern at different velocities and with different coefficient choices[34]

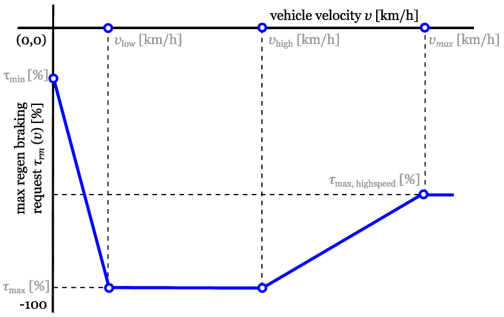

Figure 2.16: Fully released pedal characteristic[34]

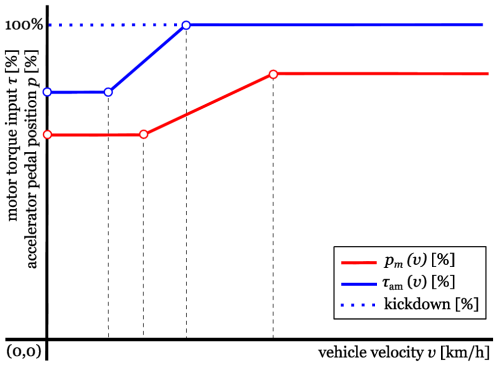

Figure 2.17: Maximum motor torque input and accelerator pedal position characteristics[34]

The drawbacks of this approach is obvious: the vehicle is controlled by the "pedal segments". If the segments are not shaped well, the strange behavior of the vehicle will confuse the driver. However, this approach has fewer parameters, making parameter tuning easier. Thus, the simulation model for this project will follow this approach with some modifications.

2.2.4 Brake Override System Modeling

A particular case needs to be considered for road vehicles: the driver presses the accelerator pedal and the brake pedal simultaneously. In this case, BOS (brake Override System)[21] requires a control logic to keep the traffic safe. The BOS system monitors the inputs from the gas and brake pedals. When it detects that the

brake pedal is activated, even if the gas pedal is pressed simultaneously, the system prioritizes the braking command. It reduces the engine power to help the driver control the vehicle and slow it down as quickly as possible. This technology significantly improves vehicle safety and prevents accidents caused by operator error. For example, Toyota applied this technology in several models to respond to several unintended acceleration incidents of high public concern during 2009-2010[6]. Toyota subsequently released a series of technical reports and white papers on implementing and enhancing BOS technology[31].

2.2.5 Differential Modeling

A Differential allows wheels on both sides to rotate at different speeds while receiving torque from the same drive shaft. Vehicles need to corner smoothly, as the outer wheel travels at a higher rotational speed than the inner one. Differentials can also provide a gear ratio between the input and output shafts[7], usually called the "axle ratio" or "diff ratio." A differential is also needed to differentiate the wheel speed for an electric vehicle that does not use hub motors because the electric motor is also fixed at the center of the front and rear wheels like a conventional vehicle.

Ring-and-pinion differentials have a simpler structure and are widely used in electric vehicles, so this differential will be modeled. It normally consists of axles, a drive gear, an output, planetary gears, a Carrier, an Input gear, and a drive shaft. The structure is illustrated in Fig. 2.18. The carrier is fixed with the drive gear. When the drive shaft transfers torque to it, the carrier rotates, which makes the planetary gears orbit with the carrier. Then, the torque is applied to both output gears, and the axles drive the wheels. When the vehicle is driven directly forward, the planetary gears only orbit without rotating on their axis, giving an equal rotation speed to the wheels on both sides. When the vehicle is cornering, the planetary gears rotate on their axis to let the wheels on both sides rotate at different speeds.

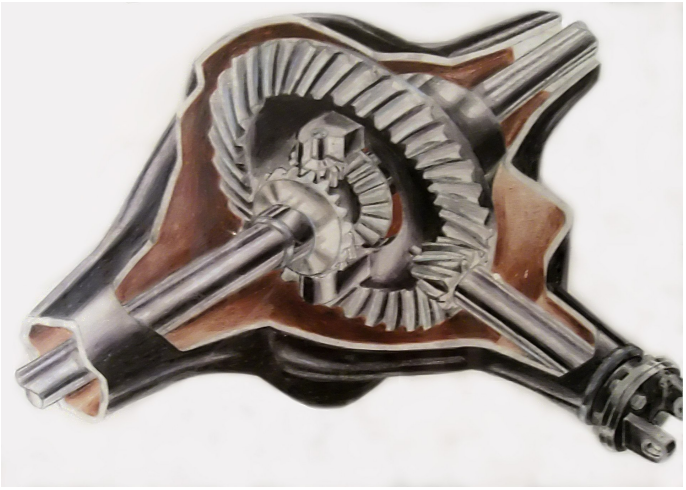

Figure 2.18: Ring-and-pinion differential structure overview[7]

The torque received on both sides are almost equal, however, if the planetary gears are rotating on its own axis, there are frictions between them and the carrier. The friction produces a torque difference M_{diff} between both side axles. Also, if the drive shaft torque is taken into consideration, this effect could be represented by a so-called differential lock coefficient K_{diff}, which equals the torque difference over drive shaft input torque: M_{diff}/M_{drv}. So, if the vehicle turns left, the torque outputs at both axles are derived as Eq. 2.21 & Eq. 2.22. If the vehicle turns right, the torque outputs are as Eq. 2.23 & Eq. 2.24[11] .

$$Tq_l = M_{drv} \cdot \frac{1 + K_{diff}}{2} \tag{2.21}$$

$$Tq_r = M_{drv} \cdot \frac{1 - K_{diff}}{2} \tag{2.22}$$

$$Tq_l = M_{drv} \cdot \frac{1 - K_{diff}}{2} \tag{2.23}$$

$$Tq_r = M_{drv} \cdot \frac{1 + K_{diff}}{2} \tag{2.24}$$

2.2.6 Brake Modeling

The simcar14 model is used first in driving simulator simIII, which has a complete physical hydraulic line for four wheels and can detect the pressure on each brake caliper. The driving simulator simIV and minisim use brake pedal position as the only brake system input, so there is a simple model converting the brake pedal position into brake caliper pressure. In order to provide a more precise description of the working process of hydraulic brake system, we decided to build a new physical brake model.

2.2.6.1 Physical Brake Process Overview

Normally, the brake system of a passenger car consists of several parts: pedal, vacuum booster, main cylinder, 4 brake calipers on 4 wheel rims, and hydraulic hoses to connect them together. There are also ABS(Anti-locked brake system) and EBD(Electric Brake force Distribution) systems to control how a simple press down on the brake pedal will be transferred to different brake torques on separate drive shafts, which will be talked about in the following sections.

When the pedal is pressed down, the force and displacement are transferred to the vacuum booster through a pushrod. Then, the vacuum booster increases the force to a higher level and pushes the primary piston with this force. There are two cylinders in the hydraulic system, the secondary piston is pushed by a spring connected to primary piston. The pushing forces on pistons are turned into the pressure of hydraulic oil in two cylinders that provide the brake pressure in the front wheels'

brake calipers, and for the rear wheels, the pressure is transferred through proportioning valves. Finally, the pressure in hydraulic oil presses the brake pads on the brake discs, turning the pressure into friction that slows the vehicle down. Normally, the process and the hydraulic system layout on a passenger vehicle[10] could be described by Fig. 2.19 and Fig. 2.19.

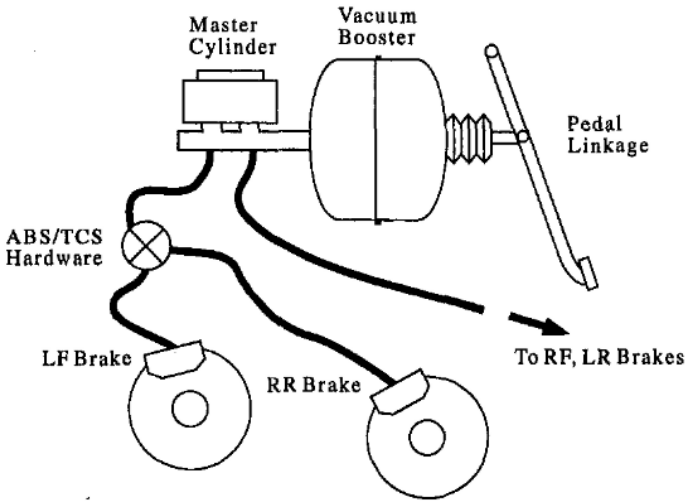

Figure 2.19: Brake system layout[10]

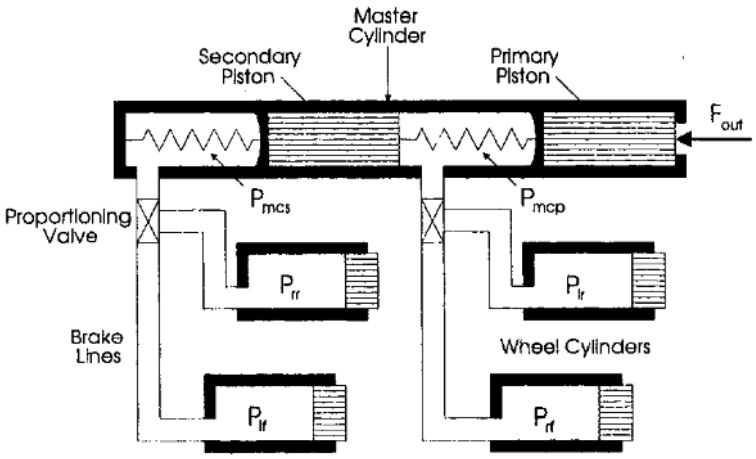

Figure 2.20: Brake hydraulic line layout[10]

2.2.6.2 Brake Force Distribution

Like distributing drive torque, each wheel's brake force must be well distributed to achieve the best performance. In a traditional four-wheel vehicle brake system layout, the left front wheel and the right rear wheel share one hydraulic line that connects to one cylinder, while the right front wheel and left rear wheel share another independent hydraulic line. This is designed to prevent the vehicle from maintaining

braking capacity on the left and right sides and front and rear wheels if one of the hydraulic lines fails. Each line has a proportioning valve to control the pressure of the hydraulic line to each rear wheel caliper.

Traditionally, the brake distribution factor, the gain value of the proportioning valve, is a fixed constant. The value requires that under any brake strength$z$ ($z = a_x/g$), the brake pedal is pressed down. The rear wheels must lock up after the front wheels. If the rear wheels lock up first, the vehicle will lose control easily with a tiny steering wheel angle change, which is extremely dangerous. So, it leads to two solutions: distribute the brake force on each wheel more perfectly and implement ABS. Now, combining them both has become very ordinary.

No matter how we apply forces and torques on axles or on rims, all of them are transferred to the interface between the tire and road surface, which is limited by the attachment condition. The condition is determined by the road, the tire, and the vertical load on the wheel. In sunny weather city drive conditions (dry tarmac road surface and rubber tires), which the project focuses on, the road and tire factor on each wheel is the same. The only influence is vertical load. A larger wheel load can provide better attachment so the tire can withstand larger longitudinal force before it slips. So, it is reasonable to distribute higher brake force on wheels with larger vertical loads to use tire attachment fully[2].

So, an ideal distribution ratio between front and rear wheels, $K_{brk,ideal}$ could be defined. If we have a mechanical analysis on a driving vehicle with acceleration on a slope, it looks like Fig. 2.21. If aerodynamic drag and rolling resistance are neglected, the vertical force on the front and rear wheels are described as Eq. 2.25 & 2.26.

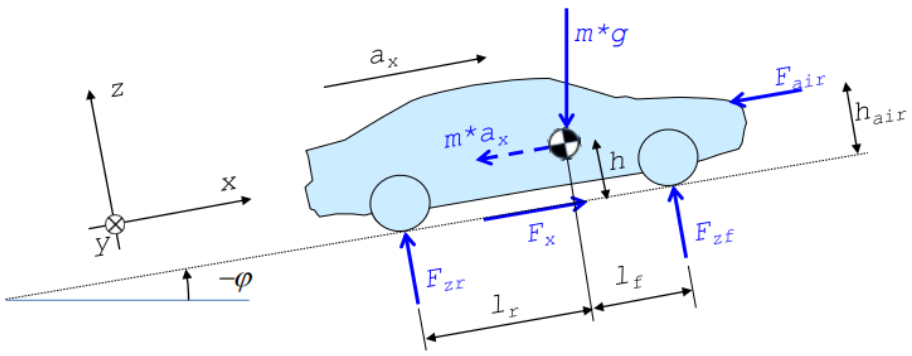

Figure 2.21: Mechanical analysis on a driving vehicle with acceleration on a slope[2]

$$F_{zf} = m \cdot \left(g \cdot \frac{l_r cos(\varphi) + h_{CG} sin(\varphi)}{l_f + l_r} - a_x \cdot \frac{h_{CG}}{l_f + l_r} \right) \tag{2.25}$$

$$F_{zr} = m \cdot \Big(g \cdot \frac{l_f cos(\varphi) - h_{CG} sin(\varphi)}{l_f + l_r} + a_x \cdot \frac{h_{CG}}{l_f + l_r}\Big) \tag{2.26}$$

The front and rear wheel load fraction will be like Eq. 2.27, and The ideal brake force distribution ratio follows this fraction.

$$F_{zf}/F_{zr} = \frac{l_r + h\Big(tan(\varphi) - \frac{a_x}{gcos(\varphi)}\Big)}{l_f - h\Big(tan(\varphi) - \frac{a_x}{gcos(\varphi)}\Big)} = K_{brk,ideal} \tag{2.27}$$

3

Electric Vehicle Model

The new electric vehicle model is created based on the simcar14dof model with Simulink. In this model, the old ICE powertrain model is replaced with a dual-motor powertrain model, which is equipped with many new features such as torque distribution, regen brake, one pedal drive, brake override, and traction control. Also, the battery model is added to the new powertrain model. The old brake system is modified to suit only one input - brake pedal position and suit the energy regeneration feature of the new powertrain model.

3.1 Powertrain Model

The most significant difference between all-electric and conventional fuel vehicles is that they use a completely different powertrain. The powertrain of a full-electric vehicle is driven by an electric motor rather than the internal combustion engine found in conventional vehicles. This fundamental change means that the powertrain must be replaced in the simulator's original model to accurately represent the performance and characteristics of an all-electric vehicle during vehicle simulation. Through this substitution, the simulation model can simulate the actual operation of an electric vehicle, including acceleration performance, energy consumption, and battery management, for simulation purposes.

3.1.1 Model for Battery

The battery system of the model is modeled using the 2nd order Thevenin Model, and the Fig.(3.1) shows the complete picture of the battery model. Firstly, the following Eq.(3.1) calculates the battery's remaining power in Ampere Hours.

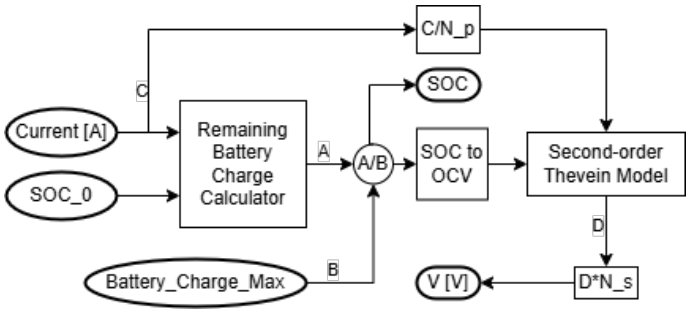

Figure 3.1: Overview of Battery Model

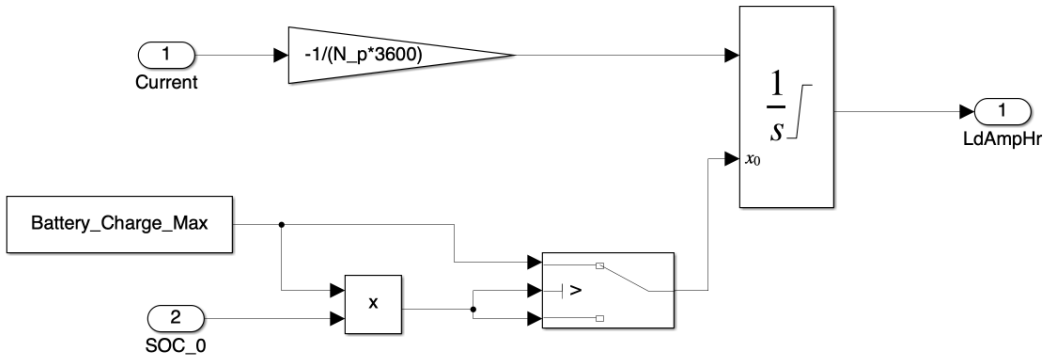

Figure 3.2: Residual Charge of batteries calculation model

$$C_{d,AmpHr} = -1 \cdot \int \frac{I}{N_p \times 3600}\, dt \tag{3.1}$$

As shown in Fig.(3.2), where N_p represents the number of parallel cells and $C_{d,AmpHr}$represents the remaining charge of the battery, this integral allows for setting the initial value. Suppose the starting SOC value is set outside the model, and the maximum battery charge is also set in the model setup. In that case, the initial residual charge in the batteries can be calculated using Eq.(3.2).

$$C_{AmpHr,0} = SOC_0 \cdot C_{AmpHr,Max} \tag{3.2}$$

After obtaining the residual battery charge in the above way, the current SOC of the battery can be calculated using Eq.(3.3). Since there is a correspondence between the battery output voltage and the battery SOC, the second module uses the existing battery OCV data for fitting[38]. This OCV-SOC relationship fitting curve is shown in Fig.(3.3).

$$SOC = \frac{C_{d,AmpHr}}{C_{AmpHr,Max}} \tag{3.3}$$

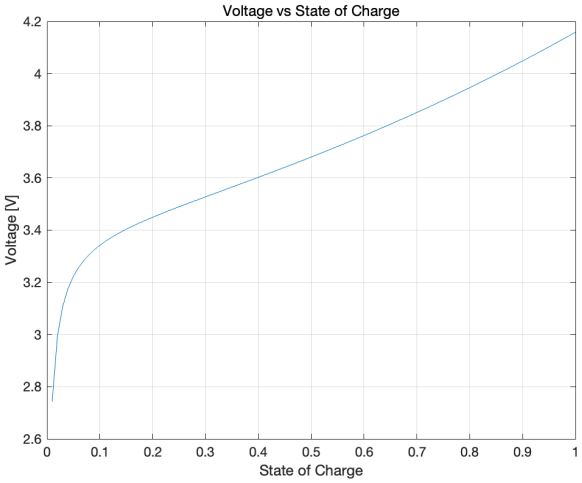

Figure 3.3: SOC-OCV Curve

After obtaining the OCV, the battery's output voltage can be modeled using the 2nd-order Thevenin Model. That is, Eq.(2.5), (2.6) and (2.7). Also, to protect the battery, the model will terminate the overall simulation process when the battery SOC is less than 10% and continuously discharged.

3.1.2 Model for Motor

The role of the electric motor is regarded as a central element in an all-electric vehicle powertrain modeling project. The aim of the electric motor model is to transfer the driver's accelerating pedal input into the drive torque and power of the motor. The electric motor not only directly determines the car's power output but also affects the energy efficiency ratio and range, making it a critical component that influences the performance of an electric vehicle. The Volvo C40 Recharge Twin version was chosen as the test model for this project. This model adopts an advanced dual-motor four-wheel drive system, providing higher power output and better driving stability, making it an ideal candidate for studying the powertrain of all-electric vehicles.

To provide comprehensive coverage of different types of electric vehicles and to meet a wide range of simulation and analysis needs, this project not only provides in-depth modeling of the two-motor system of the Volvo C40 Recharge Twin version but also simulates the powertrain of a single-motor all-electric vehicle. Such a dual-track modeling strategy ensures that the study can be applied to various available EV configurations, ranging from single-motor compact EVs to high-performance EVs equipped with multi-motor powertrains.

3.1.2.1 Single Motor Model

First, modeling a single-motor model of an all-electric vehicle powertrain is carried out, a standard configuration in electric vehicle powertrain design. In this model,

the electric motor not only serves as the vehicle's primary power source but also assumes the function of energy recovery by feeding power back to the battery through the inverter during braking. The structure of the model is shown in Fig. (3.4), covering the critical components of the EV powertrain and their interactions. The inputs and outputs of the model are shown in table (3.1).

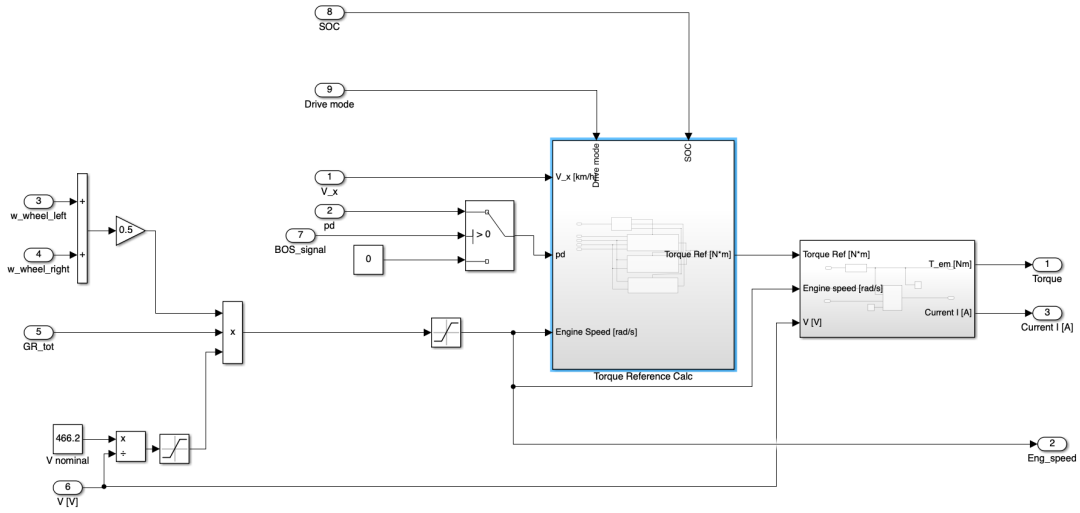

Figure 3.4: Single Motor Model Overview

Table 3.1: Input and Output Variables of the Electric Vehicle Powertrain Model

Variables Name	Descriptions	Unit
	Input	
w_wheel_left	Speed of the left wheel	rad/s
w_wheel_right	Speed of the right wheel	rad/s
GR_tot	The total gear ratio	-
V	Voltage input of motor	V
SOC	State of charge of battery	%
Drive mode	Different driving mode of the vehicle	-
V_x	Vehicle longitudinal speed	m/s
pd	Acceleration pedal position	%
BOS_signal	Brake override system control signal	-
	Output	
Torque	Motor output torque	Nm
Current I	Motor current	A
Eng_speed	Motor speed	rad/s

First, the ideal motor speed can be calculated from the wheel speed and the total transmission ratio by using Eq .(3.4). This ideal rotational speed represents the

speed at which the motor will operate when there is no influence of any external factors (e.g., motor efficiency, battery status, etc.). The ideal motor speed is based on a direct relationship between the wheel speed and the total transmission ratio. The wheel speed is derived from the vehicle tire model, while the total transmission ratio is part of the vehicle model parameters.

$$w_{motor,ref} = GR_{tot} \cdot \frac{w_{wheel,left} + w_{wheel,right}}{2} \tag{3.4}$$

Next, the relationship between the motor supply voltage and the calibrated (or rated) voltage needs to be considered to get the actual motor speed. The actual motor speed will be affected by the battery voltage level because the voltage level is directly related to the amount of power the motor can deliver. Therefore, by using the ratio of the actual voltage to the calibrated voltage as a scaling factor, the ideal speed as $w_{motor,ref}$, can be adjusted to reflect the performance of the motor under actual operating conditions. This step can be calculated by Eq.(3.5). The actual voltage is obtained from the vehicle's battery model, while the calibration voltage is the standard operating voltage set during motor design.

$$w_{motor} = w_{motor,ref} \cdot \frac{V_{nominal}}{V} \tag{3.5}$$

To comprehensively simulate and evaluate the performance of the all-electric vehicle under different driving conditions, three driving mode switching structures were specially designed to reflect the effects of different driving preferences and road conditions on vehicle performance. These driving modes are single pedal mode, normal driving mode with a regenerative braking system, and normal driving mode without a regenerative braking system. Each mode is designed to simulate the performance of an electric vehicle in real-world driving through a unique control strategy. The switching structure of these three driving modes is shown in Fig.(3.5).

To represent the performance of the electric motor, a motor map is essential for modeling all the drive modes. The motor map could be modeled with two parameters: the maximum power output and the maximum torque output from the motor, and those two parameters are rather easy to access for a mass-produced vehicle. With those two parameters the motor could be modeled as a 2-D look-up table with the method in section 2.2.2.2.
In one-pedal mode, the driver controls acceleration and deceleration with a single pedal. Pressing the pedal down indicates acceleration, and releasing the pedal automatically activates the power recovery system for deceleration. In this mode, the vehicle's power recovery efficiency is maximized, as almost all deceleration is accompanied by energy recovery. In Normal Driving Mode with power recovery, the vehicle's acceleration and deceleration are controlled by two different pedals, similar to the operation of a conventional fuel vehicle. However, unlike conventional fuel vehicles, when the driver presses the brake pedal, the power recovery system is activated, recovering a portion of the kinetic energy to be converted into electrical energy and stored in the battery. Power recovery in this mode is less efficient than in

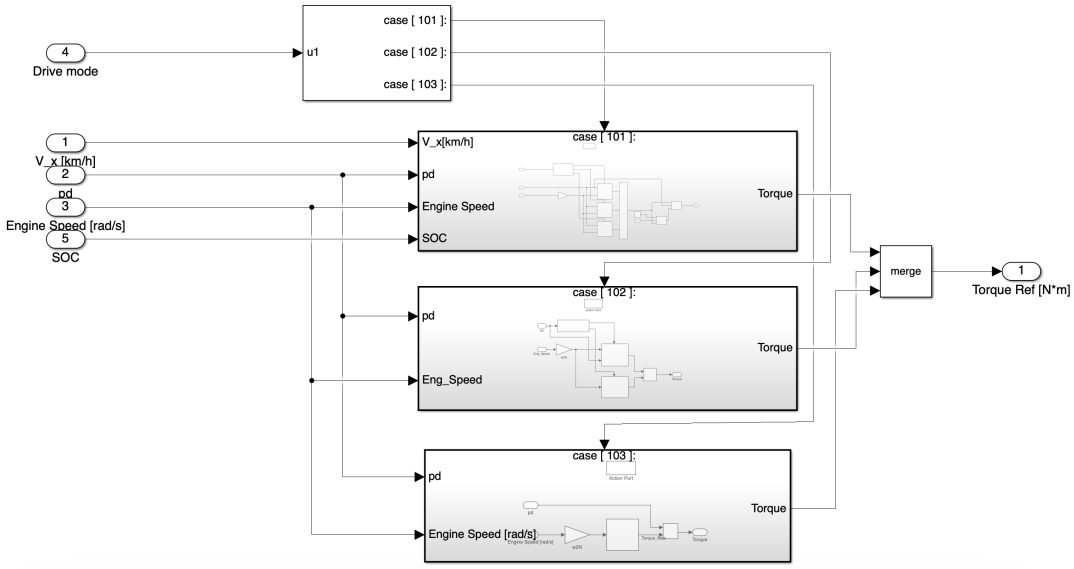

Figure 3.5: Overview of Different Drive Mode

one-pedal mode, but provides a more traditional driving experience. Normal Driving Mode without Power Recovery simulates the driving performance of an electric vehicle with no energy recovery at all. Acceleration and deceleration are controlled entirely by the accelerator and brake pedals, and releasing the accelerator pedal does not trigger power recovery.

The OPD mode is built based on the approach mentioned in 2.2.3.2, but some little modifications are applied. The motor map used here is defined by the motor on the experiment vehicle. The maximum torque output of that motor is 330Nm, the maximum power of that motor is 150KW. By using the same method used in 2.2.3.2, the motor map can be defined. The motor map is shown in the Fig.(3.6).

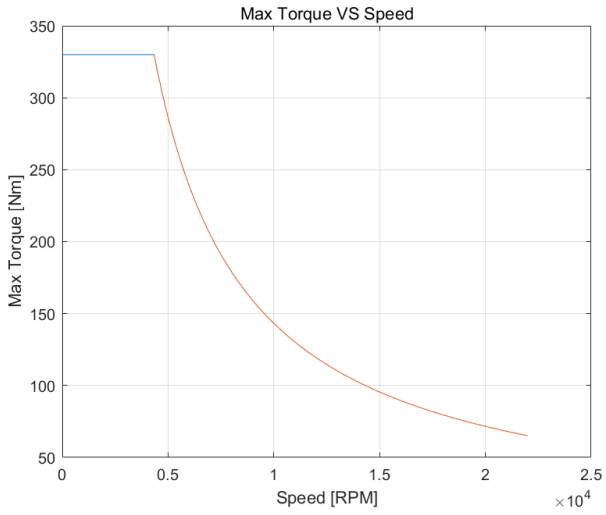

Figure 3.6: Motor Map for 330Nm 150KW Motor

The pedal segmentation of three operating conditions are divided with the same method and equation as Eq. 2.16 & 2.17.For the coasting operation, the reference torque output of the electric motor is 0 and the vehicle travels with its own inertia. For the accelerating operation, how the vehicle accelerates depends on how the accelerator pedal is pressed, the relationship is represented in Eq. 2.20. As it is mentioned, there is a reflection relation in order to slightly adjust the pedal response. The acceleration section of the model is shown in Fig. 3.7. The regenerative braking mode is modified to lower the difficulty of implementing the pedal-torque relationship to the Simulink model. The relationship is shown in Eq. 3.6. In this equation, Pd' represents a new factor that is used to calculate how much the regenerative brake torque, depending on the driver's will, is released. Then Pd' will multiply the maximum torque defined by the motor map mentioned in 2.2.2.2, and then multiply the look-up table that determines how the maximum regenerative torque varies with vehicle speed, as shown in Fig. 3.8. Then, the control logic of torque reference from pedal input is formed. The modeling of OPD mode is shown in Fig. 3.9.

$$Pd' = \Big(\frac{Pd_{cl} - Pd}{Pd_{cl}}\Big)^{m_{pd,reg}} \tag{3.6}$$

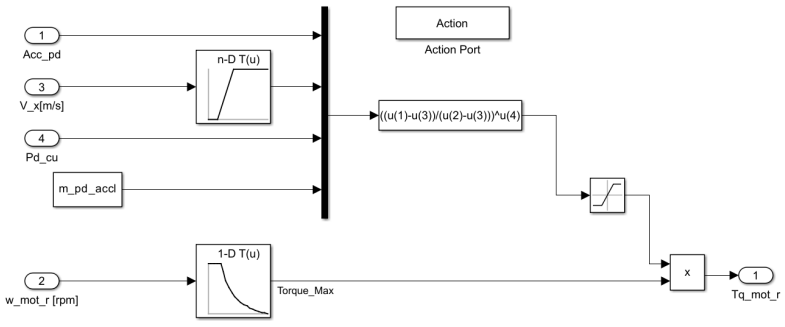

Figure 3.7: Model of accelerating with OPD mode

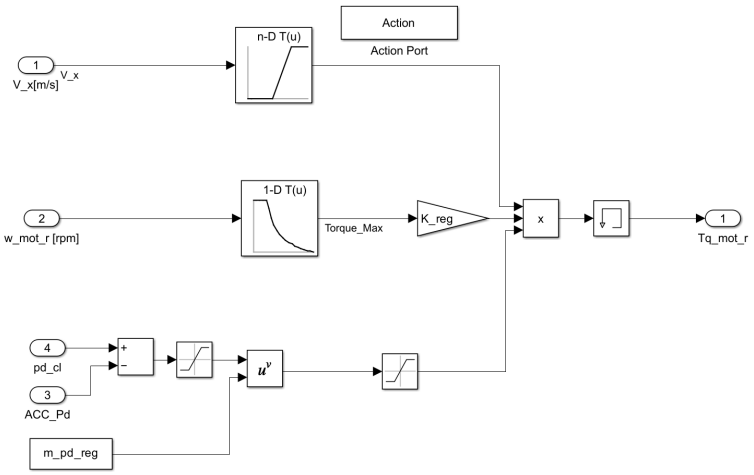

Figure 3.8: Model of regenerative braking with OPD mode

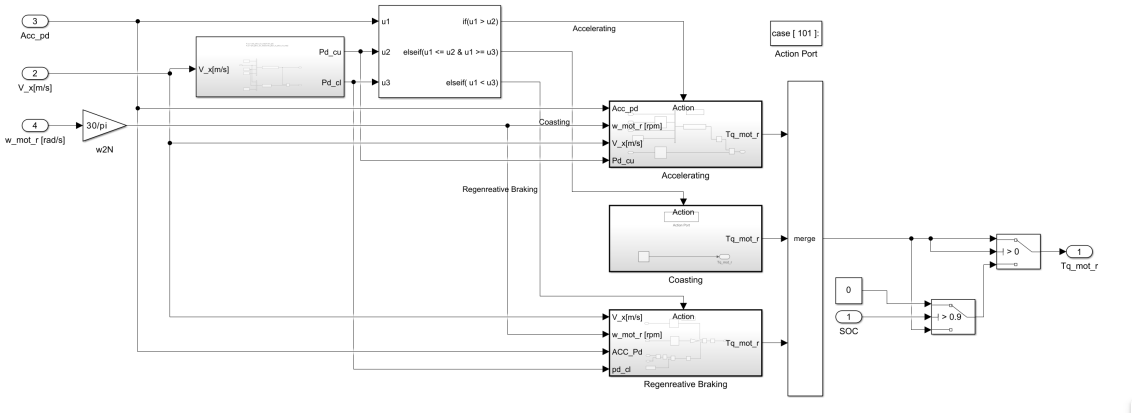

Figure 3.9: Model of OPD mode

The second mode is the conventional driving mode with brake power regeneration system when OPD is not activated. The structure of this driving mode is shown in Fig.(3.10), which allows the efficient utilization of the energy regenerated during braking without driving with a single pedal.

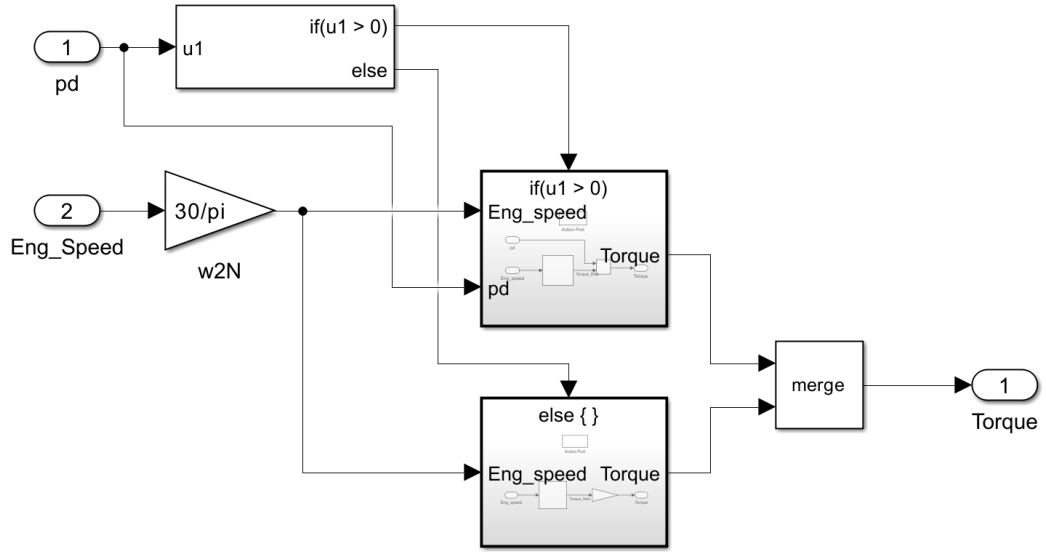

Figure 3.10: Conventional Driving Mode with Brake Power Regeneration

In this mode, the motor's operation is divided into two distinct phases: acceleration and recovery. When the accelerator pedal is depressed, the motor dynamically outputs power according to the input pedal position. The output torque is calculated in the same way as in the single-pedal driving mode, i.e. based on the current speed of the motor and the pedal position, the corresponding maximum torque value is found from the speed-torque graph and adjusted according to the pedal position to obtain the actual output torque.

When the accelerator pedal is fully lifted, the vehicle coasts like how a conventional vehicle does, and when the brake pedal is depressed, the system seamlessly transitions to the energy recovery phase, as shown in Fig.(3.11). In this phase, the motor's control system intelligently finds the appropriate torque value based on the current motor speed through the speed torque graph. This torque value is then multiplied by a preset kinetic energy recovery scaling factor to calculate the kinetic energy recovery braking torque. This mode ensures that even in regular driving mode, the vehicle's deceleration is efficiently converted into a charge for the battery.

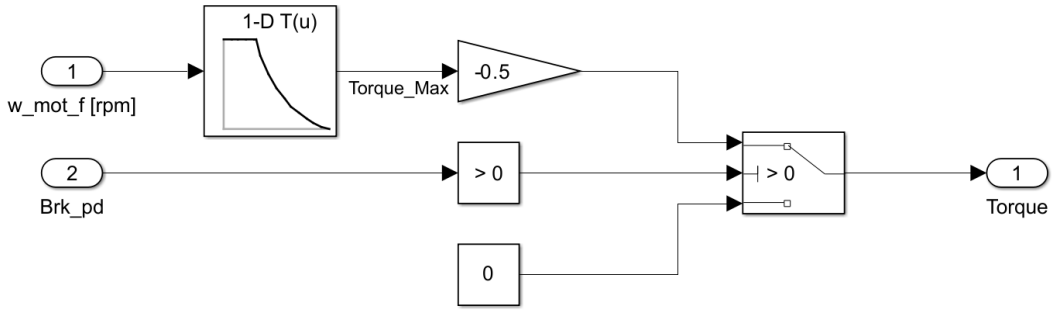

Figure 3.11: Power Regeneration System

In the last mode, OPD is not switched on, and neither is the energy regeneration system. In this mode, the driving experience is more similar to that of a conventional internal combustion engine. When there is input from the pedal, the torque output is calculated in the same way as the above. However, when there is no input from the pedal, the model does not output torque.

3.1.2.2 Dual Motor Model

Since the vehicle on which the model is based is a Volvo C40 Recharge twin motor model, there are apparently two motors in the vehicle, so two motors in total will be included in this Simulink model. It is easy to put them in the model. The key is to arrange their torque output. When the vehicle is accelerating or braking, due to the distance between the vehicle COG and the straight line connecting the front and rear wheel centers, a moment is generated. To compensate for this moment, the wheel loads of the front and rear wheels will be transferred (if all the wheels remain attached to the road surface). It is the attachment condition at the tire-road interface that influences how large a wheel can bear the power output from the shaft. It is reasonable to distribute more torque on the front or rear wheels with better attachment conditions, i.e., larger wheel loads.

From the axles subsystem, the wheel loads of 4 wheels are calculated separately. Then from that the ratio between front wheel load and rear wheel load could be calculated out.

For building the model, the single motor model in the previous text is used for the rear motor. Based on the reference torque generated by the rear motor, the front motor is controlled by the ratio between the front wheel load and the rear wheel load. Since the front motor cannot output more than the torque it could provide, a torque limiter has been implemented. The limiter calculates the maximum torque the front motor could provide at certain rotational speed and limit the ratio-calculated torque does not go beyond that value.

However, this torque control method is to make the best use of vehicle traction force.

It is not for brutal acceleration. It is proven in model tuning that when the front and rear motors both output their maximum torque, the vehicle will have the largest acceleration. So the strategy of acceleration pedal will be: try to make the front motor produce as much torque as the rear motor, if the front is not able to achieve that, output its maximum torque. So, two different dual-motor systems are built: one has a dynamic torque distribution, and the other has a fixed torque distribution ratio. The later one is what is applied in the final edition of the VDM built in our thesis work. The Simulink model for the dual motor is shown in Fig. 3.12.

Also, the torque output from the electric motor is controlled by Traction control system, which will be in the following section.

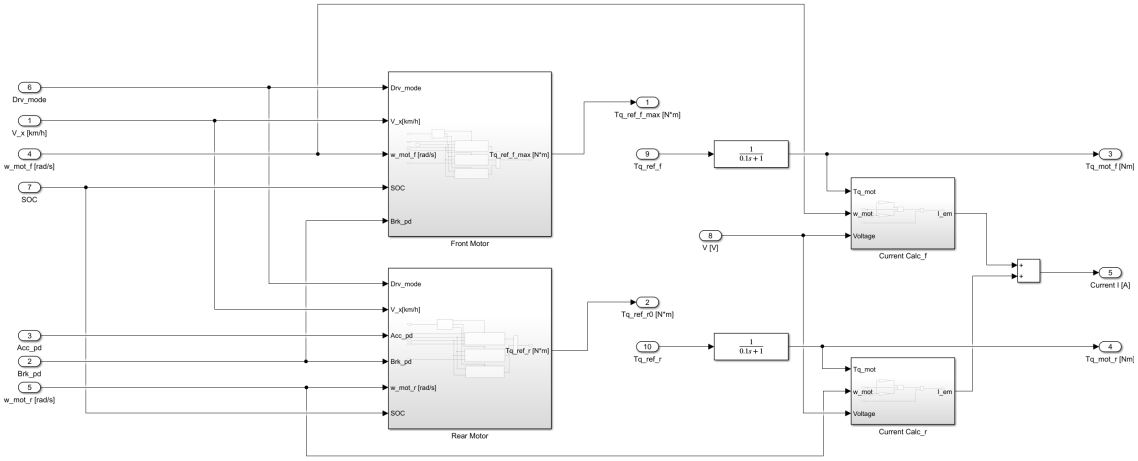

Figure 3.12: Overview of dual motor model

3.1.3 Traction Control System

Traction control system (TCS) is a vehicle safety feature designed to prevent loss of traction of the driven wheels during acceleration, particularly on slippery or uneven road surfaces. It works by detecting when one or more of the wheels is spinning faster than the others, indicating a loss of traction, and then applying individual wheel braking and/or reducing engine power to prevent wheel slip and regain traction. For this model, TCS is designed to detect only the longitudinal wheel positive slip ($\omega_{wheel} \cdot R_{wheel} > V_x$, usually occurs when accelerating), because negative slip ($\omega_{wheel} \cdot R_{wheel} < V_x$, usually occurs when braking) is controlled by ABS in the brake system As for the regenerative brake, it seldom reaches the slip limit of the tires, so the negative slip caused by regenerative brake is not considered in this model.

The basic frame of TCS is a PID controller. The error is the value of the real wheel slip exceeds the defined slip limit. Then, the torque reference is calculated by a single motor model from the pedal position minus the PID-controlled error, and the new torque reference after TCS is generated.

The torque reference bypass is also designed to achieve the "TCS on-off" function that could be controlled on the driver's control panel.

The traction control with variable torque distribution model is shown in Fig. 3.13.

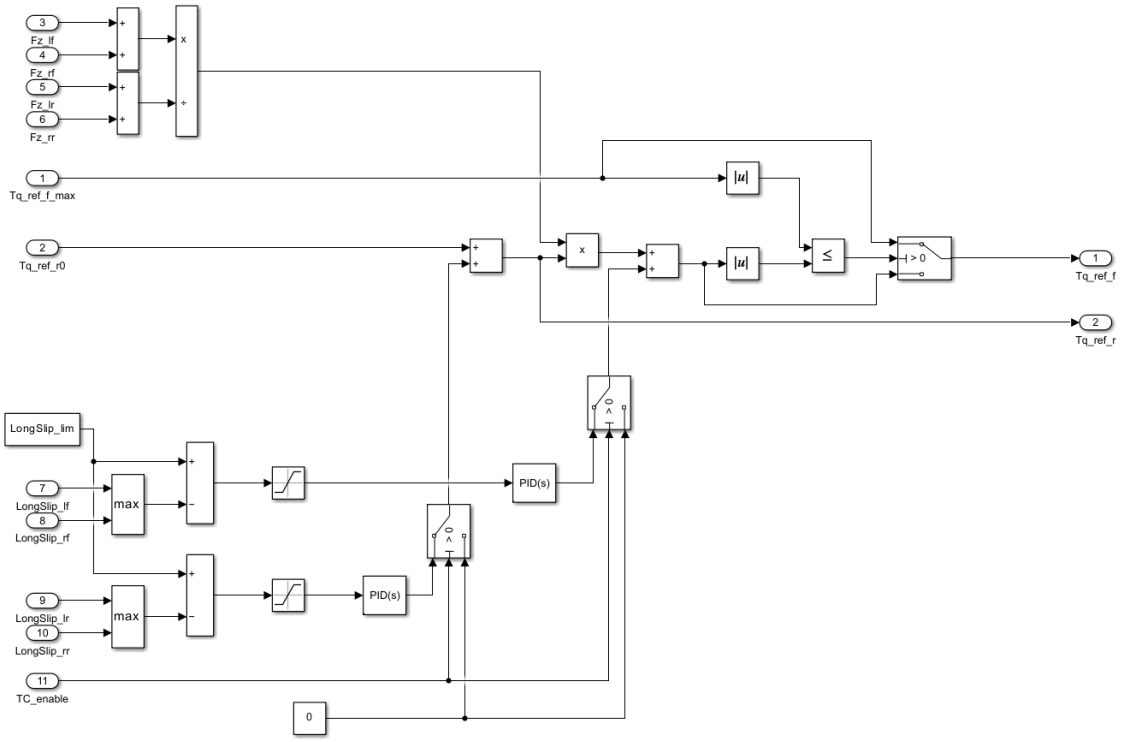

Figure 3.13: Overview of TCS and variable torque distribution

3.1.4 Model for Brake Override System

The model is divided into two parts to implement the BOS function. The BOS control unit is shown in Fig. (3.14). The BOS control unit receives the position of the accelerator pedal and the brake pedal as input signals. It first checks whether the position of these two pedals is activated (i.e., the position value is greater than 0) and generates logic signals for each of them. This step ensures the system can recognize whether the driver is operating the pedals.

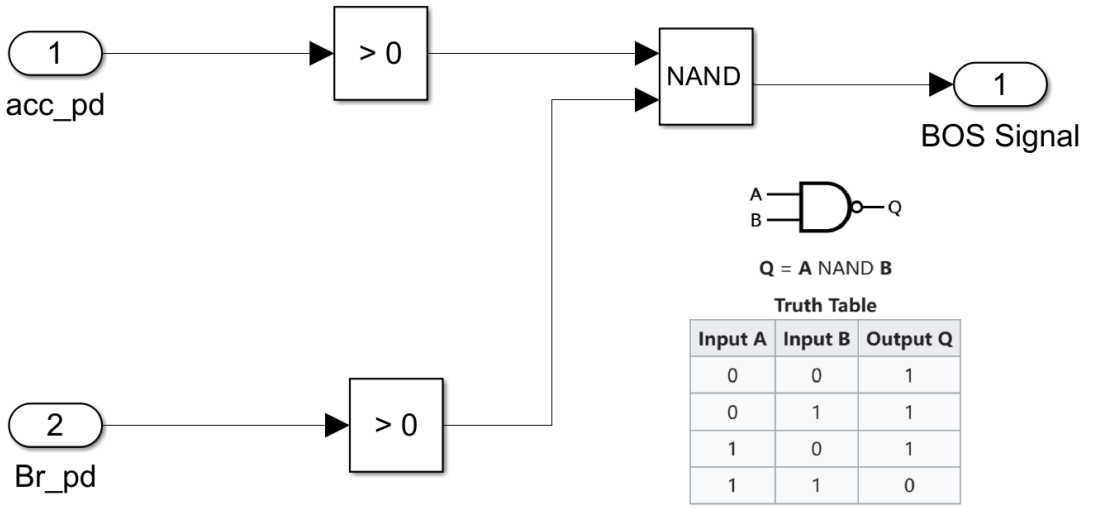

Figure 3.14: BOS Control Unit

Next, the control unit processes the two logic signals using NAND gate logic, which is a basic logic gate that outputs 0 (FALSE) when and only when all input signals are 1 (i.e., TRUE) and 1 (TRUE) for any other combination of inputs. This model means that when both the accelerator and brake pedals are activated, the output of the NAND gate is 0; if only one or none of the pedals are activated, the output is 1. The output of the NAND gate is used as the BOS control signal. This signal reflects whether the BOS system needs to be activated to prioritize the brake operation.

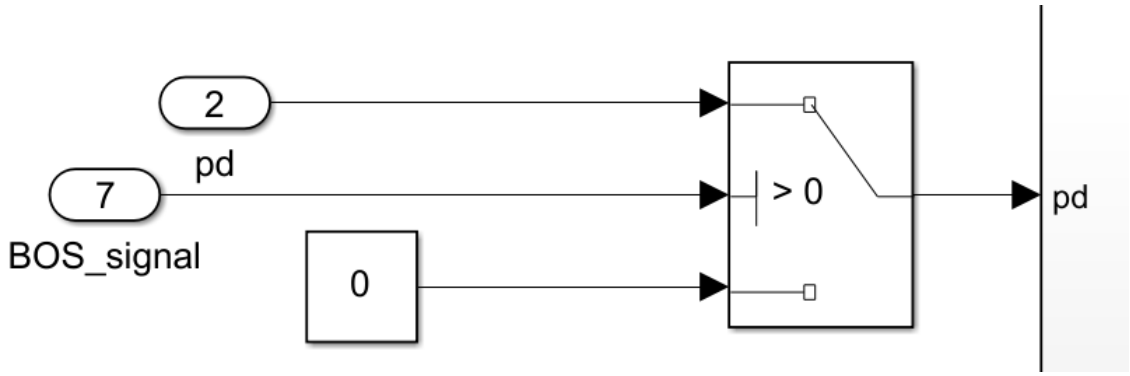

Figure 3.15: BOS in Motor Model

The system utilizes the BOS control signal through a Switch module in the motor model section, as shown in Fig. (3.15). When the BOS control signal is 0 (i.e., when both pedals are activated at the same time), the Switch module sets the accelerator pedal position signal input to the motor model to 0. In this way, the motor does not receive an acceleration command even if the accelerator pedal is pressed, thus ensuring that the braking operation can be prioritized and the basic functionality of the BOS system is achieved.

3.1.5 Differential Model

The theory of building the differential model is described in section 2.2.5. Since the vehicle modeled is a dual motor all-wheel drive vehicle, there are going to be two differentials located at both the front and rear axle, near the front and rear motor. The differential is modeled as an open differential with a lock coefficient K_{diff}. The coefficient K_{diff} could be tuned so the vehicle could have different cornering performance.

There are three working conditions for the driving direction of the vehicle model: forward, turning left, and turning right. A dead zone is added to the wheel rotational speed difference, under which the vehicle is considered driven directly forward, and the speed difference is considered zero. Each driving direction is modeled separately and selected by a logical operator comparing the two wheel speeds with the speed offset. The axle torques are calculated using equations 2.21 to 2.24. Because all torques are calculated as steady-state results, some transfer functions are added to the torques to give the model some dynamic response, which is the final axle torque output. Then, the differential model is built as Fig. 3.16.

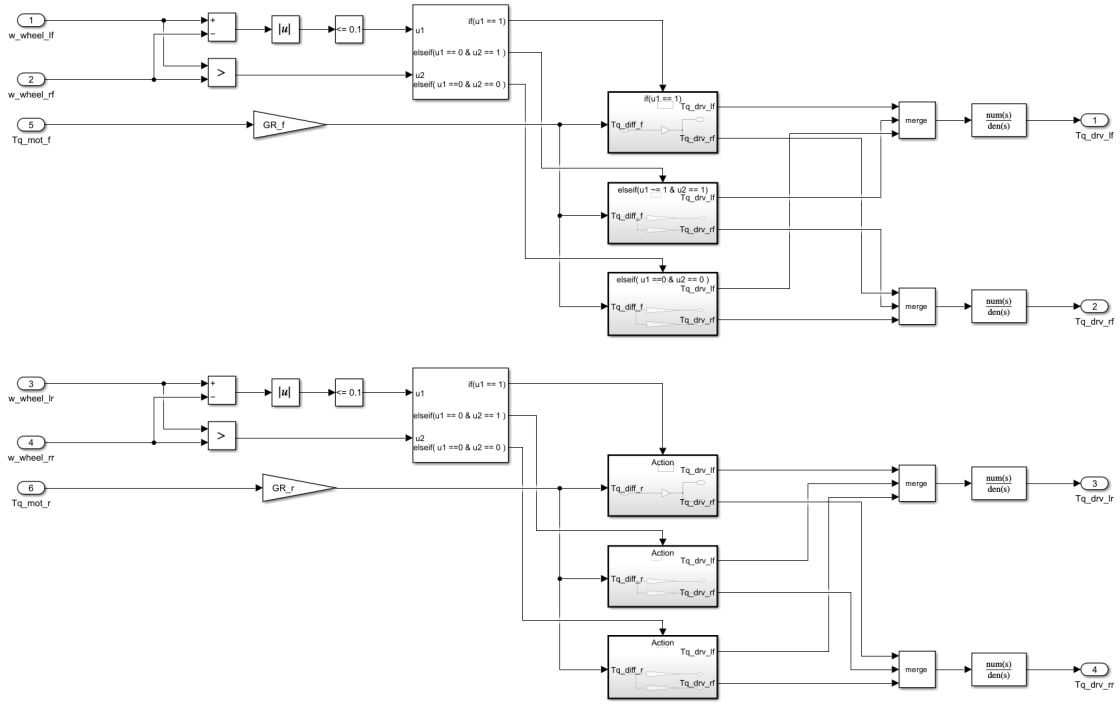

Figure 3.16: Overview of differential model

3.1.6 Powertrain Model Overview

After all the models have been built, the powertrain model could be assembled with those parts above. The completed powertrain model is shown in Fig. 3.17.

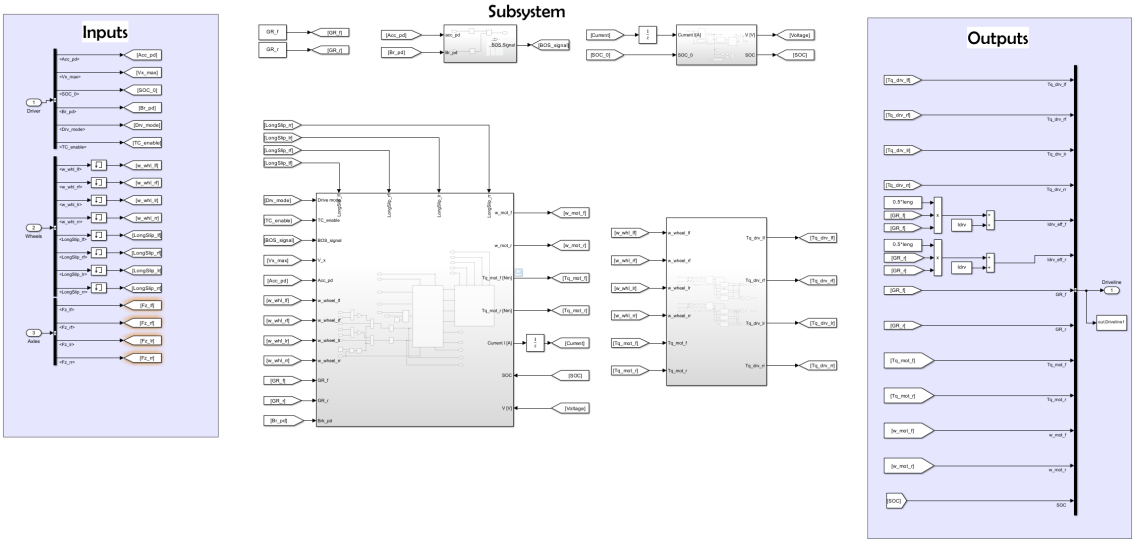

Figure 3.17: Completed powertrain model

3.2 Brake Model

The brake model used in the new EV model is modified from the old one from the simcar14dof model, changing its input from 4 separate brake hydraulic line pressure into brake pedal position. Also, to fit the regeneration function of the new driveline model, the brake distribution model is also implemented.

3.2.1 Physical Model of Brake Hydraulic Line

Apparently, the whole physical process includes many dynamic solid mechanics and fluid mechanics. To model it, the first simplification is to neglect those dynamics and build a steady-state model. The reason for doing this is we do not need to measure the inertia of the solid parts like the brake pedal, and we could also not concentrate on fluid properties of hydraulic oil, like kinetic viscosity. The second simplification is that hydraulic oil is considered not compressible. The third simplification is to only model the primary piston and cylinder, which does not have a significant drawback except making the brake torque no difference between left and right axles. Then the hydraulic line could be simplified as figure 3.18 Then some equations could be tidied up for model building.

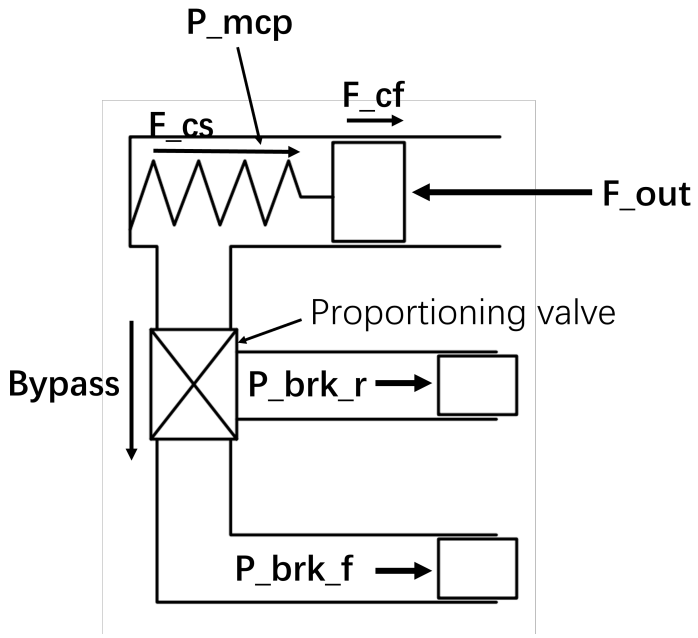

Figure 3.18: Simplified Brake hydraulic line layout

When the pedal is pressed down by a foot, there are two variables: force and displacement. In reality, the displacement is a rotation because the pedal is rotating around a rotating center. But if the rotation is in a small range, it makes nearly no difference to replace it with a linear displacement. As to the force, in our vehicle simulator, the SimIV has only the brake pedal position as an input. So, according to the solutions in the current simulators used in VTI, the pedal force could be a function of pedal position, and the function could be derived by a polynomial regression:

$$F_{pedal_{brk}} = Ax^3_{pedal_{brk}} + Bx^2_{pedal_{brk}} + Cx_{pedal_{brk}} + D \tag{3.7}$$

And then, as Fig. 3.19 shows, when the pedal is totally released, there is a small gap between the pushrod connected to the pedal and the main piston rod. The distance of this gap represents the dead zone of the brake system, and it will be zero when the pedal is slightly pressed down. Therefore, the displacement of the pushrod and main piston rod could be described as:

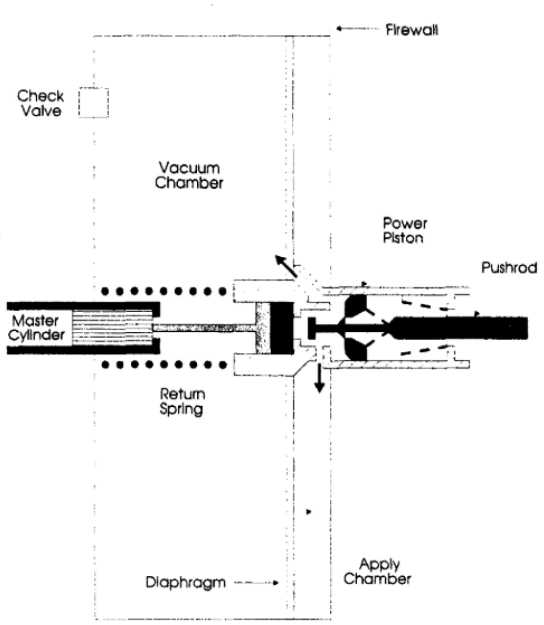

Figure 3.19: Vacuum Booster Construction[10]

$$x_{piston_{brk}} = x_{pushrod_{brk}} = x_{pedal_{brk}} - l_{gap_{brk}} \tag{3.8}$$

Then, it comes to the calculation of the pressure in the main cylinder. The pressure is produced by the force pushing the piston to compress the hydraulic oil in the cylinder, and that force could be calculated by several force equilibrium equations. The force on the pushrod and the piston are considered.

$$F_{out} = F_d + F_{in} - F_{rs} \tag{3.9}$$

$$F_{rs} = F_{rs_0} + K_{rs} x_{pedal_{brk}} \tag{3.10}$$

$$F_{piston} = F_{out} - F_{cs} - F_{cf} \tag{3.11}$$

$$F_{cs} = F_{cs_0} + K_{cs} * x_{piston_{brk}} \tag{3.12}$$

Then, the main cylinder pressure equals the force compressing the hydraulic oil over the cross-section area of the cylinder A_{mc}:

$$P_{mc} = F_{piston}/A_{mc} \tag{3.13}$$

The pressure is then transferred to two separate hydraulic lines: to the front wheels and to the rear wheels, as shown in Fig. 2.20. Normally, the hydraulic lines for the front wheels are connected directly to the main cylinder, which means the brake pressure for the front axle is equal to the pressure in the cylinder. The hydraulic lines for the rear wheels are connected to the main cylinder through a proportioning

valve, which controls the ratio of the pressures in those two hydraulic lines. The equations 3.14 show this relationship:

$$\begin{aligned} P_{brk_f} &= P_{mc} \\ P_{brk_r} &= K_{valve} \cdot P_{mc} \end{aligned} \tag{3.14}$$

After calculating the pressures of the front and rear axles, it is time to find the relationship between it and the brake effect. For a brake caliper connected to a hydraulic line and fixed to a wheel hub, the pressure in the brake line is applied to the brake pads, pressing them firmly on the brake disc, which produces friction force. Then, the friction force is transferred to the tire, and by the friction between the tire and the road surface, the car is slowed down. To simplify this process, it is accepted that the friction force on the brake disc is represented by the brake torque on the axles, which is like the torque driving the wheels. From many results of the experiment, the relationship could be linearly fitted by a segmentation function.

$$T_{brk_f} = \begin{cases} 0 & \text{if } A \cdot P_{mc} - B < 0 \\ A \cdot P_{mc} - B & \text{if } A \cdot P_{mc} - B \geq 0 \end{cases} \tag{3.15}$$

$$T_{brk_r} = K_{valve} \cdot (AP_{mc} - B) \tag{3.16}$$

In these equations, A is for the gain that transforming hydraulic pressure into brake torque, B is for the gap between brake pad and brake disc when the brake pad is at initial condition. The Simulink model of the master cylinder is shown in Fig. 3.20

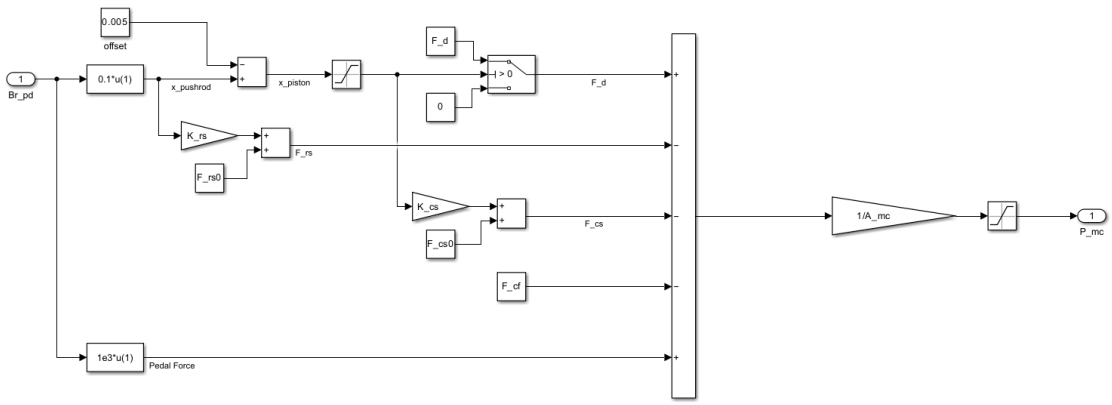

Figure 3.20: Master cylinder Simulink model

3.2.2 Brake Distribution for OPD and Series Drive Mode

From the Axle subsystem, wheel loads on 4 different wheels are calculated, and the fraction of load on the front axle and load on the rear axle will then be known. The ideal brake force distribution will follow this fraction, as shown in Eq.3.17. If the electric vehicle is driven in "series" or OPD mode, which is, without regenerative

braking or when the extra brake is required for OPD mode, this fraction K_{brk} will also be K_{valve} used in Eq.3.16. And the brake subsystem model is shown in Fig. 3.21.

$$K_{brk} = F_{zf}/F_{zr} \tag{3.17}$$

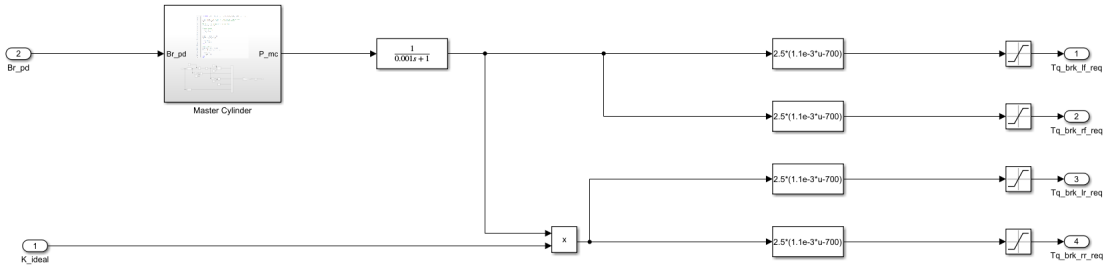

Figure 3.21: Brake subsystem model in series and OPD mode

3.2.3 Optimized Brake Distribution For EV

However, if the energy regeneration is taken into account, the vehicle is slowed down by both the brake and regenerating torque simultaneously when braking, as shown in Fig. 3.22. If the add-up of those two torques for front and rear wheels follows the ideal distribution, it will require a new K_{valve}[23]. From the torque analysis, we could have the following equations:

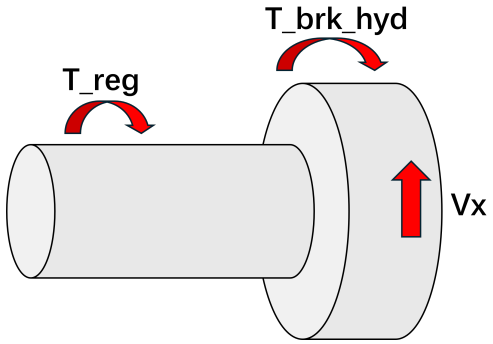

Figure 3.22: Brake torque in total, including regenerative braking and hydraulic braking

$$T_{brk_{f,tot}} = T_{reg_f} + T_{brk_{f,hyd}} \tag{3.18}$$

$$T_{brk_{r,tot}} = T_{reg_r} + T_{brk_{r,hyd}} \tag{3.19}$$

$$\frac{T_{brk_{f,tot}}}{T_{brk_{r,tot}}} = K_{brk} \tag{3.20}$$

$$K'_{valve} = \frac{T_{brk_{f,hyd}}}{T_{brk_{r,hyd}}} \tag{3.21}$$

So, K'_{valve} could deduced from those four equations above:

$$K'_{valve} = \frac{1}{K_{brk} - \dfrac{T_{reg_f}}{T_{brk_{r,hyd}} + T_{reg_r}}} - \frac{T_{reg_r}}{T_{brk_{f,hyd}}} \tag{3.22}$$

The subsystem model at "regenerative braking" mode is shown in Fig. 3.23.

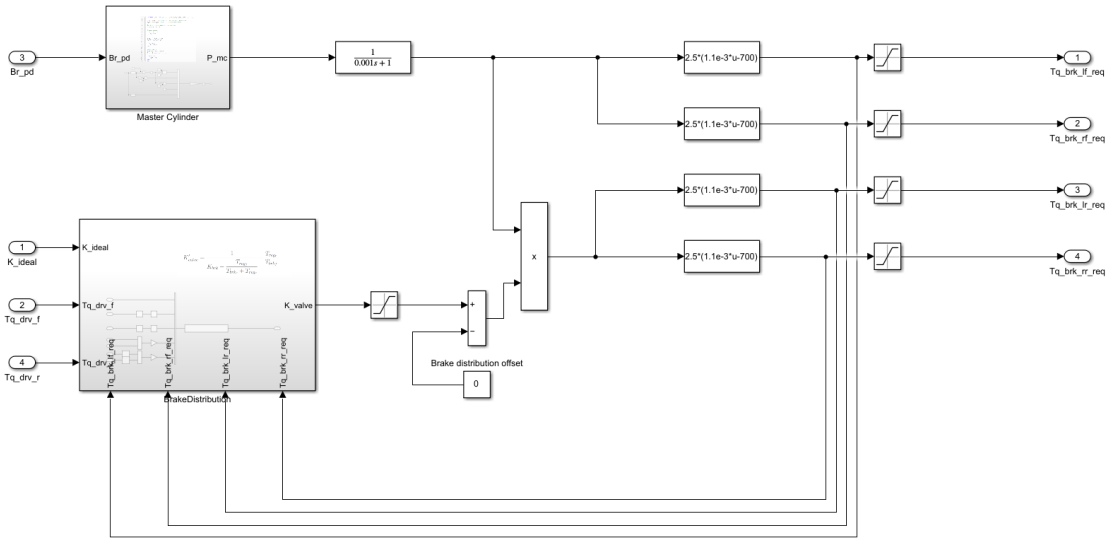

Figure 3.23: Brake subsystem model in regenerative braking mode

Then, it comes to assembling these models together so the brake subsystem model could fit those three drive modes. After that, the ABS is added on each wheel, and another link to control ABS on-off is connected to the driver's control panel. The Simulink model looks like 3.24.

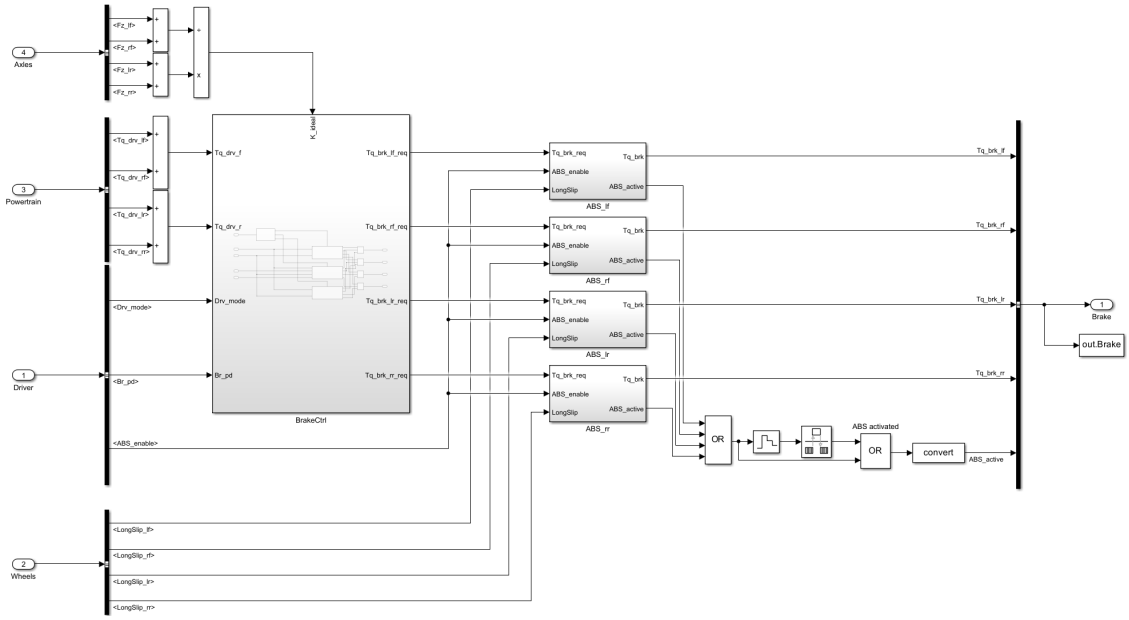

Figure 3.24: Brake subsystem model

3.3 Electric Vehicle Model

In this project, a comprehensive basic model of an all-electric vehicle was built, implemented, and optimized in the Simulink environment, as shown in Fig.(3.25). By replacing the powertrain and brake system models, the project team optimized and reconstructed the original Simulink model to achieve the all-electric vehicle's dynamic simulation. At the same time, the project converted the subsystems of the original model into Simulink library files. This improvement improves the modularity and manageability of the model and lays the foundation for subsequent updates and extensions.

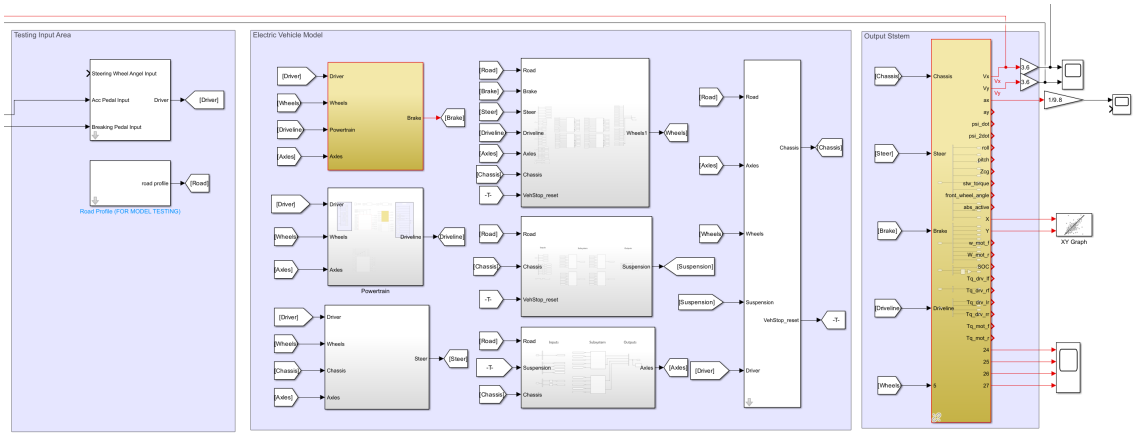

Figure 3.25: Electric Vehicle Model

The conversion to library files allowed the project team to modularly manage and update the model. By saving individual subsystems as separate library components, developers can do so directly in the library whenever a specific feature needs to be modified or improved without rebuilding the entire model. This not only speeds up development but also simplifies the process of error troubleshooting and functional verification. This approach improves the scalability of the model. As the project progresses and the technology evolves, new features and sub-models can be developed and added directly to the existing library files. In this way, the modeling framework does not need to be massively modified, but only new submodels can be replaced or added to the basic modeling framework.

The structure of these library files is illustrated in Fig.(3.26), providing a clear view of how the individual subsystems are organized and managed. In the Simulink environment, these library files can be directly called and applied to different projects and simulation scenarios, improving the development efficiency and ensuring a high degree of model consistency and reproducibility.

In the input segment of the model, a driver input module was designed to allow the user to customize and preset the initial parameters of the vehicle to suit different testing and simulation needs, as shown in Fig.(3.27). The module provides

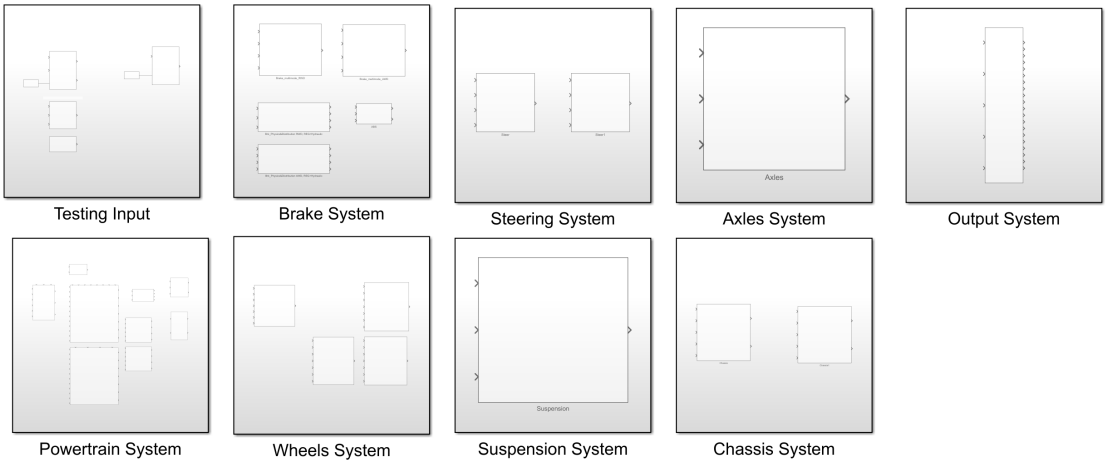

Figure 3.26: Simulink library of model

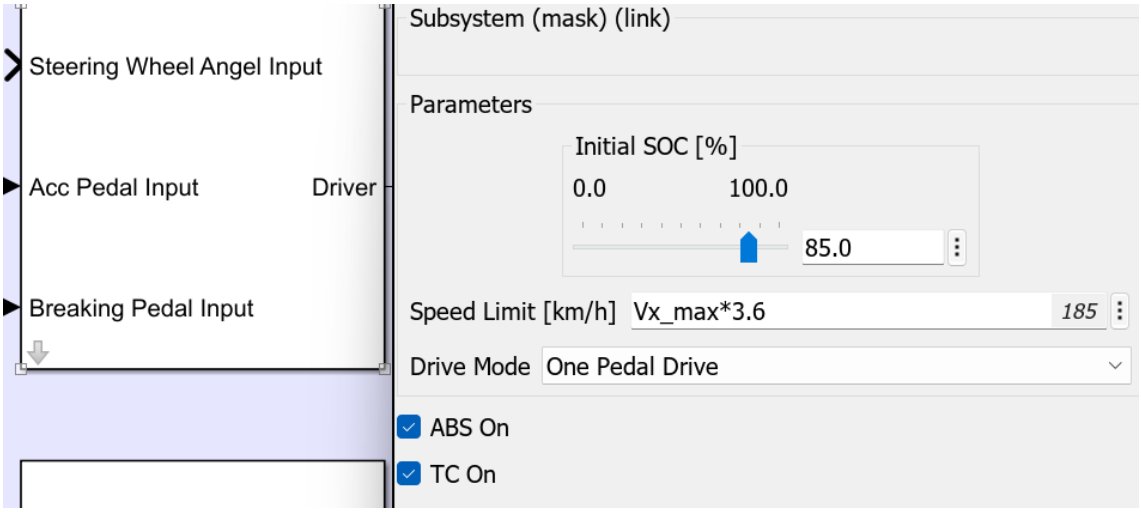

Figure 3.27: Driver Input System

an intuitive interface that allows the user to adjust the vehicle's key settings easily. The main functions of the Driver Input Module include setting the initial SOC of the vehicle, which allows the user to simulate the vehicle's driving performance under different states of charge to evaluate the effectiveness of the battery management strategy and the performance of the EV under real-world road conditions. In addition, the module supports setting the vehicle speed limit. As explained in the above section, the driver input module also supports selecting different driving modes, each with different power output and energy recovery. The module also integrates on/off controls for ABS and TC. By activating or deactivating these systems, the user can study their specific impact on the vehicle's dynamic performance.

In this project, considering the complexity of the vehicle model and the variable dynamic response, the model adopts Simulink's BUS system, which effectively manages the data transmission between different sub-modules, including the packing, sub-packing, and unpacking processing of the data, to ensure the accuracy and real-

time information flow.

The accelerator pedal signal input by the driver is fed into the powertrain module, which is responsible for calculating the torque output and speed information of the motor. At the same time, the brake pedal signal is fed into the brake model, which calculates and generates the brake torque on the four tires, and this torque information is then packaged into brake signals for further processing. In addition, the input signals from the driver's operation of the steering wheel are fed into the steering system, from which the system calculates the necessary steering adjustment information.

Next, information ranging from road information, steering information, brake information, and powertrain output, all of which are passed to the tire model, is used to calculate the dynamic performance of the tires. The dynamic response of the tires has a direct impact on the stability and safety of the vehicle. At the same time, the chassis module receives the road information and calculates the dynamic response of the vehicle chassis based on the suspension forces on the four tires, and this suspension information is not only fed back into the tire model for further dynamic calculations, but is also used in the calculation of the axle model, where the axle model combines the road information, the suspension information of the tires, and the acceleration of the vehicle in the xy-direction, to compute the force of the four tires in the z-direction. This result is fed back into the tire model to simulate how the tires will behave accurately in real-world driving.

Eventually, the outputs of all the sub-models are pooled into the chassis model, which is responsible for calculating the vehicle's acceleration in all three xyz directions and the velocity and acceleration information of the body's pitch, roll, and yaw. These dynamic parameters are fed back to the driving simulator through the output module, thus reflecting the simulated dynamic performance of the vehicle in the driving simulator in real-time, providing the driver with an all-electric vehicle driving simulation experience.

4

Experiments

The previous section described in detail the simulation modeling process of the all-electric vehicle in this project. In order to ensure that the simulation model is theoretically accurate and can truly reflect the dynamic performance of the all-electric vehicle in the natural environment, this chapter will focus on the experimental validation steps taken to improve the model's reliability. This process consists of two parts: collecting necessary vehicle operation data through information acquisition and experiments and fine-tuning and validating the simulation model using these experimental data. These data tune the model. This process involves not only applying the experimental data directly to the model but also improving the model's accuracy by tuning it and comparing the differences between the predictions of the model and the experimental observations. At the same time, the experimental data also allow for the validation of the model.

4.1 Vehicle General Data & Experiments Data

In the planning stage of the experiment, the data requirements should be defined. The type of data expected to be acquired from this experiment, the source of the data, and how the data will be applied first need to be planned and organized in detail before the experiment begins. This process involves two key data categories: static vehicle parameter information and dynamic data acquired during the experiment.

4.1.1 Vehicle General Data

For the designed simulation vehicle model to be as close as possible to the performance and behavior of a real vehicle, an important step is to collect and analyze the relevant parameters of the vehicle in detail. Table (4.1) shows the key parameters that need to be collected to refine this simulation model. These parameters include the vehicle's power performance data (e.g., maximum power, torque, etc.), dimensional parameters (e.g., vehicle length, width, height, wheelbase, etc.), mass parameters, and tire characteristics. Most of these parameters can be obtained by consulting the official website or technical manual of the subject vehicle, which provides a reliable source of information for the model's accuracy.

Table 4.1: Vehicle Data Requirement

No.	Name	Units
1	Vehicle Mass	kg
2	Vehicle Front Area	m^2
3	Vehicle Size	m∗m∗m
4	Vehicle Center of Gravity position	(x,y,z)
5	Maximum Vehicle Speed Limit	m/s
6	motor max output torque	
7	motor max power output	W
8	battery cell capacity	Ah
13	Track Width	m
14	Wheelbase	m
18	Wheel Radius	m

4.1.2 Experiments Data

An integral part of the experimental process is the collection of vehicle dynamics data that will be used for subsequent model calibration and refinement. Ensuring that a comprehensive and accurate dynamics data set is collected is fundamental to achieving high-quality model simulations. Table (4.2) systematically lists the types of vehicle dynamics data that must be collected in an experiment and their corresponding units. These data types cover all aspects of vehicle kinematics and dynamics and the sources from which the data are collected.

Table 4.2: Experiment Data Requirement

No.	Name	Units	Data source
1	speed x	m/s	sensor
2	speed y	m/s	sensor
3	speed z	m/s	sensor
4	Acceleration x	m/s^2	sensor
5	Acceleration y	m/s^2	sensor
6	Acceleration z	m/s^2	sensor
7	acceleration pedal position	0%-100%	OBD-II
15	testing time	s	sensor/OBD-II
17	Yaw velocity	°/s	sensor
18	Pitch velocity	°/s	sensor
19	Roll velocity	°/s	sensor
20	Roll angle	°	sensor
21	Pitch Angle	°	sensor
22	Yaw Angle	°	sensor

4.2 Experimental Equipment & Testing Track

The successful execution of this experiment relies on several key components: the experimental vehicle, the experimental instrumentation, and the test track. These components allow for the collection of accurate and reliable data that allows for an in-depth analysis of the vehicle's dynamics. In this section, these three key components are described in detail.

4.2.1 Experimental Vehicle

The choice of the experimental vehicle has a decisive influence on the experiment results. The vehicle should be representative of the type of vehicle under study and be able to provide the necessary performance characteristics and dynamic behavior. The experimental vehicle needs to be in good holding to avoid any mechanical failures that could interfere with the experimental data. In this project, the experimental vehicle chosen is the Volvo C40 Recharge Twin 2022, as shown in Fig. (4.1). This model is a two-motor, four-wheel drive vehicle, and its relevant technical parameters are shown in Table (4.3), table(4.4) and table (4.5).

At the same time, due to limited experimental conditions, this project could not obtain a driving robot or similar solution to control the accelerator pedal's input angle accurately. This project will use a real driver to control the vehicle, so the experimental design will be based on the full accelerator pedal experiment.

Figure 4.1: Volvo C40 Recharge Twin 2022 in REVERE Lab

Table 4.3: Electric Drive Motor Specifications

Parameter	Unit	Value
Location in Car	-	Front and Rear
Electric Motor Type	-	Synchronous Motor with Permanent Magnet
Electric Motor Model	-	EAD 3.1
Max. Power Output, per Electric Motor	kW	150
	hp	204
Max. Power Output, Total Car	kW	300
	hp	408
Max. Torque, per Electric Motor	Nm	330
Max. Torque, Total Car	Nm	660

Table 4.4: Vehicle Dimensions

Dimension	mm
Ground Clearance	171
Wheelbase	2702
Length	4440
Load Length, Floor, Folded Seat	1685
Load Length, Floor	896
Height	1596
Load Height	630
Front Track	1598
Rear Track	1603
Load Width, Floor	1059
Width	1873
Width including Folded-Out Door Mirrors	2034
Width including Folded-In Door Mirrors	1910

Table 4.5: Tire Sizes

Location	Size	
Front	235/50 R19, 7.5x19x50.5	235/45 R20, 8x20x50.5
Rear	255/45 R19, 8.5x19x56	255/40 R20, 9x20x58.5

4.2.2 IMU(Inertial measurement unit)

The experiments in this project require the acquisition of the vehicle's translational accelerations and the measurement of the angular acceleration of the experimental vehicle in the roll, pitch, and yaw directions. This experiment uses an IMU to collect the data to realize these functions. The IMU used in this experiment is Axotec RGX-840, as shown in Fig. (4.2). This IMU has 4G LTE network capability and a GPS signal input interface. The data collected during the experiment will be transmitted to the lab server through the 4G network to facilitate the subsequent data processing. The IMU has low power consumption and can be powered by the cigarette lighter in the car.

To avoid data fluctuations caused by shaking, the IMU needs to be rigidly connected to the vehicle's chassis. To accomplish this, some modifications were made to the vehicle's seating. The IMU is attached to an aluminum profile, which is attached to the vehicle seat fixing rail by two L-shaped steel plates, as shown in Fig. (4.3).

4.2.3 OBD-II Cable

To accurately obtain the accelerator pedal position information from the experimental vehicle, this project used the automotive diagnostic interface OBD-II (On-Board Diagnostics II) method to establish the connection between the vehicle and the data

Figure 4.2: Axotec RGX-840

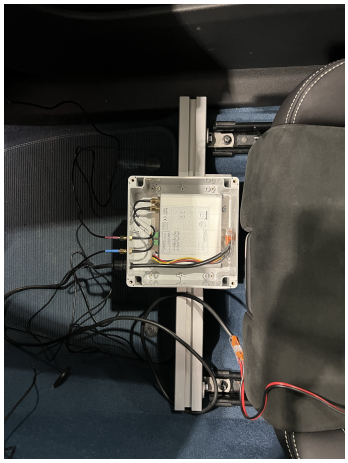

Figure 4.3: IMU in car

Figure 4.4: OBD-II Cable

acquisition system. The OBD-II system has been standard automobile equipment since 1996 and can provide real-time data on the vehicle's status. By using a specialized OBD-II connection cable, as shown in Fig. (4.4), it is possible to directly access the vehicle's internal communication network to read the position of the accelerator pedal in real time. In this project, an OBD-II scanning tool equipped with a data logging function could monitor and record the position information of the accelerator pedal in real time.

This method is efficient and enables the data to be acquired with a high degree of accuracy, as the OBD-II system extracts the information directly from the vehicle's electronic control unit (ECU). The advantage of using the OBD-II interface is its versatility. Most modern vehicles are equipped with an OBD-II interface, meaning that the same equipment and software can be used on a wide range of vehicle models, significantly increasing the flexibility and scalability of experiments.OBD-II technology allows data to be acquired with minimal invasiveness, without the need to make any modifications to the vehicle or to add additional sensors, which avoids potential damage to the vehicle while at the same time guaranteeing the originality and accuracy of the data. This avoids potential damage to the vehicle and ensures the originality and accuracy of the data.

4.2.4 Microphone & Sound Card

Although the main purpose of this project is to create VDM for electric vehicles, sounds were also collected during the experiment to reserve experimental materials for creating sound models for future electric vehicles.

The microphone used in this experiment is Core Sound OctoMic, a four-channel microphone that can capture environmental sounds containing a large amount of detail. In this experiment, the microphone was installed on the head position of the co-pilot to collect sounds while driving, as shown in Fig.4.6.

The sound card used in this project is the TASCAM official US-4X4HR sound card, as shown in Fig.4.5. The sound card is connected to the four independent channels of the four-channel microphone through an adapter cable, and the sound information of the four channels is separately collected, transcribed, and stored in the experimental computer.

Figure 4.5: Sound Card Setup

Figure 4.6: Microphone Setup

4.2.5 Testing Track

For this project, the experimental road must be as smooth as possible with cement pavement. Smooth cement pavement can reduce the impact of the external environment on vehicle driving conditions. At the same time, to carry out accelerated experiments, the experimental road should be as long as possible to meet the demand for acceleration space due to higher acceleration. To reduce the impact of climate on the experimental road, the day of the experiment should be sunny, and there should be no water on the road surface.

4.3 Experiments Design

Faced with the constraints of experimental resources and conditions, this project carefully planned a series of experiments to explore the comprehensive dynamic performance of EVs in single-pedal mode. One pedal drive mode is a driving mode unique to EVs that allows the driver to control the acceleration and deceleration of the vehicle by operating only the accelerator pedal, which allows fine control of the vehicle speed by adjusting the pedal position and, at the same time, recovers energy through the power recovery system during the deceleration process. This project plans to conduct comprehensive testing and data collection of the dynamic response of an EV to accelerate, maintain speed, and brake in this mode through experimental methods.

In the design phase of the acceleration experiment, a pre-estimation of the vehicle acceleration performance is first required, taking into account the safety of the experiment and the feasibility of its implementation. When preparing for the acceleration experiment, this project referred to the official performance data of the vehicle. I.e., the time required to accelerate from a standstill to 100km/h is 4.7 seconds. Based on this data, the theoretical distance required to accelerate the vehicle to 80km/h can be estimated with the help of the uniformly accelerated linear

motion formula, which assesses whether the selected experimental roadway meets the experimental requirements. To estimate the distance required to accelerate to 80km/h, it is assumed that the vehicle maintains uniform acceleration during the acceleration process from 0 to 100km/h. Although the actual situation may vary due to non-linear variations in power output, this simplifying assumption provides a reasonable approximation. Based on the official 0 to 100km/h acceleration time of 4.7 seconds, we can calculate the average acceleration and then use this acceleration to estimate the theoretical distance to reach 80km/h, which is about 41.8m.

4.3.1 Vehicle Normal Acceleration Test

The first full acceleration pedal acceleration experiment was implemented to analyze the performance and dynamic performance of the EV under full-force acceleration conditions. In this experimental design, attention was given to the acceleration performance of the vehicle from a standstill state to reach 80km/h, as well as the performance maintained for a period of time after reaching that speed. The following are the detailed steps and considerations of the experimental design. See table (4.6).

Table 4.6: Pre-experiment Preparation and Experiment Steps

Section	Details
Pre-experiment Preparation	• **Vehicle condition:** Ensure that the vehicle's SOC (battery charge remaining) is around 80%, which is designed to simulate the more typical daily use of EVs. Also, ensure that the electric motor can provide sufficient power for full acceleration. • **Safety measures:** Considering the safety of the full acceleration pedal test, it was conducted during a low-traffic period to ensure the safety of the vehicle and driver during the test, and the safety of other traffic participants in the vicinity.

Continued on next page

Table 4.6 continued from previous page

Section	Details
Experiment Steps	1. **Experiment start:** Place the vehicle stationary after confirming that the surrounding environment is safe and free of obstacles. 2. **Full acceleration:** Press the accelerator pedal rapidly to the maximum level and accelerate until the vehicle speed reaches 80km/h. 3. **End of the experiment:** After completing the speed holding phase, gradually decelerate the vehicle, stop it safely, and prepare for the next experiment. 4. **Repeat the experiment:** To ensure the accuracy and reliability of the experimental data, repeat the above full acceleration experiment 4 times.

4.3.2 OPD Fearture Test

A comprehensive series of experiments was designed to test the OPD function of the newly developed motor model. These experiments were designed to test the OPD function through different driving styles. This set of experiments contains tests of full throttle with OPD on, tests of OPD function, and tests of the driver driving the vehicle generally with OPD on. In addition, a random driving test was included in the experiments to obtain data from a broader range of usage scenarios and ensure that the model maintains high accuracy and reliability even under unpredictable driving behaviors.

4.3.2.1 Full Pedal test With OPD (full release after acceleration)

After fully releasing the accelerator pedal under OPD mode-activated conditions, the first experiment tested the vehicle's deceleration to a complete stop via kinetic energy recovery. Table (4.7) shows the specific experimental design.

Table 4.7: Pre-experiment Preparation and Experiment Steps for Full Pedal Acceleration and Deceleration Experiment

Section	Details
Pre-experiment Preparation	• **Vehicle conditions:** Ensure the vehicle's battery SOC (State of Charge) is approximately 80% to simulate typical daily use conditions and ensure sufficient energy for continuous operations. • **Safety Measures:** The experiment is conducted in an area with minimal traffic and good visibility to ensure the safety of the vehicle, driver, and surrounding traffic.
Experiment Steps	1. **Experiment start:** Confirm the experimental environment is safe and free of obstacles, and position the vehicle in a stationary state, ready to start the experiment. 2. **Full acceleration to 80 km/h:** Rapidly press the accelerator pedal to the maximum until the vehicle reaches 80 km/h. 3. **Full release of pedal:** Completely release the accelerator pedal and allow the vehicle to decelerate to a complete stop. 4. **Repeat:** Repeat the full acceleration and full release process four times to form an initial experimental cycle. 5. **Adjust target speed to 40 km/h:** After completing the initial cycles, adjust the target speed and repeat the acceleration to 40 km/h and full release to a stop. Repeat this reduced speed cycle. 6. **Repeat the reduced speed experimental cycle:** To ensure the accuracy and reliability of the data, repeat the entire process at the reduced speed.

4.3.2.2 Full Pedal test With OPD (half release after acceleration)

Having tested the full release of the pedal, it is also essential to consider another scenario of how the vehicle will behave when the throttle is only released halfway. This experiment was conducted to test this performance by accelerating the vehicle to a specified speed at full throttle with OPD on and then releasing the pedal halfway. The specific experimental design for this experiment is shown in Table (4.8).

Table 4.8: Pre-experiment Preparation and Experiment Steps for Full Pedal Acceleration and Half Pedal Deceleration Experiment

Section	Details
Pre-experiment Preparation	• **Vehicle conditions:** Ensure the vehicle's battery SOC (State of Charge) is approximately 80% to simulate typical daily use conditions and ensure sufficient energy for continuous operations. • **Safety Measures:** The experiment is conducted in an area with minimal traffic and good visibility to ensure the safety of the vehicle, driver, and surrounding traffic.
Experiment Steps	1. **Experiment start:** Confirm the experimental environment is safe and free of obstacles, and position the vehicle in a stationary state, ready to start the experiment. 2. **Full acceleration to 80 km/h:** Rapidly press the accelerator pedal to the maximum until the vehicle reaches 80 km/h. 3. **Half release of pedal:** Half release the accelerator pedal and allow the vehicle to decelerate for 5 seconds. 4. **Braking to Stop:** Fully release the accelerator pedal to stop the vehicle. 5. **Repeat:** Repeat the full acceleration and half-release process four times to form an initial experimental cycle. 6. **Adjust target speed to 40 km/h:** After completing the initial cycles, adjust the target speed and repeat the acceleration to 40 km/h and half release for 5 seconds. Repeat this reduced speed cycle.

4.3.2.3 Full Pedal Acceleration Speed Holding Test

A set of experiments was designed and implemented to verify that the model can control the vehicle to drive at a constant speed only through the accelerator pedal with the OPD mode on. This experiment aims to evaluate the practical effects of the OPD mode, especially the performance performance at a constant speed. In this set of experiments, the vehicle was first accelerated to a predetermined target speed with the full accelerator pedal. After reaching the target speed, the driver used only the accelerator pedal to maintain the vehicle at a constant speed, attempting to maintain stability at different speed intervals. After continuous speed driving, the

driver releases the accelerator pedal completely, allowing the vehicle to gradually decelerate to a complete stop using only the regenerative braking system. During this process, the vehicle speed, accelerator pedal position, and the effect of regenerative braking will be recorded and analyzed in detail. The specific experimental design and steps are detailed in the Table (4.9).

Table 4.9: Pre-experiment Preparation and Experiment Steps for Full Pedal Acceleration and Speed Holding Experiment

Section	Details
Pre-experiment Preparation	• **Vehicle conditions:** The vehicle's battery SOC should be kept at approximately 80% to mimic typical operational conditions and ensure adequate energy for acceleration and speed holding. • **Safety Measures:** The experiment is conducted in a controlled environment with minimal traffic to ensure the safety of the experiment, vehicle, driver, and external traffic.
Experiment Steps	1. **Experiment start:** Verify that the experimental environment is secure and free from any obstacles, ready the vehicle at a stationary state. 2. **Full acceleration to 60 km/h:** Rapidly depress the accelerator pedal fully until the vehicle reaches 60 km/h. 3. **Speed holding:** Maintain 60 km/h by modulating the accelerator pedal as needed for a duration between 5 to 10 seconds. 4. **Braking to Stop:** Fully release the accelerator pedal to stop the vehicle. 5. **Repeat:** Repeat the full acceleration and holding process four times to complete the initial set of cycles. 6. **Adjust target speed to 40 km/h:** After completing the cycles at 60 km/h, reduce the target speed to 40 km/h and repeat the full acceleration and speed holding procedure.

4.3.2.4 Full Pedal Deceleration Speed Holding Test

Following the above experiments, another set of experiments was designed and implemented to validate further the model's response to speed changes and the stability of speed holding in the OPD mode. The goal of this set of experiments was to assess

the strength of the vehicle after speed adjustment, i.e., whether the new target speed could be effectively maintained by the accelerator pedal after a speed change.

In this set of experiments, the vehicle was first accelerated to a predetermined initial target speed with the full accelerator pedal. After reaching the initial target speed, the driver would release the accelerator pedal to decelerate the vehicle to a second target speed. Once the vehicle reached the second target speed, the driver used only the accelerator pedal to maintain this state of uniform driving. After constant speed driving, the driver releases the accelerator pedal completely, allowing the vehicle to gradually decelerate to a complete stop using only the regenerative braking system. During the process, the vehicle speed, accelerator pedal position, and the effect of regenerative braking will be recorded and analyzed in detail. The specific experimental design and steps are detailed in the Table (4.10).

Table 4.10: Pre-experiment Preparation and Experiment Steps for Full Pedal Acceleration, Deceleration and Speed Holding Experiment

Section	**Details**
Pre-experiment Preparation	• **Vehicle conditions:** Ensure the vehicle's battery SOC is at approximately 80% to simulate typical operational conditions, ensuring adequate power for the experiment's demands. • **Safety Measures:** The experiment will be conducted in an area with low traffic and good visibility to safeguard the experiment, vehicle, driver, and surrounding traffic.

Continued on next page

Table 4.10 – continued from previous page

Section	Details
Experiment Steps	1. **Experiment start:** Ensure that the experimental area is safe and free from any obstacles, and prepare the vehicle in a stationary position. 2. **Full acceleration to 60 km/h:** Rapidly depress the accelerator pedal to full until the vehicle reaches 60 km/h. 3. **Deceleration to 40 km/h:** Release the accelerator pedal sufficiently to allow the vehicle to slow down to 40 km/h. 4. **Speed holding at 40 km/h:** Once at 40 km/h, use the accelerator pedal to maintain this speed for a duration of 5 to 10 seconds. 5. **Braking to Stop:** Fully release the accelerator pedal to stop the vehicle. 6. **Repeat:** Repeat the full acceleration, deceleration to 40 km/h, and holding process four times to complete the initial set of cycles. 7. **Adjust initial target speed to 40 km/h, reduce to 20 km/h:** After completing the cycles at initial conditions, start from 40 km/h and reduce the speed to 20 km/h, then maintain 20 km/h using the accelerator pedal as in previous steps.

4.3.2.5 OPD Normal Drive Speed holding Test

All of the above experiments were conducted under full accelerator pedal conditions, which are not common in daily driving behavior. This set of experiments was designed to verify that the vehicle model can accurately reflect the power output effect of the vehicle under various input environments. This set of experiments aims to simulate operations closer to actual driving situations to ensure the applicability and reliability of the model under different driving conditions. In this set of experiments, the driver was asked to gradually accelerate the vehicle to a specified speed in a usual driving manner instead of immediately using the full accelerator pedal. After reaching the target speed, the driver will use only the single-pedal function to maintain the vehicle at a constant speed. After maintaining constant speed for a certain period of time, the driver will ultimately release the accelerator pedal and allow the car to gradually decelerate to a complete stop using only the regenerative braking system. The specific experimental design and steps are detailed in the Table (4.11). Throughout the experiment, the vehicle's speed, the position of the accelerator pedal, and the effect of regenerative braking were recorded in detail.

Table 4.11: Pre-experiment Preparation and Experiment Steps for Controlled Speed Holding Experiment

Section	Details
Pre-experiment Preparation	• **Vehicle conditions:** Ensure that the vehicle's battery SOC is approximately 80% to simulate normal operating conditions, ensuring enough energy for sustained speed control. • **Safety Measures:** Conduct the experiment in a low-traffic area with clear visibility to ensure safety for the vehicle, driver, and surrounding area.
Experiment Steps	1. **Experiment start:** Verify safety of the experimental area, ensure no obstacles are present, and position the vehicle ready for normal driving. 2. **Normal driving to 40 km/h:** Drive the vehicle normally up to 40 km/h using typical acceleration. 3. **Speed holding at 40 km/h:** Use the accelerator pedal to maintain a speed of 40 km/h for 5 to 10 seconds. 4. **Braking to Stop:** Fully release the accelerator pedal to stop the vehicle. 5. **Repeat:** Repeat the process of reaching and maintaining 40 km/h three times. 6. **Adjust target speeds:** After completing initial cycles, reduce speed to 20 km/h, then to 10 km/h, maintaining each speed for 5 to 10 seconds using the accelerator pedal.

4.3.3 Vehicle braking Experiments

The braking of an all-electric vehicle consists of mechanical braking and kinetic energy recovery, which will also constitute the unique dynamic performance of an all-electric vehicle. In order to tune the braking model constructed in this project, data collection of the braking dynamics of an all-electric vehicle is required here through an experiment. Given the limitations of the data that can be obtained from the vehicle under test in this experiment, it is impossible to obtain information on the brake pedal's position. At the same time, modification of the brake pedal is an unsafe behavior. Therefore, only the dynamic performance of the fast-braking vehicle was collected for this experiment, as in table (4.12).

Table 4.12: Pre-experiment Preparation and Experiment Steps For Vehicle Braking Experiments

Section	**Details**
Pre-experiment Preparation	• Vehicle condition: Ensure the vehicle's SOC (battery charge remaining) is around 80%, which is designed to simulate the more typical daily use of EVs. Also, ensure that the electric motor can provide sufficient power for full acceleration. • Safety measures: The test is conducted during a low-traffic period to ensure the safety of the vehicle and driver, as well as the safety of other traffic participants in the vicinity.
Experiment Steps	1. Starting the experiment: After ensuring the surrounding environment is safe and free of obstacles, place the vehicle stationary. 2. Acceleration: Press the accelerator pedal until the vehicle reaches 40km/h. 3. Braking operation: After reaching 40km/h, press the brake pedal quickly until the vehicle comes to a complete stop. 4. Repeat the experiment: To ensure the accuracy and reliability of the experimental data, repeat the full acceleration experiment 3 times.

5
Results

After several experimental and modeling processes, several results have been obtained from the vehicle experiments and the model validation. This chapter will describe these results and discuss them in four main sections: experimental data and its processing, model refinement based on the processed data, comparison of the model outputs with experimental data from the same driver inputs, and limitations of the overall project. The experimental data and its processing section will present the data obtained from the vehicle experiments, including the pre-processing steps of the data and the preliminary analysis results. The model refinement based on the processed data section will detail how the processed experimental data was used to optimize and refine the EV model. The process of tuning the model parameters will be discussed, as well as how to improve the accuracy and robustness of the model through parameter tuning and validation. A comparison of model outputs with experimental data from the same driver inputs will be made to compare the differences between model outputs and actual experimental data. This section aims to validate the model's accuracy, i.e., whether the model can output a dynamic response similar to that of an actual vehicle under the same driver input conditions. The limitations section of the overall project will objectively analyze the limitations present in the project.

5.1 Experiment Data Process And Results

After obtaining the experimental data, it first needs to be processed. In view of the low frequency and average data accuracy of the experimental data, this project did not perform denoising on the experimental data. The data file format read from the ECU is a CSV file, and this type of file needs to be pre-processed before further manipulation in Matlab. Given the large number of experiments and the amount of data acquired, a Python automated script was designed for this project to perform the initial processing of CSV data. The Python script removed the table headers from the files captured for this project, leaving only the experimental data itself. The formatting of the data was also corrected. The specific code for the data processing and the flow can be found in the GitHub repository for this project.

After processing the experiment results, the experimental data can be initially observed and analyzed. Fig.(5.1) shows the results of the experiment (4.3.2.1), where the x-axis represents the time, the left y-axis represents the pedal position using a

Project	Description	Link
Vehicle Experiments Guideline	ZikunWang-Ricardo/Vehicle_Experiment_Guideline	GitHub Link

Table 5.1: GitHub Repository for Experiment Data Process

blue line, and the right y-axis represents the velocity information using a red line.

To provide a more comprehensive analysis, detailed results and corresponding graphs for all experiments are shown in the A.3. The graphs in these appendices include more experimental data covering different driving conditions and parameter settings to ensure the broad applicability of the experiments to model tuning. Further analysis of these results allows for identifying areas where the model needs to be improved and the next step of parameter tuning and optimization.

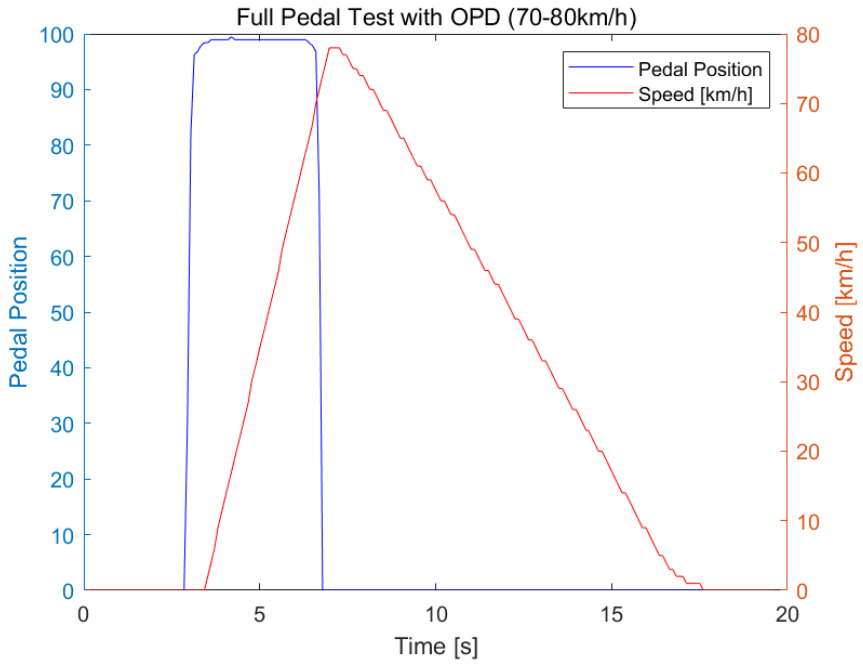

Figure 5.1: Full Pedal Test With OPD (70-80km/h)

5.2 Model Refine Process

After the experiment data are processed and ready for visualization, the next step is to adjust the model and tune the parameters to make the model outputs fit the experiment data with the same accelerator pedal input. For the Simulink model built in this project, the most focused point is how the drive torque is output by the electric motor with a certain driver's behavior. Some parameters had already been set based on either the physical parameter and the technical specification found on the official web page of the test vehicle or based on our model tuning experiences.

However, some parameters still require to be tuned in order to enable the vehicle model to reflect the real handling at a more accurate level.

First, referencing the data from the "speed holding at 60 km/h at OPD mode" experiment, the model is analyzed. If the accelerator pedal signal from the experiment is input to the vehicle model with no steering wheel angle (straight run), and the model is at OPD mode, the longitudinal velocity from the experiment and the model output are shown in Fig. 5.2.

Apparently, this model is far from reflecting reality. So, some of the parameters must be tuned. After the parameters for shaping the pedal regenerative braking-coasting-accelerating segmentation are tuned, the model could give a better judgment on when to accelerate and to brake, compared with the experiment data. the outputs are like figure 5.3.

After the "pedal segments" are shaped as the behavior of the real vehicle does, the accelerating, regenerative braking and speed-holding behavior of the model still are not fit. Further tuning on that performance will be the next step. In this step, the parameters that define the mapping relation between drive torque and pedal position input and the look-up table defining how the maximum regenerate rate varies with velocity are adjusted. The comparison between the experiment data and the model output then looks like Fig. 5.4. It could be observed that the model fits reality.

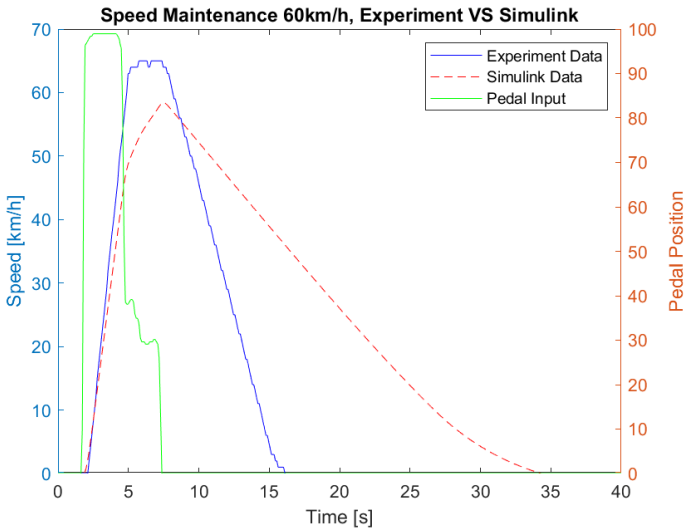

Figure 5.2: Longitudinal velocity of experiment VS simulation model output, OPD mode, before tuning the parameters

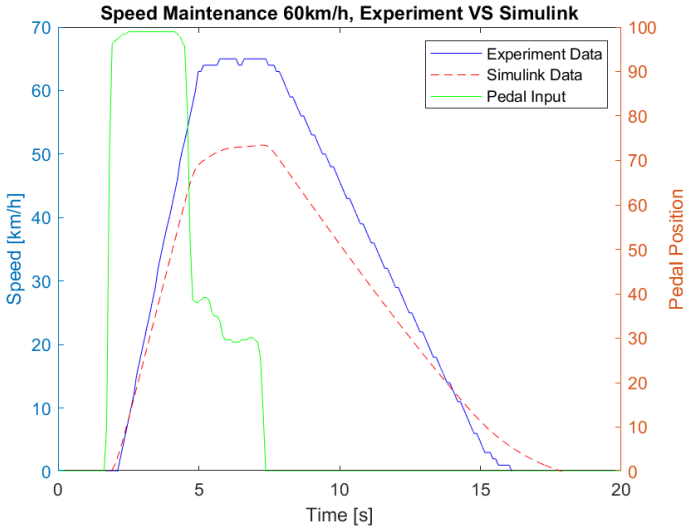

Figure 5.3: Longitudinal velocity of experiment VS simulation model output, OPD mode, after shaping the "pedal segments"

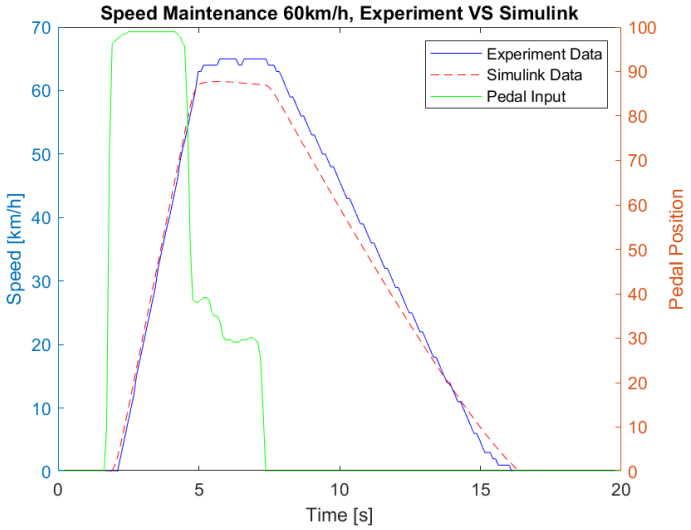

Figure 5.4: Longitudinal velocity of experiment VS simulation model output, OPD mode, after further tuning

Then different experiment data are input to the model, and smaller changes on the parameters are applied for the robustness and accuracy under different driver operations. The final fitting results are talked about in the following section of this thesis.

5.3 Model Results Using Experiment Input

After all the parameters are tuned until the model produces a rather proximate fit to the experimental data, the results are as follows. Those results include the experiment input data, the experiment result, and the model's result. The Results

show that this Simulink model performs well in most situations, but there are still some limitations in the model.

5.3.1 Vehicle Normal Acceleration Simulation Result VS Experiment Result

This result shows the vehicle's normal acceleration experiment results vs. simulation results. For this experiment, due to the limitation of not getting access to the braking pedal data, only the acceleration part of the result has been considered. As shown in Fig.(5.5), the model has a good result for normal acceleration performance, but the response time is not good enough. Also it could be noticed that the simulated vehicle acceleration response is slower instead of faster as shown in former figures. This is because the drive mode in this experiment is normal drive using two pedals, not in OPD mode, and so is the VDM switched into. The two drive modes in VDM are using different control logic, so the direction of delay comparing to experimental data are opposite. Yet the delay is within tolerance.

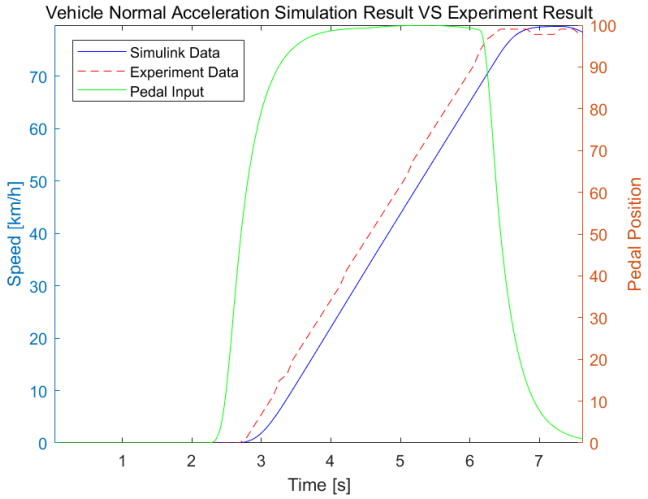

Figure 5.5: Full Pedal Test Without OPD

5.3.2 OPD Feature Test Result

After normal driving without OPD, the project's focus is on the unique feature of the fully electric vehicle. In this section, some different model vs. experiment results are shown. All those experiments try to rebuild a vehicle model that behaves like an OPD-driving vehicle in the real world.

5.3.2.1 Vehicle Full Pedal With OPD (full release after acceleration) Simulation Result VS Experiment Result

These results show the experiments for full pedal driving and full release after acceleration. There are two groups of experiments for different target speeds. As shown in Fig.(5.6) and Fig.(5.7), the Simulink model gives a very similar result to the experiment result. This means the model created is good enough to present the performance of extreme acceleration and deceleration through OPD.

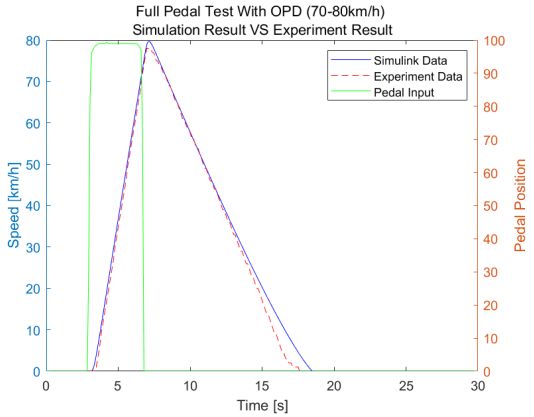

Figure 5.6: Full Pedal Test With OPD (70-80km/h) Simulation Result VS Experiment Result

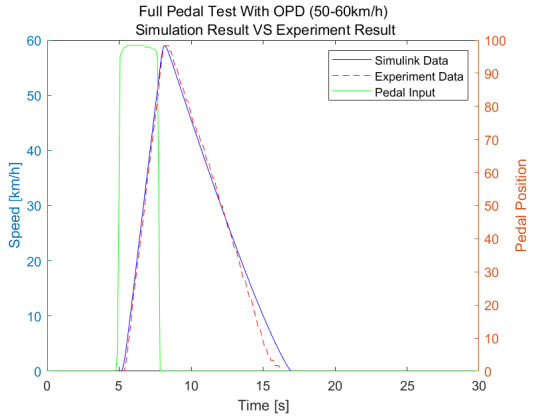

Figure 5.7: Full Pedal Test With OPD (50-60km/h) Simulation Result VS Experiment Result

5.3.2.2 Full Pedal test With OPD (half release after acceleration)

OPD vehicles have different strategies for different speeds and pedal positions. Two different experiments have been done to verify the model's performance in half-pedal positions released after full pedal acceleration. The results in Fig.(5.8) and Fig.(5.9) show that the model gives a similar result to the experiments.

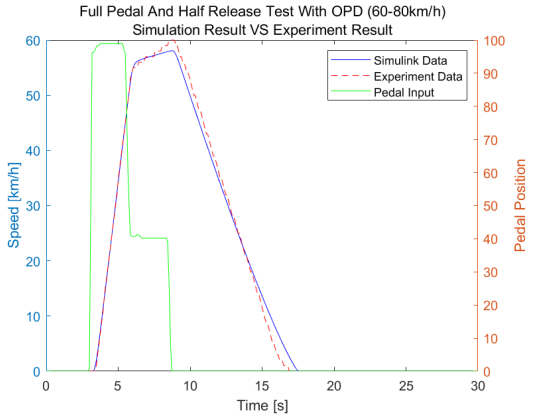

Figure 5.8: Full Pedal And Half Release Test With OPD (60-80km/h)Simulation Result VS Experiment Result

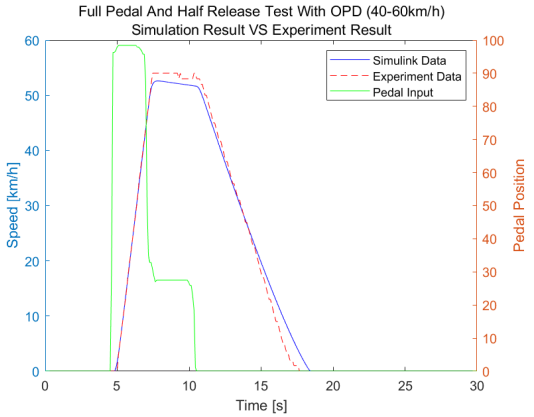

Figure 5.9: Full Pedal And Half Release Test With OPD (40-60km/h)Simulation Result VS Experiment Result

5.3.2.3 Full Pedal Acceleration Speed Holding Test

When a driver is driving a fully electric car in real life, many scenarios require the vehicle to maintain a certain speed. For an OPD vehicle, using one pedal to do speed holding is a unique experience to driving an ICE car. The results in Fig.(5.10) and Fig.(5.11) show that the model has a similar result as the experiment design. That means the model gives the same driving feeling when people drive it at a certain speed after acceleration.

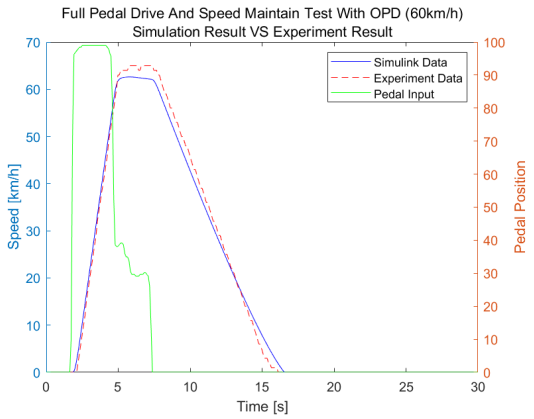

Figure 5.10: Full Pedal Drive And Speed Maintain Test With OPD (60km/h) Simulation Result VS Experiment Result

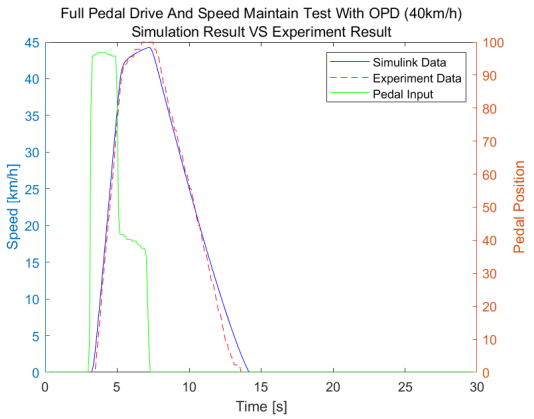

Figure 5.11: Full Pedal Drive And Speed Maintain Test With OPD (40km/h) Simulation Result VS Experiment Result

5.3.2.4 Full Pedal Deceleration Speed Holding Test

In OPD, the driver needs to release the acceleration pedal to control the speed decrease. In some scenarios, the driver wants to decrease and maintain a lower speed rather than stop the car. The results in Fig.(5.12) and Fig.(5.13) show that when

the real driver sent the same acceleration pedal input to the car and the model, the result was from those two parts. The Simulink model gives an excellent result that fits the experiment.

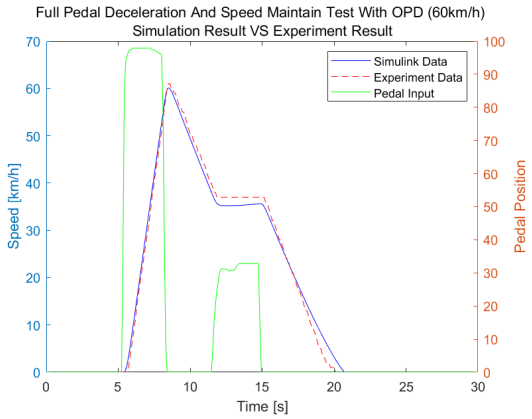

Figure 5.12: Full Pedal Deceleration And Speed Maintain Test With OPD (60km/h) Simulation Result VS Experiment Result

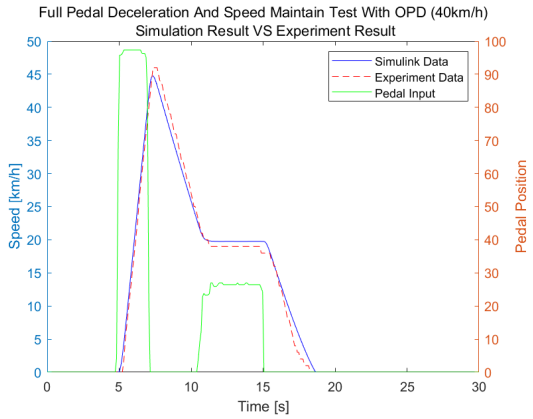

Figure 5.13: Full Pedal Deceleration And Speed Maintain Test With OPD (40km/h) Simulation Result VS Experiment Result

5.3.2.5 OPD Normal Drive Speed Holding Test

In most real-life scenarios, the driver won't use a full acceleration pedal most of the time. In that case, the experiments should apply some normal driving conditions to verify the model's performance. The results in Fig.(5.14) and Fig.(5.15) show the vehicle and the model performance when the driver tries to maintain a low speed at standard pedal position input. The Simulation result for the 40 km/h target speed is good, but the result from the 20 km/h target speed is higher than the experiment. This result shows that the model is not good enough when dealing with low-speed simulations of imperfect roads. This might be due to the road where the experiment happens not being perfectly horizontal, including a tiny slope and some bumps, and the influence from that will increase when the vehicle speed is decreased.

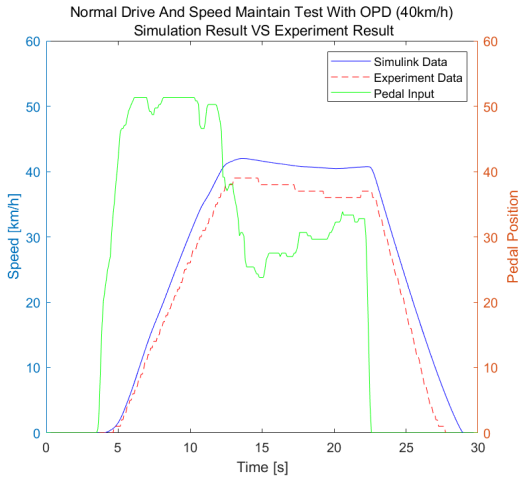

Figure 5.14: Normal Drive And Speed Maintain Test With OPD (40km/h) Simulation Result VS Experiment Result

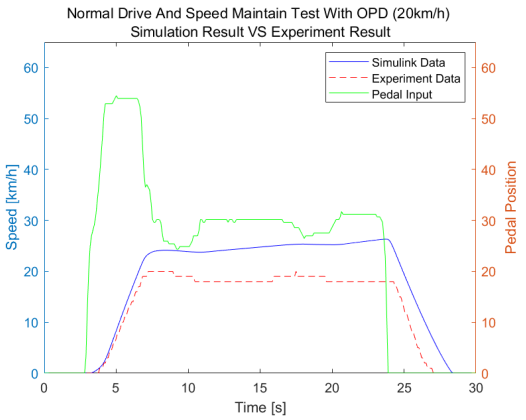

Figure 5.15: Normal Drive And Speed Maintain Test With OPD (20km/h) Simulation Result VS Experiment Result

5.3.3 Vehicle braking Experiments

The model contains a newly built braking system model. Thus, the experiment needs to contain a design to verify it. The results in Fig.(5.16) and Fig.(5.17) show the braking performance after the vehicle reaches 40km/h and 20km/h. The OPD feature in the car has been turned off since the experiment's design was to verify the brake itself. The result is that the target speed is 40km/h, and the vehicle braking performance is as good as that of the experiments. However, for a target speed of 20km/h, the simulation model continuously accelerates while the experiment data is cruising. The possible reason for that is the road influences the experiment input to maintain speed at 20km/h. This result also shows that the model is not good enough when dealing with low-speed simulations of imperfect roads.

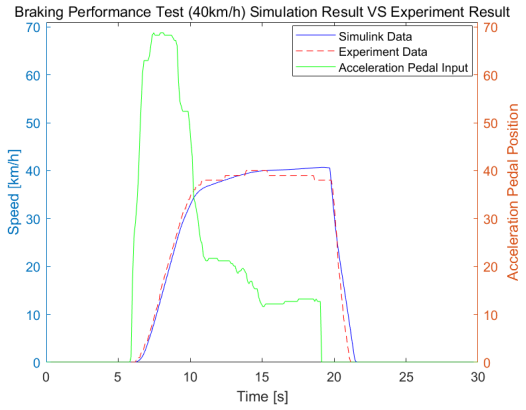

Figure 5.16: Certain Speed Braking Test (40km/h) Simulation Result VS Experiment Result

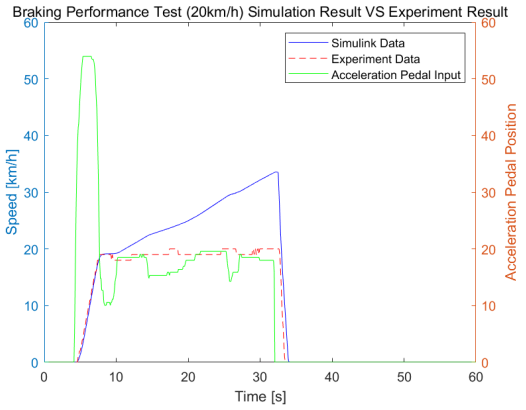

Figure 5.17: Certain Speed Braking Test (20km/h) Simulation Result VS Experiment Result

6
Conclusion

6.1 Outcomes

This master's thesis presents a fully electric vehicle model in Simulink. In the future, the model can be implemented in the SIM IV simulator for people to drive. The model has the OPD, BOS, and regenerate braking feature for the simulator driver to feel like driving an electric vehicle.

We created a vehicle simulation toolbox for future work. The toolbox and base model are modular, and the appropriate modules can be replaced when simulating other vehicles without redeveloping the entire model.

Also, when experimenting, we create a workflow for students like us who will work with cars but only have minimal access to the data from cars. The modern vehicle always comes with an OBD port. Hence, we created a guideline on how to get data from OBD and how to process it. The guideline is open-sourced and distributed on GitHub.

6.2 Limitations

There are some limitations in this model. First, there are many unknown parameters of the test vehicle, such as the spring stiffness and damping in the suspension subsystem, the toe and camber of the wheel, and the stiffness of the tire. These parameters are only tuned to achieve robust longitudinal performance; the lateral performance is not included in this study. The real vehicle test is also done only in the longitudinal direction, which is another reason why the lateral performance of this vehicle model could not be tuned. Second, the tire model uses the magic formula approach, the parameters in the magic formula are beyond our ability to modify. Third, the electric motor is built based on the motor map. The motor map represents the steady state operating performance of an electric motor rather than dynamic, though a first-order transfer function is added in the model to describe the dynamic, which is also theoretical.

There are some limitations in the experiment design. Given that this project encountered certain technical limitations in accessing critical information for communication within the vehicle control system, particularly the inability to access the decoded DBC file for CAN (Controller Area Network) messages, the information

read directly from the vehicle was very limited. This limitation is mainly reflected in the fact that the accelerator pedal position information can only be read through the OBD-II interface. At the beginning of the experimental design, the project envisaged analyzing the vehicle's dynamic behavior in depth through several tests, including tests with different accelerator pedal positions, brake pedal positions, power recovery under different pedal changes, and dual lane change tests. These experimental designs can be accessed in A.2.

However, the tests with different brake pedal positions could not be conducted as scheduled due to the inability to obtain pedal position information quantitatively. Specifically, the lack of a means to accurately control and record the accelerator pedal position made this part of the experimental design challenging to implement. Similarly, tests on brake pedal position could not be executed due to the inability to read brake pedal position information via CAN messages and the questionable safety of physically modifying the brake pedal to obtain position information for testing on public roads.

In addition, the initial design of the dual-lane change test was to use the brake pedal information, accelerator pedal information, and steering wheel information collected in the experiment as inputs and to verify the accuracy of the model established by the project by comparing it with the data derived from the calculation. However, due to the limitation of data collection capability, critical data such as steering wheel angle could not be obtained, leading to this test plan's abandonment.

Secondly, the project team could not obtain access to a professional test track, which meant that all data collection had to be carried out on public roads, where the actual road conditions had an unknown impact on the accuracy and reliability of the data collection. Although the project team made every effort to select straight and level road sections for the experiments to minimize the impact of road conditions on data quality, the experimental data were still inevitably affected to a certain extent.

6.3 Future Work

There could be plenty of future work carry on over our outcomes. First, further experiments with more precision and better design could be conducted to make the model fit the real vehicle more accurately, such as lateral performance and battery performance. Additionally, the experiment design could include more sensors and, if possible, the official DBC file. Also, the model is not running perfectly in low-speed situations when the road has slop and other influences, it might due to the road, but there is also a possibility that the model is not refined at low speed scenario. Second, the model is not interpreted into the driving simulator yet, it must be another interesting work to let people drive the "Simulink vehicle" in the driving simulator to experience the fast change of the acceleration on an electric vehicle. Third, the drive modes on the vehicle model is rather rough. As we know there are different drive modes on a real vehicle such as "sport" "comfort" "snow" etc. It will

be a nice project to find differnce of the drive modes on the vehicle and how they could be modeled into a vehicle simulation model.

Bibliography

[1] Prognos nyregistreringar för 2024, 2024.

[2] Bengt Jacobson et al. Vehicle dynamics, 2015.

[3] D. Arosio, F. Braghin, F. Cheli, and E. Sabbioni. Identification of pacejka's scaling factors from full-scale experimental tests. *Vehicle System Dynamics*, 43(sup1):457–474, 2005.

[4] M Sh Asfoor, AM Sharaf, and S Beyerlein. Use of gt-suite to study performance differences between internal combustion engine (ice) and hybrid electric vehicle (hev) powertrains. In *The International Conference on Applied Mechanics and Mechanical Engineering*, volume 16, pages 1–16. Military Technical College.

[5] Mohamed El Baghdadi, Laurent De Vroey, Thierry Coosemans, Joeri Van Mierlo, Wim Foubert, and Rafael Jahn. Electric vehicle performance and consumption evaluation. IEEE.

[6] Wikipedia contributors. 2009–2011 toyota vehicle recalls.

[7] Wikipedia contributors. Differential (mechanical device), 2024.

[8] Hongyang Cui, Dale Hall, and Nic Lutsey. Update on the global transition to electric vehicles through 2019. 2020.

[9] Charles F. P. George. Driving simulators in clinical practice. *Sleep Medicine Reviews*, 7(4):311–320, 2003.

[10] J. Christian Gerdes and J. Karl Hedrick. Brake system modeling for simulation and control. *Journal of Dynamic Systems, Measurement, and Control*, 121(3):496–503, 1999.

[11] Wenda Guan. *Vehicle Construction*. Tsinghua University Press Co., 2004.

[12] Jorge Gómez Fernández. *A Vehicle Dynamics Model for Driving Simulators*. Thesis, 2019. Accession Number: cst.20.500.12380.160346; Publication Type: Thesis; Language: English.

[13] Steven C Hageman. Simple pspice models let you simulate common battery types. *EDN*, 38(22):117–, 1993.

[14] Marah Al Halabi and Anas Al Tarabsheh. Modelling of electric vehicles using matlab/simulink. *SAE Technical Paper Series*, 2020-10-14.

[15] P. Hansson, A. Stenbeck, A. Kusachov, F. Bruzelius, and B. Augusto. Prepositioning of driving simulator motion systems. *International Journal of Vehicle Systems Modelling and Testing*, 10(3):288, 2015.

[16] Arne Helland, Gunnar D. Jenssen, Lone-Eirin Lervåg, Andreas Austgulen Westin, Terje Moen, Kristian Sakshaug, Stian Lydersen, Jørg Mørland, and Lars Slørdal. Comparison of driving simulator performance with real driving after alcohol intake: A randomised, single blind, placebo-controlled, cross-over trial. *Accident Analysis Prevention*, 53:9–16, 2013.

[17] Mattias Hjort, Sogol Kharrazi, Olle Eriksson, and Magnus Hjälmdahl. Limit handling in a driving simulator. Report 03476030 (ISSN), Statens väg- och transportforskningsinstitut, 2015 2015. 2020-09-11T08:53:42.368+02:00.

[18] Mari Iwata, Kunihiro Iwamoto, Iwao Kitajima, Takasuke Nogi, Koichi Onishi, Yu Kajiyama, Izumi Nishino, Masahiko Ando, and Norio Ozaki. Validity and reliability of a driving simulator for evaluating the influence of medicinal drugs on driving performance. *Psychopharmacology*, 238(3):775–786, 2021.

[19] Fenzhu Ji, Yong Pan, Yu Zhou, Farong Du, Qi Zhang, and Guo Li. Energy recovery based on pedal situation for regenerative braking system of electric vehicle. *Vehicle System Dynamics*, 58(1):144–173, 2020.

[20] Sangshin Kwak. Four-leg-based fault-tolerant matrix converter schemes based on switching function and space vector methods. *IEEE Transactions on Industrial Electronics*, 59(1):235–243, 2011.

[21] Jun-Ho Lee and Ki-won Song. A study on the safety assessment process in end effector based on brake override system. *Journal of Knowledge Information Technology and Systems (JKITS)*, 15(2):245–253, 2020.

[22] Wei Liu, Hongzhong Qi, Xintian Liu, and Yansong Wang. Evaluation of regenerative braking based on single-pedal control for electric vehicles. *Frontiers of Mechanical Engineering*, 15(1):166–179, 2020.

[23] Zhengwei Ma and Daxu Sun. Energy recovery strategy based on ideal braking force distribution for regenerative braking system of a four-wheel drive electric vehicle. *IEEE Access*, 8:136234–136242, 2020.

[24] Ned Mohan, Tore Marvin Undeland, and William P. Robbins. *Power electronics : converters, applications and design*. Wiley, 3. edition, 2003. Main Library Johanneberg tk Mohan + 1 CD-ROM Accession Number: clpc.oai.edge.chalmers.folio.ebsco.com.fs00001000.d8fd2703.b1b9.4d68.a2a1.381ad40bb434; Other Notes: Media enhanced third edition, 18. pr.; Publication Type: Book; Physical Description: xvii, 802 s. ill. 1 CD-ROM; Language: English.

[25] Abdallah Moujahid, Mounir Elaraki Tantaoui, Manolo Dulva Hina, Assia Soukane, Andrea Ortalda, Ahmed Elkhadimi, and Amar Ramdane-Cherif. Machine learning techniques in adas: A review. IEEE.

[26] Emanuele Obialero. *A Refined Vehicle Dynamic Model for Driving Simulators*. Thesis, 2019. Accession Number: cst.20.500.12380.179787; Publication Type: Thesis; Language: English.

[27] Gwangmin Park, Seonghun Lee, Sungho Jin, and Sangshin Kwak. Integrated modeling and analysis of dynamics for electric vehicle powertrains. *Expert Systems with Applications*, 41(5), 2014/04/01.

[28] Mariarosaria Picone, Arcangelo Errichiello, and Armando Cartenì. How often are adas used? results of a car drivers' survey. *WSEAS TRANSACTIONS ON SYSTEMS*, 22:566–577, 2023.

[29] Ahmad Rahmoun and Helmuth Biechl. Parameters identification of equivalent circuit diagrams for li-ion batteries. In *2012 11th International Symposium PÄRNU, PÄRNU, Estonia*.

[30] Gaizka Saldaña, José Ignacio San Martín, Inmaculada Zamora, Francisco Javier Asensio, and Oier Oñederra. Analysis of the current electric battery models for electric vehicle simulation. *Energies*, 12(14):2750, 2019.

[31] U.S. News Best Cars Staff. Toyota to install brake override systems in all new vehicles, 2010.

[32] Carlos Renato Storck and Fatima Duarte-Figueiredo. A survey of 5g technology evolution, standards, and infrastructure associated with vehicle-to-everything communications by internet of vehicles. *IEEE Access*, 8:117593–117614, 2020.

[33] Mengjian Tian, Qiyuan Hu, Bingzhao Gao, Haitao Ding, and Hong Chen. Design and handling dynamic analysis of electric vehicle chassis with yaw direction oscillatable battery pack. *Vehicle System Dynamics*, 60(3):951–972, 2022.

[34] J. J. P. Van Boekel, I. J. M. Besselink, and H. Nijmeijer. Design and realization of a one-pedal-driving algorithm for the tu/e lupo el. *World Electric Vehicle Journal*, 7(2):226–237, 2015.

[35] Jeffrey Wishart, Steve Como, Uilani Forgione, Jack Weast, Lewis Weston, Andrew Smart, George Nicols, and Ramesh S. Literature review of verification and validation activities of automated driving systems. *SAE International Journal of Connected and Automated Vehicles*, 3(4):267–323, 2021.

[36] Boyi Xiao, Huazhong Lu, Hailin Wang, Jiageng Ruan, and Nong Zhang. Enhanced regenerative braking strategies for electric vehicles: Dynamic performance and potential analysis. *Energies*, 10(11):1875, 2017.

[37] De Jong Yeong, Gustavo Velasco-Hernandez, John Barry, and Joseph Walsh. Sensor and sensor fusion technology in autonomous vehicles: A review. *Sensors*, 21(6):2140, 2021.

[38] Caiping Zhang, Jiuchun Jiang, Linjing Zhang, Sijia Liu, Leyi Wang, and Poh Chiang Loh. A generalized soc-ocv model for lithium-ion batteries and the soc estimation for lnmco battery. *Energies*, 9(11):900, 2016.

[39] Yuanjian Zhang, Yanjun Huang, Haibo Chen, Xiaoxiang Na, Zheng Chen, and Yonggang Liu. Driving behavior oriented torque demand regulation for electric vehicles with single pedal driving. *Energy*, 228:120568, 2021.

[40] Yunfei Zhang, Can Zhao, Bin Dai, Zhiheng Li, Yunfei Zhang, Can Zhao, Bin Dai, and Zhiheng Li. Dynamic simulation of permanent magnet synchronous motor (pmsm) electric vehicle based on simulink. *Energies 2022, Vol. 15, Page 1134*, 15(3), 2022-02-03.

A
Appendix

A.1 Model Equations

A.1.1 Chassis

The equations for planar motion of the vehicle:

$$ma_x = m(\dot{u} - vr) = F_{x,tot} \tag{A.1}$$

$$ma_y = m(\dot{v} + ur) = F_{y,tot} \tag{A.2}$$

$$I_z\dot{r} = M_{z,tot} \tag{A.3}$$

where:

$$F_{x,tot} = \Sigma_{i=1}^{4} F_{xi} + F_{x,slope} + F_{x,Air} \tag{A.4}$$

$$F_{y,tot} = \Sigma_{i=1}^{4} F_{yi} + F_{y,slope} \tag{A.5}$$

$$M_{z,tot} = \Sigma_{i=1}^{4} (F_{zi}a_i - F_{xi}b_i + M_{zi}) \tag{A.6}$$

The road slope are given by:

$$F_{x,slope} = -mg\theta_{sl} \tag{A.7}$$

$$F_{y,slope} = \Sigma_{i=1}^{4} F_{zi}\theta_{cfi} \tag{A.8}$$

The aerodynamic drag is given by:

$$F_{x,Air} = -0.5C_{Ax}\rho_A A_0 u^2 \tag{A.9}$$

The roll, pitch and vertical vibrations are given by:

$$\ddot{\varphi} = \frac{\Sigma_{i=1}^{4} b_i F_{suspi} + m_s a_y h_{sr} + m_s g\varphi h_{sr}}{I_R} \tag{A.10}$$

$$\ddot{\theta} = \frac{\Sigma_{i=1}^{4} a_i F_{suspi} + m_s a_x h_{sp} + m_s g\varphi h_{sp}}{I_R} \tag{A.11}$$

$$\ddot{Z}_{CG} = \frac{\Sigma_{i=1}^{4} F_{suspi}}{m_s} \tag{A.12}$$

A.1.2 Steer

$$\delta_i = \frac{\delta_{SW,filtered} - \theta_{tb}}{i_{steer}} + F_{yi}c_{sfi} + M_{zi}c_{tori} + \varphi_{mot}\varepsilon_i + \delta_{toei} \tag{A.13}$$

$$\theta_{tb} = \frac{T_{SW}}{K_{tb}} \tag{A.14}$$

$$P_{servo} = c_1(T_{SW} - T_0) + [P_{max} - c_1(T_{max} - T_0)]\frac{(T_{SW} - T_0)^5}{(T_{max} - T_0)^5} \tag{A.15}$$

$$T_{kp} = T_{SW}i_{steer} + P_{servo}A_{piston}\frac{n_r i_{steer}}{2\pi} \tag{A.16}$$

A.1.3 Wheels

Magic formula:

$$(F_{Xi}, F_{Yi}, M_{Zi}, M_{Yi}, M_{Xi}) = MFfnc(\alpha_i, k_i, \gamma_i, F_{Zi}) \tag{A.17}$$

$$F_{xi} = F_{Xi}cos(\delta_i) - F_{Yi}cos(\delta_i) \tag{A.18}$$

$$F_{yi} = F_{Yi}cos(\delta_i) + F_{Xi}cos(\delta_i) \tag{A.19}$$

The equations for the longitudinal slips are given by:

$$\begin{cases} k_i = \dfrac{R_W\omega_i - u_i}{R_W\omega_i} & \text{for traction} \\ k_i = \dfrac{R_W\omega_i - u_i}{u_i} & \text{for braking} \end{cases} \tag{A.20}$$

$$u_i = u - b_i r \tag{A.21}$$

$$I_{Weffi} = I_{Wi} + 0.5(i_{gear}^2 I_{eng} + I_{DRV}) \tag{A.22}$$

$$T_i = T_{BRKi} + T_{DRVi} + M_{Yi} \tag{A.23}$$

$$T_{BRKi} = -P_{BRKi}C_{BRKi} \tag{A.24}$$

$$T_{DRV1} = T_{DRV2} = 0.5T_{DRVf} \tag{A.25}$$

$$T_{DRV3} = T_{DRV4} = 0.5T_{DRVr} \tag{A.26}$$

$$M_{Yi} = -F_{zi}R_w c_r \tag{A.27}$$

The side slip angle is given by:

$$\alpha_i = \delta_i - atan\frac{v + a_i r}{u - b_i r} \tag{A.28}$$

$$\frac{\sigma}{u}\dot{\alpha}_i + \alpha_i = \delta_i - atan\frac{v + a_i r}{u - b_i r} \tag{A.29}$$

The camber angle is given by:

$$\gamma_i = \gamma_{sti} + F_{yi}\tau_{sfi} + \varphi_{mot}\tau_{\varphi i} \tag{A.30}$$

A.1.4 Suspension

The deflection of the spring and the damper at each wheel is given by:

$$d_{si} = Z_{CG} - \theta a_i + \varphi b_i - z_{Wi}, i = 1:4 \tag{A.31}$$

$$\dot{d}_{si} = \dot{Z}_{CG} - \dot{\theta} a_i + \dot{\varphi} b_i - \dot{z}_{Wi}, i = 1:4 \tag{A.32}$$

Consequnently the spring and damper forces are given by:

$$F_{si} = -K_{Si} d_{Si} \tag{A.33}$$

$$F_{Di} = -C_{Di}\dot{d}_{Si} \tag{A.34}$$

The total suspension force on each wheel is given by:

$$F_{suspi} = F_{si} + F_{Di} - \frac{K_{arb}\varphi}{2b_i} \tag{A.35}$$

$$\ddot{Z}_{Si} = \frac{-K_{Ti}(Z_{Wi} - Z_{Ri}) - C_{Ti}(\dot{Z}_{Wi} - \dot{Z}_{Ri}) - F_{Si} - F_{Di} + \frac{K_{arb}\varphi}{2b_i}}{m_{usi}} \tag{A.36}$$

A.1.5 Axles

The static load on each wheel are given by:
For the front wheels:

$$F_{Zi,st} = 0.5 m_f g cos\theta_{sl} \tag{A.37}$$

For the rear wheels:

$$F_{Zi,st} = 0.5 m_r g cos\theta_{sl} \tag{A.38}$$

The change in the wheel load are calculated by:
For the front wheels:

$$\Delta F_Z = \pm\frac{m_f a_y h_{rf}}{tw} \tag{A.39}$$

For the rear wheels:

$$\Delta F_z = \pm \frac{m_r a_y h_{rr}}{tw} \tag{A.40}$$

Due to the longitudinal acceleration, the changes of the wheel load is given by:

$$\Delta F_z = \pm \frac{m a_x h_p}{2wb} \tag{A.41}$$

The load on each wheel can be derived by:

$$F_{Zi} = F_{Zi,st} + F_{suspi} \pm \frac{m a_x h_p}{2wb} \pm \frac{m_{f,r} a_y h_r}{tw} \tag{A.42}$$

A.2 Experimental design for complete testing

To test the single-pedal mode with regenerative braking function, unique to all-electric vehicles, this experimental design is derived from the experimental design proposed in Jorge's master thesis with modifications.

A.2.1 Straight-ahead Run

The experimental part is to collect data in different driving modes and braking modes, which is used to tune the braking system and the powertrain system model to make their output fit the experiment results with the same input.

A.2.1.1 Experiment 1: Constant Acceleration Pedal position Test

In this round of testing, the initial SOC should be higher than 80%. The starting state of the vehicle is stationary. After starting the experiment, the acceleration pedal is first stepped down to 20% and maintained for 10s and the data is recorded. Afterwards, the vehicle was returned to the initial state and the acceleration pedal was stepped down to 40%, maintained for 10s, and the data was recorded. Repeat the above experimental operation and record the data at 60%, 80%, and 100% of the acceleration pedal.
The data recorded in this experiment contains the output states of the vehicle's powertrain at different constant acceleration pedal positions, as well as the transient response states as the pedal is increased from 0 to the enacted pedal position.

A.2.1.2 Experiment 2: Variable Pedal Experiments at Specific Speeds

In this experiment, the effect of different degrees of acceleration pedal release on single-pedal mode driving at different vehicle speeds will be investigated. The pre-requisites for this experiment are that the SOC state meets the requirements to activate the single-pedal mode and that the single-pedal mode should be enabled in the vehicle system.
First, the car was driven with 100% acceleration pedal position to reach 150km/h, and at the moment of reaching 150km/h the acceleration pedal was released to 80% and the data was recorded. Repeat the above operation to release the acceleration

pedal from 100% to 60%, 40%, 20%, and 0%. Record the data.
Then, the above experimental procedure was repeated with the acceleration pedal position of 80%, 60%, 40%, and 20% as the starting state. It should be noted that there may be cases where the car is unable to reach the desired 150km/h at lower positions, such as 20%. In this case, the test will be carried out at the highest achievable speed and this will be stated in the experiment report.
All the above experimental procedure will be tested for all the different target speeds i.e. 100 km/h, 80 km/h, 60 km/h,40 km/h,20 km/h.

A.2.1.3 Experiment 3: Experiments for rapidly changing acceleration pedal position

This experiment looks at whether rapidly changing accelerator pedal position has an effect on powertrain output performance. This experiment is divided into two parts, one part is a test of the effect of rapidly depressing the accelerator pedal on the output performance of the powertrain, and the other part is a test of the effect of rapidly lifting the accelerator pedal on the output performance of the regenerative braking system. For the initial state setting of the car, the regenerative braking system should be activated in the system as well as the single pedal mode.
In the first part, the initial speed of the car was 20 km/h. this speed was reached by 50% of the accelerator pedal position. After reaching 20km/h, the pedal was pressed down to 100% maintained for 5s and the data was recorded. Change the initial speed to 40, 60, 80 and 100km/h and repeat the experiment.
In the second part, the initial speed of the car was 150 km/h which was reached by accelerating the pedal position to 100%. After reaching this initial speed, the pedal was quickly lifted to 50% position for 30s to record the data. The speed of the car was returned to the initial state and the pedal was quickly released to the 0% position and data was recorded continuously until the vehicle speed was 0.

A.2.1.4 Experiment 4: Straight-ahead Free Ride

The vehicle's initial speed is 0, and the initial SOC should be less than 80% but greater than 30%. The driver is supposed to freely depress both pedals without any steering wheel angle input. When the free ride is over, the vehicle speed should be 0 km/h.

A.2.2 Circular Run

The experiment consists of driving the vehicle describing a constant radius circular path, starting from 0km/h speed and slowly increasing until the stability limits are reached. From this experiment, the main vehicle motions that can be studied are the vehicle's lateral velocity, acceleration, and yaw rate.

A.2.2.1 Constant Radius Test

First, drive the car onto a route of that set radius, using the smallest speed that will maintain that path. Keep the position of the accelerator pedal and the angle of

the steering wheel fixed, and record the data at this point. Subsequently, increase the vehicle speed to the next level, maintain the same path, and when the vehicle is stabilized, keep the position of the accelerator pedal as well as the angle of the steering wheel fixed and record the data. The experimental procedure was repeated until the vehicle was unable to maintain the steady-state condition.

A.2.3 Double lane-change track and designation of sections

This part of the experiment was obtained by adapting ISO 3888-1. This part of the experiment simulates the behavior of a driver changing lanes during driving, and the purpose of this part of the experiment is to validate the results of the model in more detail. By comparing the results of this part of the experiment with those of the model, the model's representation of real-world driving dynamics is demonstrated.

A.3 Experiments Results

A.3.1 Vehicle Normal Acceleration Test Result

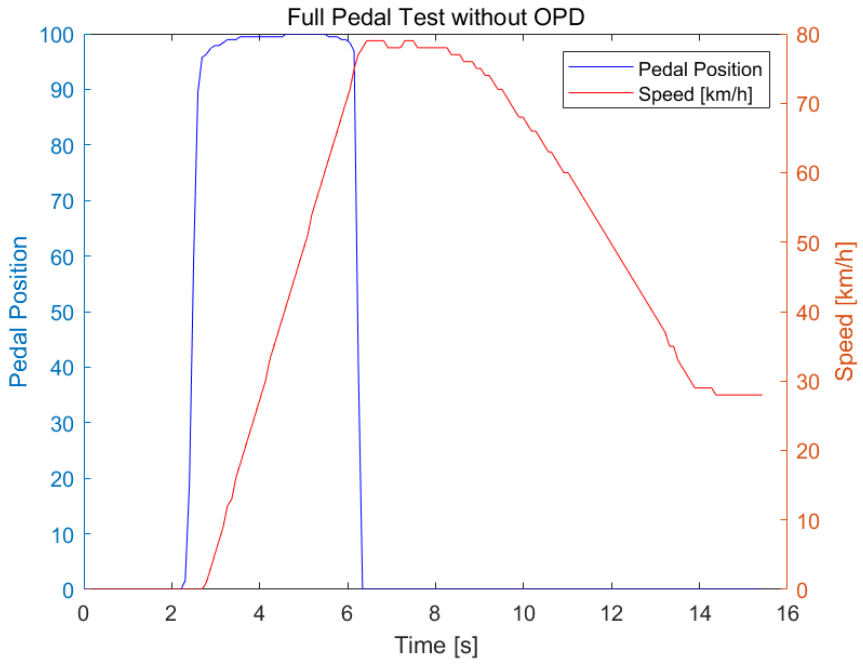

Figure A.1: Full Pedal Test Without OPD

A.3.2 OPD Feature Test Result

A.3.2.1 Full Pedal test With OPD (full release after acceleration)

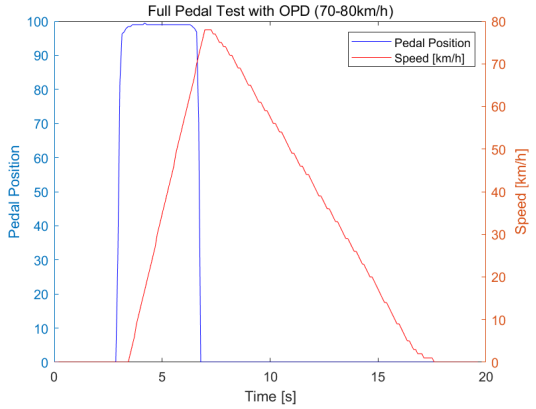

Figure A.2: Full Pedal Test With OPD (70-80km/h)

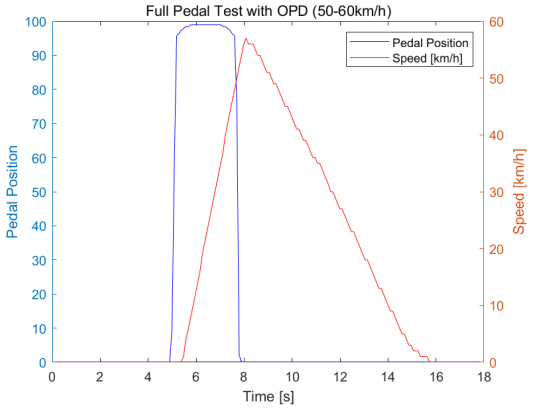

Figure A.3: Full Pedal Test With OPD (50-60km/h)

A.3.2.2 Full Pedal test With OPD (half release after acceleration)

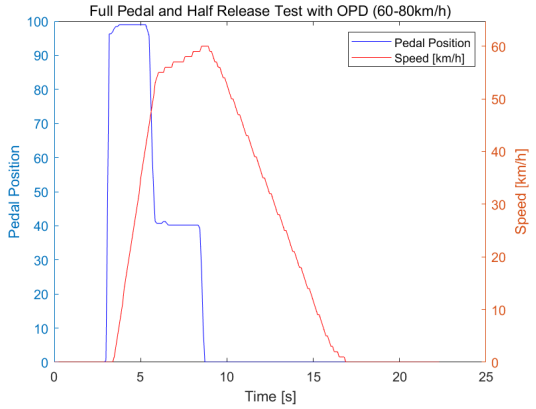

Figure A.4: Full Pedal Test With OPD (60-80km/h)

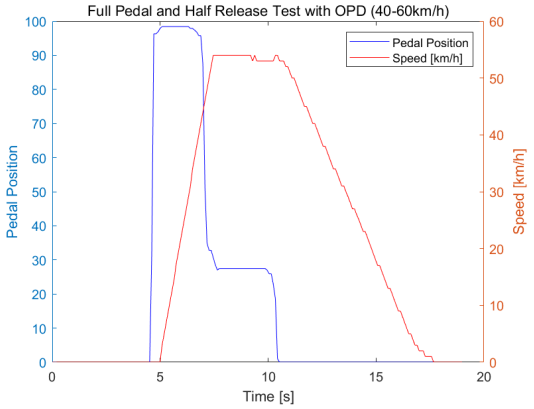

Figure A.5: Full Pedal Test With OPD (40-60km/h)

A.3.2.3 Full Pedal Acceleration Speed Maintenance Test

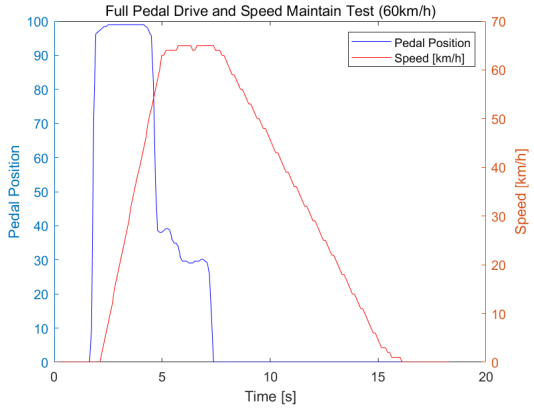

Figure A.6: Full Pedal Drive And Speed Maintain Test With OPD (60km/h)

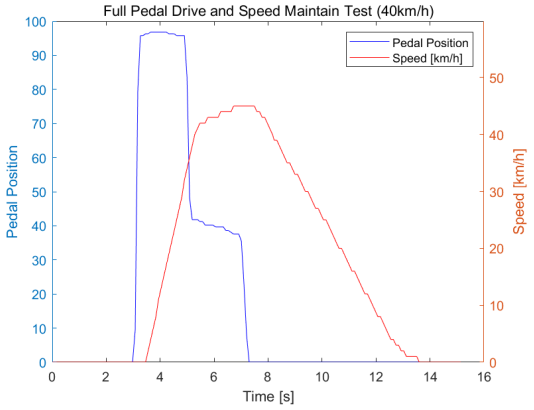

Figure A.7: Full Pedal Drive And Speed Maintain Test With OPD (40km/h)

A.3.2.4 Full Pedal Deceleration Speed Maintenance Test

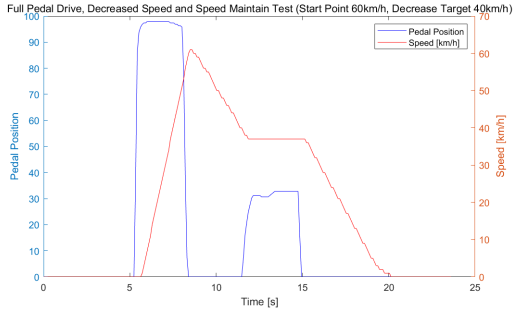

Figure A.8: Full Pedal Deceleration And Speed Maintain Test With OPD (60km/h)

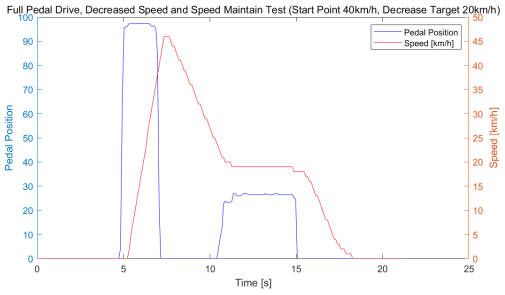

Figure A.9: Full Pedal Deceleration And Speed Maintain Test With OPD (40km/h)

A.3.2.5 OPD Normal Drive Speed Maintenance Test

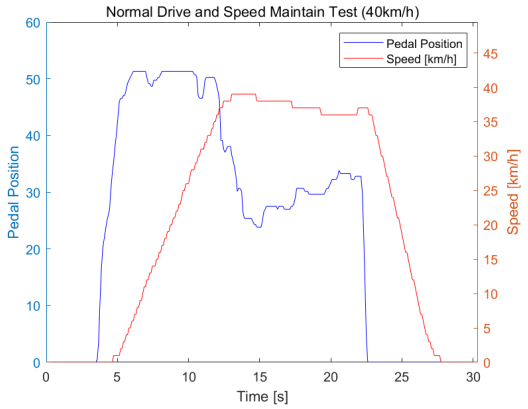

Figure A.10: Normal Drive And Speed Maintain Test With OPD (40km/h)

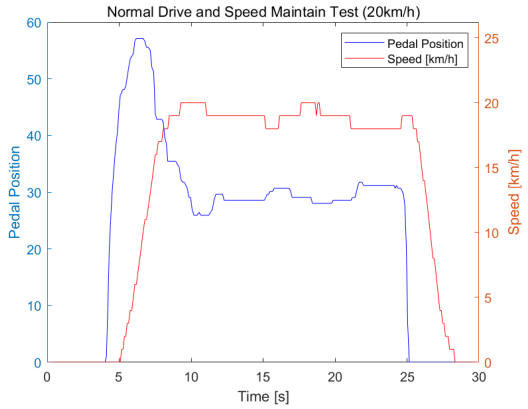

Figure A.11: Normal Drive And Speed Maintain Test With OPD (20km/h)

A.3.3 Vehicle braking Experiments

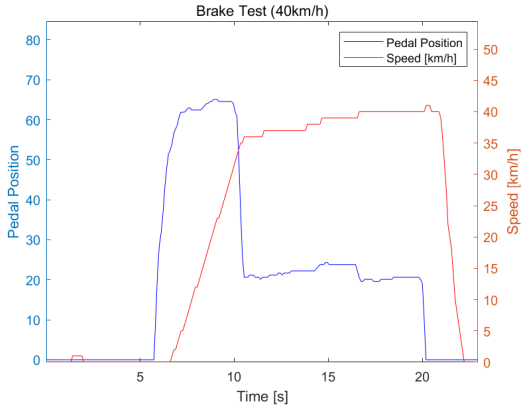

Figure A.12: Certain Speed Braking Experiment (40km/h)

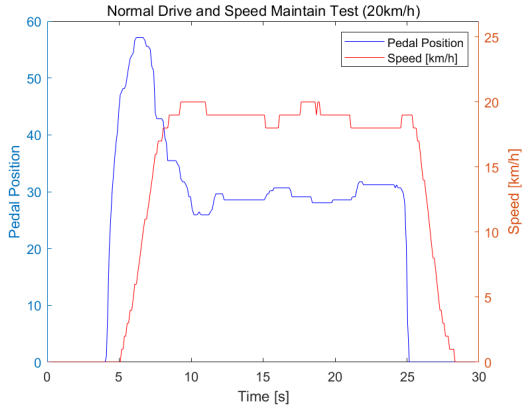

Figure A.13: Certain Speed Braking Experiment (20km/h)

A.4 Nomenclature for Appendix

A_{piston}	Piston area of the steering servo system
A_0	Projected front area of the vehicle
a_i	Longitudinal position (wrt CG) of wheel i
a_x	Longitudinal acceleration of the vehicle
a_y	Lateral acceleration of the vehicle
b_i	Lateral position (wrt CG) of wheel i
C_{Ax}	Air drag coefficient

$C_{BRK,i}$	Brake torque-pressure gradient for wheel i
$C_{D,i}$	Damping coefficient at wheel i
$C_{T,i}$	Tyre vertical damping coefficient at wheel i
C_{ϕ}	Suspension roll damping
c_r	Rolling resistance coefficient
$c_{sf,i}$	Suspension compliance for lateral force at wheel i
$c_{tor,i}$	Suspension torsional compliance at wheel i
clutch	Clutch engagement
dS_i	Suspension deflection at wheel i
$F_{D,i}$	Damper force at wheel i
$F_{S,i}$	Spring force at wheel i
$F_{Susp,i}$	Suspension force at wheel i
$F_{X,i}$	Longitudinal force, in tyre coordinate, at wheel i
$F_{x,Air}$	Air drag
$F_{x,i}$	Longitudinal force, in vehicle coordinate, at wheel i
$F_{x,Slope}$	Longitudinal force due to the road slope
$F_{x,Tot}$	Total longitudinal force
$F_{Y,i}$	Lateral force, in tyre coordinate, at wheel i
$F_{y,i}$	Lateral force, in vehicle coordinate, at wheel i
$F_{y,Slope}$	Lateral force due to the road crossfall
$F_{y,Tot}$	Total lateral force
$F_{z,i}$	Vertical force at wheel i
$F_{zi,st}$	Static load at wheel i
h_p	Pitch centre height
h_{rf}	Front roll centre height
h_{rr}	Rear roll centre height
h_{sp}	Height of centre of gravity above the pitch centre
h_{sr}	Height of centre of gravity above the roll centre
I_{DRV}	Driveshaft inertia
I_{eng}	Engine inertia
I_R	Vehicle moment of inertia about roll axis
$I_{Weff,i}$	Effective inertia at wheel i
$I_{W,i}$	Inertia of wheel i
I_P	Vehicle moment of inertia about pitch axis
I_z	Vehicle moment of inertia about z axis
i_{gear}	Gear ratio (gearbox+end gear)
i_{steer}	Steering gear ratio
K_{arb}	Anti-roll bar stiffness

$K_{S,i}$	Spring stiffness at wheel i
K_{tb}	Torsion bar stiffness
$K_{T,i}$	Tyre vertical stiffness at wheel i
K_{ϕ}	Suspension roll stiffness
$M_{X,i}$	Overturning moment at wheel i
$M_{Y,i}$	Rolling resistance torque at wheel i
$M_{z,i}$	Aligning torque at wheel i
$M_{z,Tot}$	Total moment about z axis
m	Vehicle mass
m_f	Front mass
m_r	Rear mass
m_s	Sprung mass
$m_{us,i}$	Unsprung mass at wheel i
n_r	Rack ratio, i.e., rack linear motion per turn of steering wheel
$P_{BRK,i}$	Brake pressure at wheel i
P_{servo}	Pressure at steering servo system
R_W	Wheel radius
r	Vehicle yaw rate
$T_{BRK,i}$	Brake torque at wheel i
$T_{DRV,i}$	Driving torque at wheel i
T_{eng}	Engine Torque
T_i	Total torque at wheel i
T_{kp}	Torque about the kingpin (sum of the torque at both sides)
T_{SW}	Steering wheel torque
t_w	Track width
u	Vehicle longitudinal speed
u_i	Longitudinal speed at wheel i
v	Vehicle lateral speed
w_b	Wheelbase
z_{CG}	Vertical position of vehicle centre of gravity
$z_{R,i}$	Road surface vertical position at wheel i
$z_{W,i}$	Vertical position of wheel i
α_i	Side slip angle at wheel i
γ_i	Camber angle at wheel i
γ_{sti}	Static camber angle at wheel i
κ_i	Longitudinal slip at wheel i
θ	Vehicle pitch angle
$\theta_{cf,i}$	Crossfall of the road at wheel i

θ_{sl}	Longitudinal slope of the road
θ_{tb}	Torsion bar deflection
δ_i	Steer angle of wheel i
δ_{SW}	Steering wheel angle
$\delta_{SW,filtered}$	Filtered steering wheel angle
$\delta_{toe,i}$	Toe angle at wheel i
ϵ_i	Roll steer coefficient for wheel i
ρ_A	Air density
σ	Tyre relaxation length
$\tau_{sf,i}$	Coefficient for camber due to lateral force, for wheel i
$\tau_{\phi,i}$	Roll camber coefficient at wheel i
ϕ	Vehicle roll angle
ϕ_{mot}	Roll angle due to the vehicle motion
ω_{eng}	Engine speed
ω_i	Rotational speed of wheel i
ΔF_z	Load transfer

DEPARTMENT OF MECHANICS AND MARITIME SCIENCES
CHALMERS UNIVERSITY OF TECHNOLOGY
Gothenburg, Sweden 2024
www.chalmers.se

CHALMERS
UNIVERSITY OF TECHNOLOGY